

**UCSF**

**UC San Francisco Electronic Theses and Dissertations**

**Title**

Regulation of cell migration and cell polarity by a C. elegans Wnt gene

**Permalink**

<https://escholarship.org/uc/item/24h059bf>

**Author**

Whangbo, Jennifer S.

**Publication Date**

1999

Peer reviewed|Thesis/dissertation

Regulation of Cell Migration and Cell Polarity by a *C. elegans* Wnt gene

by

Jennifer S. Whangbo

DISSERTATION

Submitted in partial satisfaction of the requirements for the degree of

DOCTOR OF PHILOSOPHY

in

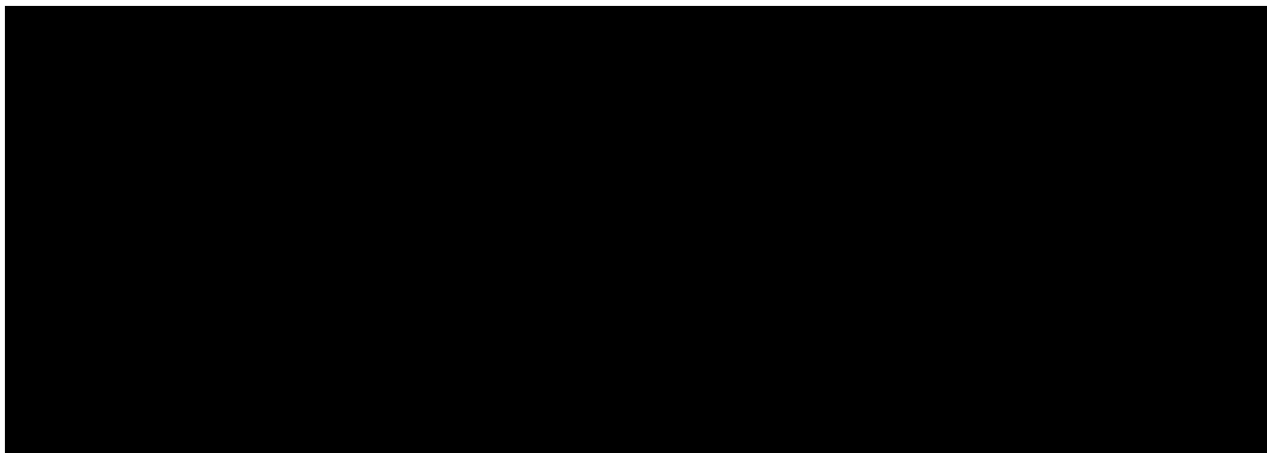
Biochemistry

in the

GRADUATE DIVISION

of the

UNIVERSITY OF CALIFORNIA SAN FRANCISCO



Date

University Librarian

Degree Conferred: .....

**Copyright 1999**

**by**

**Jennifer S. Whangbo**

To my family and friends

UCSF LIBRARY  
LIBRARY

## **Preface**

I would like to thank Cynthia Kenyon for her generous support and encouragement. Especially during the past year, she has been instrumental in helping me to achieve my goals. I truly admire her energy and enthusiasm for science, and I appreciate her ability to create a fun and stimulating lab environment. I thank my committee members, Cori Bargmann and Tom Kornberg, for expeditiously reading and commenting on my thesis. They have also given me helpful suggestions and assurance during the course of my project. In addition, I thank Joachim Li for his continued interest in my progress and well being.

I am grateful to many members of the Kenyon lab for their insights and positive reinforcement throughout graduate school. In particular, I thank Jeanne Harris for beginning the *egl-20* project and Gregg Jongeward for facilitating the cloning of *egl-20*. I feel fortunate to have overlapped with Steve Salser, Lisa Wrischnik and Supriya Shivakumar; their extensive knowledge combined with their wry sense of humor generated many memorable group meetings. I feel privileged to have had the opportunity to observe Craig Hunter in action. I thank Craig, Scott Alper, Javier Apfeld and Joy Alcedo for always being eager to engage in deep scientific discussions. I would also like to thank my past and present bay mates: Lucie Yang for her friendship, Mary Sym for inspiring me to be more efficient, Lisa Williams for being my only rotation student ever and Ilan Zipkin for his view of the world.

Our lab is extremely fortunate to have Bella Albinder, who cares about everyone and makes the lab a warm place. We are also prevented from complete dysfunction by Kathleen Rañeses, who is the source of all interesting knowledge.

My friends have given me a life outside of lab and have kept me sane. I thank Maki Inada for mochi runs to Yamada Seika; Tom Wang, Mike Pollard and Wei Wei for settling Catan; David Tobin for teaching me how to dance salsa; and Dorothy, Claudine and Trisha for fun visits. My family has always been supportive of my endeavors. I would like to thank my parents for giving me the strength and confidence to pursue my goals. I thank my brother, Albert, for his email correspondence and weekly phone calls, which always give me something to look forward to.

Finally, I thank Javier Apfeld, who coincidentally falls into many of the categories mentioned above. He has made my life infinitely more interesting, debatable and meaningful.

110211DDADV

**Regulation of Cell Migration and Cell Polarity by a *C. elegans* Wnt gene**

Wnt signaling molecules have essential functions in a wide range of developmental processes. This work describes the role of a Wnt family member, *egl-20*, in patterning cell migrations and asymmetric cell fates along the anteroposterior (A/P) body axis of *C. elegans*. The *egl-20/Wnt* gene plays two essentially opposite roles in the migrations of the descendants of QL and QR, two bilaterally symmetrical cells that migrate in opposite directions along the A/P axis. In the QL lineage, *egl-20* promotes posterior migration, whereas in the QR lineage it promotes anterior migration. In addition, *egl-20* activity is required for the correct A/P polarity of an asymmetric cell division in the lateral epidermis.

How does a single protein control these diverse processes? The expression of an *egl-20::gfp* fusion gene is restricted to a group of cells in the tail region of the animal.

Despite its localized distribution, EGL-20 does not act as a spatially-graded morphogen to specify the distinct migratory fates in the Q lineages or the polarity of the V5 epidermal cell. In the QL and QR lineages, EGL-20 acts in a dose-dependent manner to specify opposite patterns of migration. High levels of EGL-20 promote posterior migration by activating a canonical Wnt signal-transduction pathway, whereas low levels promote anterior migration by a separate, undefined mechanism. The two Q cells are able to respond differently to EGL-20 because they have different response thresholds.

Thus, in this system, two distinct dose-dependent responses are determined by left-right asymmetrical differences in the cellular responsiveness to Wnt signaling.

EGL-20 also influences the V5 division in a position-independent manner. The regulation of polarity in this single epidermal cell is complex and involves multiple signaling systems. In the wild type, EGL-20 appears to play a role in repressing or overriding local perturbations in polarity signals, rather than a role in providing essential polarity information to the V5 cell.



**Table of Contents**

Chapter 1: Introduction .....1

    BACKGROUND.....3

        Wnt pathways.....3

        Regulation of Hox gene expression.....7

        Cell migrations during development .....9

        Polarity of asymmetric cell divisions .....13

        Planar polarity .....17

    OVERVIEW .....18

    CONCLUSIONS.....20

    REFERENCES.....22

Chapter 2: *egl-20*, a Gene Involved in Anteroposterior Patterning,  
Encodes a Wnt Homolog.....33

    SUMMARY .....33

    INTRODUCTION.....34

    RESULTS .....35

*egl-20* encodes a Wnt family member.....35

        Isolation of new *egl-20* alleles .....35

        Molecular lesions associated with *egl-20* alleles .....36

    DISCUSSION .....37

    MATERIALS AND METHODS .....38

        General Methods and Strains .....38

        Cloning of *egl-20*.....38

UCSF LIBRARY  
JUN 17 2007

Complementation tests to identify new <i>egl-20</i> alleles.....	40
Sequencing <i>egl-20</i> alleles .....	40
<b>Chapter 3: A Wnt Signaling System that Specifies Two Patterns of</b>	
<b>Cell Migration in <i>C. elegans</i>.....</b>	<b>47</b>
SUMMARY.....	47
INTRODUCTION.....	48
RESULTS .....	49
Expression of <i>egl-20</i> is not left-right asymmetrical .....	49
The EGL-20/Wnt protein does not act as a positional signal for	
<i>mab-5</i> activation.....	50
The Q cells respond to EGL-20 in a dose-dependent manner .....	51
Both QL and QR can activate <i>mab-5</i> expression in response to	
EGL-20, but QL is more sensitive to EGL-20 than is QR.....	52
Low levels of EGL-20 promote anterior migration.....	53
DISCUSSION .....	55
MATERIALS AND METHODS.....	58
<i>egl-20</i> Reporter Genes and Transgenic Arrays .....	58
Heat Shock Constructs and Conditions .....	59
$\beta$ -galactosidase Detection .....	59
Examination of TGF- $\beta$ Pathway Mutants.....	60
ACKNOWLEDGEMENTS.....	60

Chapter 4: Multiple layers of signaling regulate the polarity of an asymmetric cell division.....77

SUMMARY.....77

INTRODUCTION.....78

RESULTS .....80

    Mutations in *egl-20* reverse the polarity of the asymmetric V5-cell division80

    Establishment of asymmetry does not appear to require lateral signaling between the V5 daughter cells .....82

    Genes that act with *egl-20* to activate *mab-5* expression do not influence the polarity of the V5-cell division .....83

    The polarity of the V5-cell division is not determined by the spatial pattern of *egl-20* expression in the animal.....84

    Overexpression of EGL-20 causes ectopic polarity reversals in the V cells .85

    Signals from neighboring cells orient the V5-cell division in *egl-20* mutants, but not in wild-type animals.....86

*lin-44* does not encode the polarity-reversing signal.....87

    Mutations in *lin-17/Frizzled* prevent V5 polarity reversals from occurring in *egl-20/Wnt* mutants .....88

    Mutations in *pry-1* enhance the frequency of V5 polarity reversals in *egl-20* mutants .....89

    LIN-44 is not required in order for the ablation of V6 and T to rescue the V5 polarity defect in *egl-20* mutants .....89

*egl-20* and *lin-44* can functionally replace each other.....90

DISCUSSION .....	90
Signals from posterior neighbors polarize the V5-cell division in <i>egl-20</i> mutants .....	93
<i>lin-17</i> and <i>pry-1</i> influence the polarity of V5 in <i>egl-20</i> mutants. ....	94
What orients the V5-cell division along the A/P body axis? .....	95
MATERIALS AND METHODS .....	96
General Procedures, Nomenclature, and Strains .....	96
Strains .....	96
Construction of double mutant strains.....	96
Determining the fates of V5.a and V5.p.....	97
Immunofluorescence .....	98
Cell Ablations.....	98
Temperature shift experiments.....	99
Reporter Genes and Transgenic Arrays.....	100
<i>Heat Shock Conditions</i> .....	100
ACKNOWLEDGEMENTS.....	100
REFERENCES.....	112
Chapter 5: Future directions .....	114
SUMMARY.....	114
I. <i>egl-20</i> and its role in Q cell migrations .....	115
How does <i>egl-20</i> promote anterior migration in the QR lineage? .....	115
What makes QL more sensitive than QR to levels of EGL-20? .....	117
Where does the EGL-20 signal transduction pathway act? .....	119

II. EGL-20 and its role in establishing polarity of the V-cell divisions .....	120
What is the <i>egl-20</i> signal transduction pathway for determining	
V5 polarity?.....	120
What is the signal that causes V5 polarity reversals in	
<i>egl-20</i> mutants? .....	122
What signals polarize the other V-cell divisions? .....	123
CONCLUSIONS.....	124
Appendix A: Final positions of the QL.pa and QR.pa descendants and	
polarity of the V5-cell division in <i>egl-20(mu241)</i> and <i>egl-20(mu320)</i>	
at 15°C, 20°C and 25°C.....	125
Appendix B: The final positions of the QL.pa and QR.pa descendants in	
<i>egl-20(n585); bar-1(ga80)</i> double mutants.....	128
Appendix C: A high dose of <i>hs-egl-20</i> causes posterior migration of the	
Q descendants in a <i>mab-5</i> and <i>egl-5</i> -independent manner.....	130
Appendix D: <i>mig-14(mu71)</i> suppresses the <i>mab-5</i> -independent response	
to high levels of <i>hs-EGL-20</i> .....	133
Appendix E: <i>mig-1</i> and <i>mig-13</i> mutants can exhibit the low dose	
response to <i>hs-egl-20</i> .....	135
Appendix F: Later polarity reversals in the V cell lineages of	
<i>egl-20(n585)</i> animals.....	138
Figure F.1. Polarity reversals also occur later in the V-cell lineages	
of <i>egl-20(-)</i> mutants.....	138
Appendix G: The temperature sensitive period (TSP) of V5 polarity .....	140

Appendix H: Screening through candidate mutants for V cell polarity .....143  
Appendix I: Overexpression of *lin-17* causes *egl-20(-)* phenotypes.....147  
Appendix J: Peptide antibodies against the EGL-20 protein.....149  
Appendix K: LIN-39 staining in *egl-20(n585)* mutants.....151

INCE IIDDADY

## List of Tables

Table 2.1. Phenotypes and molecular lesions of <i>egl-20</i> alleles .....	44
Table 4.1. The polarity of the V5-cell division in <i>egl-20</i> mutants.....	107
Table 4.2. V5 polarity phenotype of single and double mutants .....	108
Table 4.3. <i>hs-egl-20</i> causes polarity defects in all V-cell divisions.....	109
Table 4.4. Polarity of the V5-cell division following ablations.....	110
Table 4.5. <i>egl-20</i> and <i>lin-44</i> can substitute for each other .....	111
Table A.1 Polarity of the V5-cell division in <i>mu241</i> and <i>mu320</i> .....	126
Table H.1 Mutant strains with wild-type V5 polarity .....	146
Table I.1 Overexpression of <i>lin-17</i> causes <i>egl-20(-)</i> phenotypes .....	148

## List of Figures

Figure 1.1. A summary of the <i>egl-20(-)</i> phenotypes.....	21
Figure 2.1. The cosmid W08D2 contains <i>egl-20</i> rescuing activity.....	41
Figure 2.2. <i>egl-20</i> encodes a Wnt homolog.....	42
Figure 3.1. <i>egl-20</i> regulates Q cell migration and is expressed in the posterior.....	61
Figure 3.2. EGL-20 does not act as a positional signal.....	64
Figure 3.3. Cells in the QL and QR lineages have different response thresholds to the EGL-20 signal .....	67
Figure 3.4. The threshold for anterior migration is lower than the threshold for <i>mab-5</i> expression in both Q cells .....	70
Figure 4.1. <i>egl-20</i> activity is required to orient the V5-cell division.....	101
Figure 4.2. Posterior localization of EGL-20 is not required to orient the V5-cell division.....	103
Figure 4.3. The EGL-20::GFP distribution is altered in a <i>mig-14(k124)</i> mutant background.....	105
Figure A.1. Final positions of the QL.pa and QR.pa descendants in <i>egl-20(mu241)</i> at 15°C, 20°C and 25°C.....	127
Figure A.2. Final positions of the QL.pa and QR.pa descendants in <i>egl-20(mu320)</i> at 15°C, 20°C and 25°C.....	127
Figure B.1 Final positions of the QL.pa and QR.pa descendants in <i>egl-20(n585); bar-1(ga80)</i> double mutants at 20°C and 25°C.....	129



Figure C.1 Final positions of the QL.pa and QR.pa descendants in <i>mab-5(e2088); egl-20(n585); mul53(hs-egl-20)</i> following heat shock.....	131
Figure C.2 Final positions of the QL.pa and QR.pa descendants in <i>mab-5(e1289); egl-5(n945); mul53(hs-egl-20)</i> following heat shock.....	132
Figure D.1. Final positions of the QL.pa and QR.pa descendants in <i>mig-14(mu71); mab-5(e2088); mul53(hs-egl-20)</i> following heat shock.....	134
Figure E.1. Final positions of the QR.pa descendants in <i>mig-1(e17870); mul53</i> and <i>mul53; mig-13(mu31)</i> animals following heat shock .....	136
Figure F.1. Polarity reversals also occur later in the V-cell lineages of <i>egl-20(-)</i> mutants.....	138
Figure G.1. The TSP for V5 polarity determination in <i>egl-20(-)</i> mutants .....	142
Figure J.1. Staining of wild-type animals with unpurified EGL-20 anti-sera #45585 .....	150
Figure K.1. $\alpha$ -LIN-39 staining of wild type and <i>egl-20(n585)</i> .....	153

WILEY-LIBRARY

## Chapter 1: Introduction

During the post-embryonic development of the nematode *C. elegans*, the *egl-20* gene patterns diverse events such as the migration of neuroblasts and the orientation of asymmetric cell divisions along the anteroposterior (A/P) body axis (Figure 1.1). In *egl-20* mutants, the QL neuroblast fails to express the Hox gene *mab-5*, and consequently, its descendants migrate into the anterior rather than into the posterior (Harris et al., 1996). *egl-20* mutants also exhibit a guidance defect in the anterior migrations of certain neural cells in the QR lineage. In the absence of *egl-20* activity, these neural cells migrate to positions that are posterior to the normal stopping points (Harris et al., 1996). Thus, *egl-20* plays two essentially opposite roles in Q cell migration. In the QL lineage it promotes posterior migration, whereas in the QR lineage it promotes anterior migration. In addition, mutations in *egl-20* can reverse the A/P orientation of certain asymmetric cell divisions in the lateral epidermis of the worm.

Several aspects of nematode development make *C. elegans* an ideal model organism for the study of cell migration and cell polarity. The invariant cell lineage generates reproducible and defined patterns of cell migrations and divisions from animal to animal. The transparency of *C. elegans* enables direct observation of both stationary and migratory cells. In addition, the short generation time and genetic tractability of *C. elegans* facilitate the process of identifying mutant animals and characterizing the nature of their defects at the molecular and cellular levels.

The Q neuroblasts display a wide range of interesting migratory behaviors. The QL and QR neuroblasts are born in equivalent A/P positions on the left and right sides of

PROOF REVISION

the animal. QL and QR undergo identical patterns of division and differentiation, yet their migrations are left-right asymmetric. QL and its descendants express the Hox gene *mab-5*, which in turn specifies their posterior migration. QR and its descendants, which do not express *mab-5*, migrate anteriorly. Each descendant migrates to a unique position along the body axis and subsequently differentiates into a sensory neuron. Thus, the Q cell migrations provide a system for studying topics such left-right asymmetry, Hox gene regulation and the encoding of positional information along the A/P axis.

Similarly, the epidermal V cells provide a useful system for studying the regulation of asymmetric cell fate determination. In newly hatched *C. elegans* larvae, the six V cells (V1-V6) extend in a row along each side of the body. In hermaphrodites, these cells undergo several rounds of asymmetric divisions to generate sensory and cuticular structures. The first asymmetric division is oriented such that the posterior daughter adopts the seam cell fate and the anterior daughter adopts the syncytial fate. These two cell types are relatively large and can be distinguished by their morphology using Nomarski optics. Thus, misoriented or misspecified cell fates can be readily identified.

Using a combination of molecular biology, genetics and cell biology techniques, I have investigated the role of *egl-20* in patterning cell migrations and in establishing cell polarity. My entry point for this project was the cloning of *egl-20*. Jeanne Harris previously mapped the *egl-20* locus relative to physical markers on chromosome IV. Gregg Jongeward identified a pool of three cosmids which contained *egl-20(+)* rescuing activity. Subsequently, I demonstrated that *egl-20* encodes a member of the Wnt family of secreted glycoproteins. This molecular characterization was followed by a

WING LIDDON

more detailed analysis of EGL-20 function in regulating diverse A/P patterning events. Before summarizing my findings, I will provide a brief review of research in fields relevant to this work.

## **BACKGROUND**

### **Wnt pathways**

Wnt genes were first cloned as candidate protooncogenes from the mouse genome. Subsequently, Wnt homologs have been identified in a wide range of organisms and have been found to regulate important developmental processes ranging from the segmentation of insect embryos to embryonic axis specification in vertebrates (Cadigan and Nusse, 1997; Nusse and Varmus, 1992). Wnt family members are defined by homology to the founding members *Wnt-1* in the mouse (first called *int-1*) and *wingless* (*wg*) in *Drosophila*. Wnt genes encode secreted glycoproteins that are typically 350-400 amino acids in length. These signaling molecules are characterized by an amino terminal signal sequence, one or more sites for N-linked glycosylation and a conserved pattern of 23-24 cysteine residues. Analyses of *wg* alleles in *Drosophila* have suggested the presence of functional domains in the Wg protein that have different signaling activities (Bejsovec and Wieschaus, 1995). Evidence for different domains in Wnt proteins is also provided by studies of chimeric Wnt proteins in *Xenopus* embryos (Du et al., 1995).

The first mutations in a Wnt gene were isolated in the *wg* gene of *Drosophila*. Based on the segment polarity phenotype of *wg* mutant embryos, other genes with similar mutant phenotypes were identified and led to the elucidation of the *wg* signal

transduction pathway (Nusse and Varmus, 1992). The Wg receptor was identified in cell culture through a biochemical binding assay. Cell lines transfected with members of the Frizzled family of seven transmembrane receptors were able to bind Wg on their cell surface (Bhanot et al., 1996). In addition, these cells were able to accumulate a downstream effector, the Armadillo protein, in a Wg-dependent manner. The current understanding of signaling events downstream of the activated Wg receptor is as follows: the Dishevelled (Dsh) phosphoprotein antagonizes the zeste-white 3/GSK-3 kinase (Zw3), which in turn leads to intracellular accumulation of Armadillo/ $\beta$ -catenin (Arm). In the nucleus, the Arm protein interacts with the TCF/LEF1 transcription factor to regulate target gene expression. The mechanism by which these proteins work as signaling components is poorly understood and the identification of new components continue to add further complexity to the pathway. For example, studies in tumor cell lines have identified the adenomatous polyposis coli (APC) protein in a complex with GSK-3 and  $\beta$ -catenin. In this complex, APC appears to play a negative role in the Wnt pathway by precipitating  $\beta$ -catenin degradation (Rubinfeld et al., 1996; Rubinfeld et al., 1993). In contrast, studies in *Xenopus* and *C. elegans* suggest that APC acts as a positive regulator of Wnt signaling (Cadigan and Nusse, 1997). Recent evidence implicates heparan sulfate proteoglycans in Wg signaling (Lin and Perrimon, 1999). In addition, secreted factors with Wnt inhibiting activity have been identified (Cadigan and Nusse, 1997).

What is known about how Wnt proteins function in vivo? In *Drosophila*, the Wg protein is able to influence cell fates at both short and long ranges. For example, in embryos, Wg is secreted by subpopulations of cells within each segment and received by

their adjacent nonsecreting neighbors (van den Heuvel et al., 1989). In addition, the Wg protein can organize the pattern of cells located at a distance from the secreting cells. Several studies have suggested that Wg functions as a graded morphogen to organize tissues such as the developing wing, leg and midgut (Hoppler and Bienz, 1995; Lecuit and Cohen, 1997; Neumann and Cohen, 1997; Zecca et al., 1996). In this model, the localized expression of *wg* leads to the formation of a Wg protein gradient, which in turn alters gene expression of the responding cells in a concentration-dependent manner. Thus, Wg can function at distinct signaling thresholds to determine multiple cell fates in several tissues.

The first Wnt genes to be identified in *C. elegans*, *Ce-Wnt-1* and *Ce-Wnt-2*, were obtained by a PCR screen of genomic DNA and by the Caenorhabditis Genome Project, respectively (Kamb et al., 1989). Northern blot analysis of these two genes indicated that both genes were expressed most strongly in embryos, but transcripts were also present at lower levels in the larval and adult stages (Shackleford et al., 1993). Mutational analysis of *Ce-Wnt-1* indicates that it has both maternal and zygotic functions. Disruption of the maternal function results in an early cytokinesis defect which results in arrested multinucleate embryos (Shivakumar, 1996). The zygotic function of *Ce-Wnt-1* has not been characterized. Mutations in *Ce-Wnt-2* have not been isolated. Mutations in another Wnt gene, *mom-2*, also result in an embryonic-lethal phenotype. *mom-2* mutants are defective in the specification of the E blastomere, which gives rise to all the endoderm. The cloning of other *mom* (more mesoderm) genes combined with RNAi experiments have elucidated a Wnt signaling pathway including the *mom-1/porcupine*, *mom-5/frizzled*, *apr-1/APC* and *wrm-1/armadillo* genes (Rocheleau et al., 1997; Thorpe et al.,

1997). In addition, the *pop-1* gene, which is defective in the specification of the mesodermal fates, was found to encode a TCF/LEF-1 transcription factor (Lin et al., 1995). Interestingly, the Wnt pathway activates TCF in *Drosophila*, whereas in *C. elegans*, Wnt signaling downregulates the TCF protein. Recent evidence indicates that a MAP-kinase pathway interacts with the Wnt pathway to downregulate POP-1 activity (Meneghini et al., 1999). The ability of MAP-kinase-related activities to modulate Wnt signaling appears to be conserved between *C. elegans* and vertebrates (Ishitani et al., 1999). The LIN-44/Wnt protein acts post-embryonically to orient asymmetric divisions of tail blast cells such as B, F, U and T (Herman and Horvitz, 1994; Herman et al., 1995; Lin et al., 1995). In *lin-44* mutants, these cells continue to divide asymmetrically, but the A/P and dorsoventral (D/V) polarities of many divisions within these lineages are reversed. The LIN-17/Frizzled protein is a candidate receptor for LIN-44 (Sawa et al., 1996). However, mutations in *lin-17* disrupt the asymmetry of these divisions rather than causing polarity reversals. In *lin-17* mutants, the B and T cells divide to generate two daughters that both adopt the anterior cell fate (Sternberg and Horvitz, 1988). One model to explain this difference in phenotypes is that another Wnt protein signals through LIN-17 in the absence of LIN-44 (Sawa et al., 1996). Alternatively, LIN-44 may be required to activate or cluster LIN-17 asymmetrically within the mother cell. In summary, *C. elegans* possesses multiple Wnt pathways that are active in a variety of different tissues.

### **Regulation of Hox gene expression**

The Hox genes, which encode homeodomain-containing transcription factors, play a major role in specifying body pattern along the A/P axis. First characterized in

insects and vertebrates, the Hox genes are organized in clusters on chromosomes and they are expressed broad stripes along the A/P axis that correspond to their domains of function (Carroll, 1995; Lawrence and Morata, 1994; McGinnis and Krumlauf, 1992). Despite its non-segmented body plan and unique mode of development that involves asymmetric embryonic cleavages and invariant cell lineages, the nematode *C. elegans* generates many position-specific structures along the A/P axis and also expresses Hox cluster genes similar to those of insects and vertebrates (Kenyon et al., 1997; Salser and Kenyon, 1994). Hox gene specificity appears to have been conserved substantially during evolution since Sex combs reduced (Scr) and Antennapedia (Antp), two *Drosophila* Hox proteins, can substitute for their *C. elegans* homologs (Hunter and Kenyon, 1995). The *C. elegans* Hox cluster consists of *ceh-13*, a *labial* homolog, *lin-39*, a *Sex combs reduced* homolog, *mab-5*, an *Antennapedia* homolog, and *egl-5*, an *Abdominal-B* homolog (Wang et al., 1993). Recently, the *C. elegans* genome sequencing project has indicated that the Hox cluster contains two additional *abd-B*-like genes (Ruvkun and Hobert, 1998).

Restricting the expression of the Hox genes to their appropriate domains is essential for normal development: lack of expression or ectopic expression of Hox genes can change the identity of one region to another. Classic examples of homeotic transformations in *Drosophila* include mutations that change antennae into legs or halteres into wings. In *C. elegans*, restriction of *mab-5* expression to the posterior is important for proper cell fate specification in the epidermal V cells. In the wild type, *mab-5* expression is limited to the posteriormost V cells. In males, this expression pattern leads to the production of sensory structures known as rays instead of cuticular



structures known as alae, which are produced by the anterior V cells. Ectopic expression of *mab-5* in the anterior causes the anterior V cells to adopt the posterior fate, generating rays instead of alae (Salser and Kenyon, 1996).

In some cases, Hox genes are expressed in dynamic patterns and must be regulated both spatially and temporally within their general domains. In *Drosophila*, the differentiation of the parasegments 5 and 6 into thoracic and abdominal morphologies, respectively, results from the dynamic pattern of *Ubx* expression in these two metameres (Castelli and Akam, 1995). In *C. elegans*, *mab-5* is switched “on” and “off” multiple times in the V5 lineage to specify three different cell fates (Salser and Kenyon, 1996). In the migrating Q neuroblasts, *mab-5* expression turns on in QL, but not QR, to specify posterior migration (Salser and Kenyon, 1992).

What mechanisms regulate Hox gene expression? In *Drosophila* embryos, maternal genes such as the homeobox gene *bicoid* act with the zygotic gap genes to set up gradients of positional information, which in turn position the expression of the pair-rule genes. Together, the gap genes and pair-rule genes initiate and refine the stripes of Hox gene expression. The post-establishment patterns of Hox gene expression are regulated by the *Polycomb (Pc)* group and *trithorax (trx)* group genes, which function to maintain transcriptional repression and activation, respectively (Lawrence and Morata, 1994; McGinnis and Krumlauf, 1992). In the visceral mesoderm of *Drosophila*, *Wg* and the TGF- $\beta$  family member, Decapentaplegic (*Dpp*), act cooperatively both to stimulate and repress *Ubx* expression (Yu et al., 1998). *Wg* also controls expression of *labial* in the inner cell layer of the midgut to specify two distinct cell types (Hoppler and Bienz, 1995).

In *C. elegans*, regulators of Hox genes include the Ras, EGF and Wnt pathways (Jiang and Sternberg, 1998; Maloof and Kenyon, 1998; Maloof et al., 1999). For example in the vulval precursor cells, the Ras signaling pathway can upregulate *lin-39* expression. *egl-5* is a downstream target of the *lin-3* EGF/*let-23* EGFR pathway in specifying the P12 neuroectoblast fate. In addition, the *egl-20/Wnt* gene and a canonical Wnt signal transduction pathway regulate expression of *mab-5* in the QL neuroblast (Harris et al., 1996; Maloof et al., 1999).

### **Cell migrations during development**

During the development of multicellular organisms, cell migrations are crucial to the establishment of organ systems such as the nervous system, respiratory system and reproductive system. The process of cell migration requires the integration of extracellular cues with intracellular responses that ultimately lead to the modulation of the actin cytoskeleton (Lauffenburger and Horwitz, 1996). A number of extracellular signals and cellular components that direct various cell migrations have been identified through a combination of *in vitro* analyses of cultured cells and classical genetic screens (Tear, 1999).

A vertebrate model for the study of cell migration is the neural crest in developing embryos. The neural crest cells emerge from the neural tube and migrate to characteristic sites within the embryo, where they subsequently differentiate into diverse cell types including neurons, pigment cells and the adrenal medulla (Bronner-Fraser, 1993). Experimental data suggest that the spatial and temporal distribution of extracellular

matrix-associated cues such as proteoglycans, fibronectin and collagen are involved in the guidance of these cells through various tissues (Perris, 1997).

The major model systems for genetic studies of cell migration in *Drosophila* are the border cells of the egg chamber, the tracheal cells of the developing tracheal system and the germ cells of the developing gonad (Montell, 1994). Visual screens for mutations that disrupt the various migrations have led to the identification of genes required for cell migration in all three systems. In border cell migrations, mutations in the *slow border cells (slbo)* gene can cause a complete failure of migration or a delayed initiation of migration. *slbo* encodes a homolog of vertebrate CCAAT enhancer binding protein (C/EBP), a basic region-leucine zipper transcription factor (Montell et al., 1992). One target of C/EBP in the control of border cell migration is the fibroblast growth factor (FGF) receptor homolog encoded by the *breathless (btl)* gene (Murphy et al., 1995). The *Drosophila* FGF pathway has also been implicated in the regulation of tracheal cell migration. In *btl* mutants, cells cannot migrate out of the tracheal pits to form the tracheal tree, a system of air-filled tubules required for respiration. The FGF homolog, Branchless (Bnl), is the putative ligand for Btl and acts as a key determinant of tracheal branch formation. For example, misexpression of *bnl* can direct branch formation and outgrowth to new positions (Sutherland et al., 1996). An extensive mutagenesis has been carried out to identify genes required for the guidance of the primordial germ cells (Moore et al., 1998). One of the genes isolated in this screen, *columbus*, encodes 3-hydroxy-3-methylglutaryl coenzyme A (HMG-CoA). This enzyme is expressed in the somatic gonad and may help to produce an attractive cue. Misexpression of HMG-CoA

reductase can attract the primordial germ cells to tissues other than the gonadal mesoderm (Van Doren et al., 1998).

Migratory cells in *C. elegans* include the sex myoblasts, the distal tip cells, the P blast cells and neurons such as HSN, CAN, BDU, QL and QR. Genes involved in the guidance of some of these migrations are homologous to guidance systems identified in other organisms, implying conservation in the control of cell movement. For example the FGF pathway, defined by EGL-17/FGF and EGL-15/FGFR, controls the migrations of the sex myoblasts (Chen and Stern, 1998). Mutations in *unc-6*, *unc-5* and *unc-40*, cause dorsal migration defects in the distal tip cells. In addition, *unc-40* mutants exhibit occasional defects in the migrations of the QL and QR descendants and in the ventral migrations of the P blast cells (Hedgecock et al., 1990). *unc-6* encodes a homolog of the vertebrate Netrin molecules, whereas *unc-5* and *unc-40/deleted in colorectal cancer* encode its putative receptors (Chan et al., 1996; Ishii et al., 1992; Leung-Hagesteijn et al., 1992). The Netrin family of guidance molecules play an important role in attracting and repelling developing axons in the vertebrate nervous system (Tear, 1999; Tessier-Lavigne and Goodman, 1996). Guidance along the A/P axis is less well understood. The *C. elegans vab-8* gene, which encodes a protein with kinesin motor similarity, functions cell-autonomously in posteriorly directed migrations (Wolf et al., 1998). Recently, the *mig-13* gene has been shown to encode a novel protein that is capable of promoting anterior migration in a cell non-autonomous manner (Sym et al., 1999). A number of genes have been isolated in screens for defective CAN and Q cell migrations (Harris et al., 1996; Forrester et al., 1998; Sym et al., unpublished data), however, a clear pathway for regulating these migrations has not yet emerged. Thus, many of the molecules

involved in guiding cell migrations remain to be identified. In addition, very little is known about how extracellular guidance molecules are transduced by their target cells to generate a migratory response.

Much of our current understanding of how the response to guidance molecules is mediated during migration come from studies of axon guidance in vertebrates and *Drosophila*. In these systems, a number of attractive and repulsive guidance cues have been identified, including the Ephrin, Netrin, Semaphorin and Slit protein families. In addition, different classes of transmembrane receptors for these signals have been identified (Seeger and Beattie, 1999; Tessier-Lavigne and Goodman, 1996). Some of these guidance cues can interact with different receptors and act as both attractants and repellents. For example, Netrin receptors of the Deleted in Colorectal Cancer (DCC) family mediate attraction, whereas receptors of the UNC5 family mediate repulsion (Keino-Masu et al., 1996; Leung-Hagesteijn et al., 1992). During the development of the nervous system, growth cones often express receptors that mediate attraction and receptors that mediate repulsion simultaneously. Yet, these growth cones are able to exhibit specific responses. Recent studies have demonstrated that the level of the transmembrane receptor is important in determining the response of the growth cone. In addition, the cytoplasmic domain of the guidance receptor can determine the response of the growth cone in vivo, independent of the ectodomain (Bashaw and Goodman, 1999; Hong et al., 1999). The mechanism by which signal transduction through the receptor impinges upon the cytoskeleton remains unknown. However, the use of different pharmacological inhibitors in a *Xenopus* axon turning assay has begun to elucidate some

of the signaling pathways required for the attractive and repulsive responses of growth cones (Song et al., 1998)

### **Polarity of asymmetric cell divisions**

Asymmetric cell divisions are a fundamental means of generating diversity during the development of both unicellular and multicellular organisms. The mechanisms by which a single cell can divide to yield two cells with different developmental potentials have been studied in a wide range of organisms (Horvitz and Herskowitz, 1992; Jan and Jan, 1998; Knoblich, 1997). Two distinct mechanisms, one involving intrinsic factors and one involving extrinsic factors, appear to be employed in the generation of diversity. Intrinsically asymmetric cell divisions create daughter cells that are different from birth. These divisions arise when cell-fate determinants within a polarized mother cell are partitioned unequally into the daughter cells. With extrinsic factors, the daughter cells are initially equivalent, but adopt different fates as a result of interactions with each other or with neighboring cells. The identification of intrinsic determinants in yeast, *Drosophila* and *C. elegans* has enabled the study of these mechanisms on a molecular level.

The budding yeast *Saccharomyces cerevisiae* displays asymmetry in the regulation of mating-type switching. Only cells that have budded previously (mother cells) possess the HO endonuclease which catalyzes the genetic recombination event that leads to mating-type switching. The newly budded cells (daughter cells) do not express the HO gene and cannot undergo mating-type switching. The Ash1 protein, a member of the GATA family of transcriptional regulators, is an intrinsic determinant for this

asymmetry. In wild-type strains, Ash1 is found only in the daughter cells, where it acts as a transcriptional repressor of *HO* (Sil and Herskowitz, 1996). The asymmetric distribution of Ash1 appears to be achieved by the localization of ASH1 mRNA to the distal tip of the budding daughter cell during mitosis (Takizawa et al., 1997).

The development of the peripheral nervous system (PNS) and central nervous system (CNS) in *Drosophila* require a number of asymmetric cell divisions (Jan and Jan, 1998; Knoblich, 1997). The external sensory (ES) organs of the PNS derive from a single sensory organ precursor (SOP) cell. The SOP cell divides into a IIA and a IIB cell. The IIA and IIB cells, in turn, undergo asymmetric divisions to generate hair and socket cells and neuron and sheath cells, respectively. A number of asymmetric factors that are required for these divisions have been identified. The membrane-associated Numb protein localizes in a crescent overlying one of the two spindle poles during mitosis. Upon division of the SOP, Numb segregates preferentially into the IIB daughter cell. Numb functions as an intrinsic cell-fate determinant because the amount of Numb is sufficient to determine the cell fate: in loss-of-function *numb* mutants, both daughter cells become IIA cells; conversely, if Numb is overexpressed, then both daughters adopt the IIB fate (Rhyu et al., 1994; Uemura et al., 1989). A similar function for Numb has been demonstrated in the CNS, where it is required for specification of the ganglion mother cell fate (Spana et al., 1995). In both the PNS and CNS, a homeobox-containing transcription factor, Prospero, colocalizes with Numb during part of the mitotic cycle and is required for proper neuronal differentiation (Knoblich et al., 1995; Vaessin et al., 1991). Miranda, a membrane protein with a predicted coiled-coil structure, appears to be required for the proper asymmetric localization of Prospero (Shen et al., 1998). The

Inscuteable (Insc) protein, which contains a putative Src homology domain and ankyrin repeats, is asymmetrically localized to the apical pole of dividing neural precursors, and is subsequently required for the localization of Numb, Miranda and Prospero to the basal pole of these cells in the CNS (Kraut and Campos-Ortega, 1996; Kraut et al., 1996). The Insc protein is thought to provide positional information for the localization of Numb, but does not localize it directly. The *partner of numb* (*pon*) gene was identified in a yeast two-hybrid screen for genes that interact with the phosphotyrosine-binding domain of Numb (Lu et al., 1998). The PON protein colocalizes with Numb in vivo and is sufficient to direct its asymmetric localization in all cell types where it is normally present. Interestingly, the control of cell fate in the *Drosophila* nervous system appears to be mediated by both intrinsic and extrinsic mechanisms. Cell-cell interaction between the SOP daughter cells mediated by the transmembrane receptor Notch is also required for the proper specification of their fates (Hartenstein and Posakony, 1990). The intrinsic determinant Numb appears to bias the Notch-mediated cell-cell interaction by inhibiting Notch activity, thereby creating an asymmetry between the daughter cells (Frise et al., 1996; Guo et al., 1996). Thus, it is possible that other signaling pathways such as the Wnt pathway may be integrated with the function of intrinsic cell fate determinants.

The invariant cell lineage of *C. elegans* consists of many asymmetric cell divisions. The HAM-1 protein has been identified as an intrinsic cell fate determinant during development of the nervous system. Like the Numb protein in *Drosophila*, the HAM-1 protein is localized asymmetrically into a crescent in the HSN/PHB precursor cell (Guenther and Garriga, 1996). Nothing is known about how HAM-1 is localized or how HAM-1 controls cell fate.



Genetic screens for embryonic-lethal mutations have identified several groups of genes that are required to establish cell polarity and orient asymmetric divisions during embryonic development. For example, the maternally expressed *par* (abnormal cytoplasmic partitioning) genes establish and maintain A/P polarity in the one-celled zygote (Bowerman, 1998). Mutations in many of the *par* genes disrupt the asymmetry of the first cell division and disrupt the asymmetric distributions of transcriptional regulators such as SKN-1 and PAL-1, which specify posterior fates. The molecular identities of all six *par* genes are known and the localization patterns of several PAR proteins have been determined (Rose and Kemphues, 1998). The PAR-3 and PAR-6 proteins colocalize at the anterior periphery of the one-cell embryo whereas PAR-1 and PAR-2 localize to the posterior periphery. Since these proteins form nonoverlapping domains in the embryo, they are thought to act by recruiting different signaling molecules to the opposite poles of asymmetrically dividing cells. However, the mechanisms by which the PAR proteins recruit downstream cell fate determinants are unclear (Rose and Kemphues, 1998). The mechanism of generating asymmetry by the *par* genes appears to be conserved in evolution. A *par-1* homolog has been identified in the mouse (*mpar-1*) and the *Drosophila bazooka* gene encodes a *par-3* homolog (Böhm et al., 1997; Kuchinke et al., 1998). Both proteins are asymmetrically localized in their respective tissues and regulate polarized cell divisions.

The *mom* genes, which define a Wnt signaling pathway (described above), are required for asymmetric divisions in the early embryo. During normal development, the EMS blastomere receives a polarizing signal from its neighbor, the P2 germline precursor (Goldstein, 1992). This Wnt signal from P2 polarizes EMS such that POP-1 activity is

downregulated in the posterior daughter of EMS, which then adopts the endoderm precursor fate. In the absence of the Wnt signal, POP-1 activity remains high in both the anterior and posterior daughters of EMS and consequently, both daughters adopt the mesoderm precursor fate (Rocheleau et al., 1997; Thorpe et al., 1997). A different Wnt signaling pathway defined by the *lin-44/Wnt* and *lin-17/frizzled* genes control asymmetric cell divisions in certain post-embryonic blast cells (described above). Unlike the previously described genes, *lin-44* is not required to create asymmetry. Instead, LIN-44 functions to establish the polarity of asymmetric cell divisions along the A/P axis. This is similar to the role of EGL-20 in the lateral epidermis. How does the LIN-44/Wnt protein generate polarity? Expressing *lin-44* under the control of a heat shock promoter is able to rescue the *lin-44(-)* mutant phenotype, raising the possibility that LIN-44 plays a permissive rather than instructive role in specifying cell polarity (Herman et al., 1995).

### **Planar polarity**

The orientation of the V cell divisions in the lateral epidermis of *C. elegans* also resembles the generation of planar polarity in vertebrate and *Drosophila* epithelia. The planar polarization of epithelial cells is essential for normal function in many tissue systems (Eaton, 1997). For example, planar polarity in reproductive tract epithelia is required for the directional transport of an ovum toward the uterus. In the vertebrate ear, specialized hair cells are oriented coordinately to maximize the ear's sensitivity to sound. In *Drosophila*, adult cuticular structures such as bristle sense organs and hairs uniformly point toward the posterior on the thorax and abdomen. Planar polarity is also evident in the uniformly oriented clusters of photoreceptor cells in the eye. The mechanisms of

AMERICAN  
LIBRARY

planar polarity specification have been studied most extensively in *Drosophila*, where several mutations affecting the orientation of bristles and ommatidia have been identified and cloned (Shulman et al., 1998). The *frizzled* (*fz*) gene, which encodes a seven transmembrane receptor (Adler et al., 1990; Park et al., 1994), was first identified for its role in planar polarity. Subsequently, *frizzled* homologs have been found in many organisms, where they have been proposed to function as receptors for Wnt signaling molecules (described above). However, the ligand for Fz in specifying planar polarity remains unknown. Mutations in two *Drosophila* Wnt genes, *wg* and *Dwnt-2*, do not exhibit any polarity defects. Interestingly, both the Wg and Fz signaling pathways require *dishevelled* (*dsh*) activity, but diverge in the more downstream factors. In the planar polarity signaling pathway, Dsh is thought to act through small GTPases such as RhoA and the Jun-N-terminal kinase (JNK) subfamily of MAPK pathways (Boutros et al., 1998; Strutt et al., 1997).

## OVERVIEW

Chapter 2 describes the cloning of *egl-20*. In addition to demonstrating transformation rescue of the *egl-20(-)* mutant phenotypes with a transgene encoding a Wnt homolog, I sequenced several *egl-20* mutant alleles and identified molecular lesions in conserved residues of the predicted Wnt protein. These sequences reveal that the different functions of EGL-20 can be mutated separately.

Chapter 3 examines the mechanism by which EGL-20 promotes opposite migratory behaviors in the QL and QR lineages. A genomic *egl-20* transgene tagged with *gfp* reveals that *egl-20* is expressed in a group of epidermal and muscle cells in the

tail region. I tested whether the left-right asymmetric expression of *mab-5* in the Q cells was dependent on the posterior localization of EGL-20. By misexpressing *egl-20* in the anterior body region, I demonstrated that EGL-20 does not act as a positional signal for the specification of different migratory fates in the QL and QR lineages. Instead, EGL-20 acts through distinct signaling thresholds. High levels of EGL-20 promote posterior migration by activating a canonical Wnt signal-transduction pathway, whereas low levels promote anterior migration by activating a separate, undefined pathway. Furthermore, the two Q cells respond differently to EGL-20 because they have different response thresholds. This Wnt system differs from previously described systems because the distinct dose-dependent responses are specified not by graded levels of the Wnt signal, but instead by left-right asymmetrical differences in the cellular responsiveness to Wnt signaling.

Chapter 4 describes characterization of the V5 polarity reversals in *egl-20* mutants. Together with Jeanne Harris, I showed that the orientation of the V5 cell division requires the *egl-20* and *mig-14* genes, but does not require any of the other known components of the EGL-20 signal transduction pathway for *mab-5* activation in the QL neuroblast. By performing cell ablation experiments, we showed that signals from adjacent V cells can influence the polarity of the V5 cell division in *egl-20(-)*, but not wild-type animals. In addition, we found that mutations in *lin-17*, a *C. elegans* *frizzled* homolog, can suppress the V5 polarity reversal defect of *egl-20* mutants. This suggests that *lin-17* might mediate the signaling pathway that causes polarity reversals in *egl-20* mutants. Misexpression of *egl-20* in the anterior body region indicates that EGL-20 is permissive, rather than instructive in establishing V5 polarity. Using a heat shock-

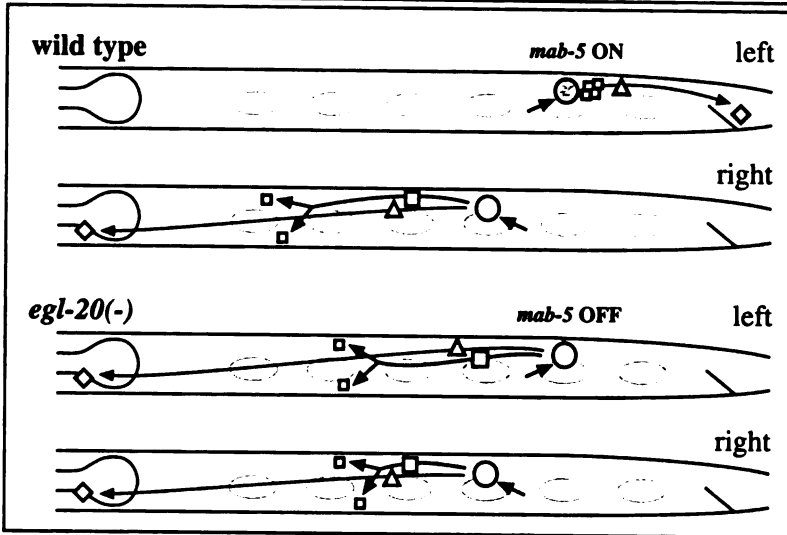
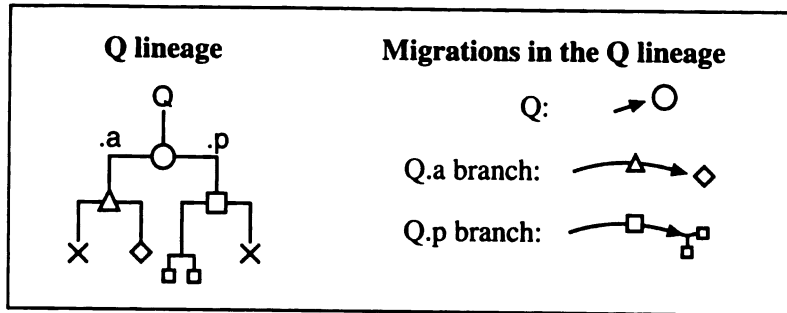
*egl-20* fusion transgene, I determined that relatively low levels of *hs-egl-20* can rescue the V5 polarity defect of *egl-20* mutants, whereas relatively high levels of *hs-egl-20* cause ectopic polarity defects in all the V cell lineages. Although mutations in *lin-17* do not suppress these ectopic polarity defects, mutations in *mig-14* completely suppress the effects of *hs-egl-20*. EGL-20::GFP localization appears to be altered in a *mig-14* mutant background, suggesting that *mig-14* might be responsible for the secretion or processing of the EGL-20 signal. Finally, I demonstrated that *egl-20* can functionally replace *lin-44*, another *C. elegans* Wnt homolog required for the orientation of asymmetric cell divisions. Together these experiments indicate that the regulation of polarity in a single cell division is complex and involves several different signaling systems. The misexpression and heat shock experiments show that the V5 cell does not receive A/P polarity information directly from EGL-20, but rather from a yet unidentified system.

## CONCLUSIONS

In summary, the molecular and phenotypic characterization of *egl-20* has provided insights into several fundamental topics of developmental biology. For example, mechanisms that regulate Hox gene expression, anterior cell migration and cell polarity have been elucidated by altering the location and levels of EGL-20 in vivo. In addition, the cloning of *egl-20* has revealed a new function for the highly conserved Wnt pathway in the guidance of migrating cells. Part of Chapter 2 originally appeared as “A Wnt signaling pathway controls Hox gene expression and neuroblast migration in *C. elegans*” in *Development* 126, 37-49 (1999), Chapter 3 has been submitted to *Molecular Cell*; Chapter 4 is being prepared for submission to *Development*.

RECEIVED  
MAY 17 2001

***egl-20* promotes posterior migration in the QL lineage and anterior migration in the QR lineage**



***egl-20* is required to establish wild-type polarity of the V5-cell division**

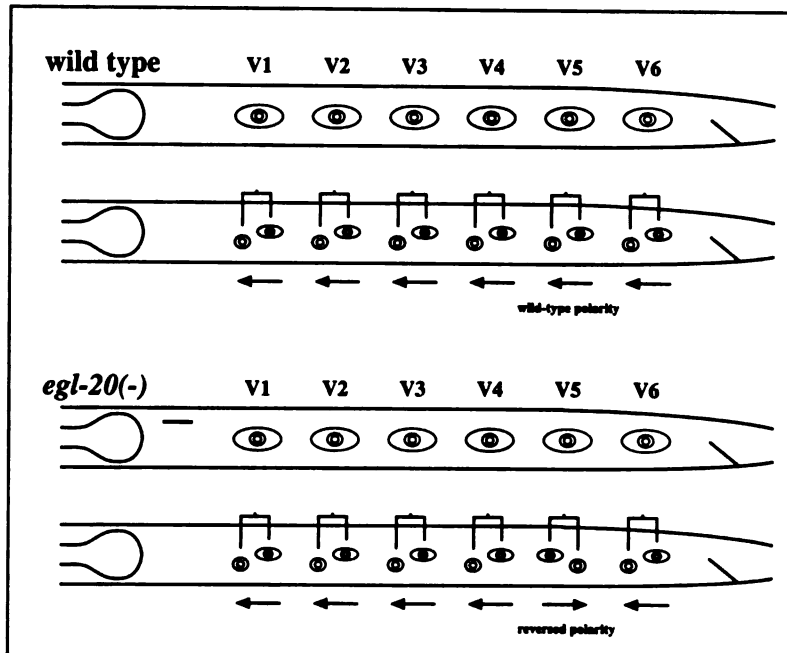


**Figure 1.1.** A summary of the *egl-20*(-) phenotypes.

## **REFERENCES**

- Adler, P. N., Vinson, C., Park, W. J., Conover, S., and Klein, L. (1990). Molecular structure of frizzled, a *Drosophila* tissue polarity gene. *Genetics* *126*, 401-16.
- Bashaw, G. and Goodman, C. (1999). Chimeric axon guidance receptors: the cytoplasmic domains of slit and netrin receptors specify attraction versus repulsion. *Cell* *97*, 917-926.
- Bejsovec, A., and Wieschaus, E. (1995). Signaling activities of the *Drosophila* wingless gene are separately mutable and appear to be transduced at the cell surface. *Genetics* *139*, 309-20.
- Bhanot, P., Brink, M., Samos, C. H., Hsieh, J., Wang, Y., Macke, J. P., Andrew, D., Nathans, J., and Nusse, R. (1996). A new member of the frizzled family from *Drosophila* functions as a Wingless receptor. *Nature* *382*, 225-30.
- Boutros, M., Paricio, N., Strutt, D. I., and Mlodzik, M. (1998). Dishevelled activates JNK and discriminates between JNK pathways in planar polarity and wingless signaling. *Cell* *94*, 109-18.
- Bowerman, B. (1998). Maternal control of pattern formation in early *Caenorhabditis elegans* embryos. *Current Topics in Developmental Biology* *39*, 73-117.
- Bronner-Fraser, M. (1993). Mechanisms of neural crest cell migration. *Bioessays* *15*, 221-30.
- Cadigan, K. M., and Nusse, R. (1997). Wnt signaling: a common theme in animal development. *Genes and Development* *11*, 3286-305.
- Carroll, S. B. (1995). Homeotic genes and the evolution of arthropods and chordates. *Nature* *376*, 479-85.

Castelli, G. J., and Akam, M. (1995). How the Hox gene Ultrabithorax specifies two different segments: the significance of spatial and temporal regulation within metameres. *Development* *121*, 2973-82.

Chan, S. S., Zheng, H., Su, M. W., Wilk, R., Killeen, M. T., Hedgecock, E. M., and Culotti, J. G. (1996). UNC-40, a *C. elegans* homolog of DCC (Deleted in Colorectal Cancer), is required in motile cells responding to UNC-6 netrin cues. *Cell* *87*, 187-95.

Chen, E. B., and Stern, M. J. (1998). Understanding cell migration guidance: lessons from sex myoblast migration in *C. elegans*. *Trends in Genetics* *14*, 322-7.

Du, S. J., Purcell, S. M., Christian, J. L., McGrew, L. L., and Moon, R. T. (1995). Identification of distinct classes and functional domains of Wnts through expression of wild-type and chimeric proteins in *Xenopus* embryos. *Molecular and Cellular Biology* *15*, 2625-34.

Eaton, S. (1997). Planar polarization of *Drosophila* and vertebrate epithelia. *Current Opinion in Cell Biology* *9*, 860-6.

Forrester, W. C., Perens, E., Zallen, J. A., and Garriga, G. (1998). Identification of *Caenorhabditis elegans* genes required for neuronal differentiation and migration. *Genetics* *148*, 151-65.

Frise, E., Knoblich, J. A., Younger-Shepherd, S., Jan, L. Y., and Jan, Y. N. (1996). The *Drosophila* Numb protein inhibits signaling of the Notch receptor during cell-cell interaction in sensory organ lineage. *Proceedings of the National Academy of Sciences of the United States of America* *93*, 11925-32.

Goldstein, B. (1992). Induction of gut in *Caenorhabditis elegans* embryos. *Nature* *357*, 255-7.

LIBRARY  
UNIVERSITY OF  
MICHIGAN



Guenther, C., and Garriga, G. (1996). Asymmetric distribution of the *C. elegans* HAM-1 protein in neuroblasts enables daughter cells to adopt distinct fates. *Development* 122, 3509-18.

Guo, M., Jan, L. Y., and Jan, Y. N. (1996). Control of daughter cell fates during asymmetric division: interaction of Numb and Notch. *Neuron* 17, 27-41.

Hacohen, N., Kramer, S., Sutherland, D., Hiromi, Y., and Krasnow, M. A. (1998). sprouty encodes a novel antagonist of FGF signaling that patterns apical branching of the *Drosophila* airways. *Cell* 92, 253-63.

Harris, J., Honigberg, L., Robinson, N., and Kenyon, C. (1996). Neuronal cell migration in *C. elegans*: regulation of Hox gene expression and cell position. *Development* 122, 3117-31.

Hartenstein, V., and Posakony, J. W. (1990). A dual function of the Notch gene in *Drosophila* sensillum development. *Developmental Biology* 142, 13-30.

Hedgecock, E. M., Culotti, J. G., and Hall, D. H. (1990). The *unc-5*, *unc-6*, and *unc-40* genes guide circumferential migrations of pioneer axons and mesodermal cells on the epidermis in *C. elegans*. *Neuron* 4, 61-85.

Herman, M. A., and Horvitz, H. R. (1994). The *Caenorhabditis elegans* gene *lin-44* controls the polarity of asymmetric cell divisions. *Development* 120, 1035-47.

Herman, M. A., Vassilieva, L. L., Horvitz, H. R., Shaw, J. E., and Herman, R. K. (1995). The *C. elegans* gene *lin-44*, which controls the polarity of certain asymmetric cell divisions, encodes a Wnt protein and acts cell nonautonomously. *Cell* 83, 101-10.

Hong, K., Hinck, L., Nishiyama, M., Poo, M., Tessier-Lavigne, M., and Stein, E. (1999). A ligand-gated association between cytoplasmic domains of UNC5 and DCC family receptors converts netrin-induced growth cone attraction to repulsion. *Cell* 97, 927-941.

Hoppler, S., and Bienz, M. (1995). Two different thresholds of wingless signalling with distinct developmental consequences in the *Drosophila* midgut. *Embo J* 14, 5016-26.

Horvitz, H. R., and Herskowitz, I. (1992). Mechanisms of asymmetric cell division: two Bs or not two Bs, that is the question. *Cell* 68, 237-55.

Hunter, C. P., and Kenyon, C. (1995). Specification of anteroposterior cell fates in *Caenorhabditis elegans* by *Drosophila* Hox proteins. *Nature* 377, 229-32.

Ishii, N., Wadsworth, W. G., Stern, B. D., Culotti, J. G., and Hedgecock, E. M. (1992). UNC-6, a laminin-related protein, guides cell and pioneer axon migrations in *C. elegans*. *Neuron* 9, 873-81.

Ishitani, T., Ninomiya-Tsuji, J., Nagai, S., Nishita, M., Meneghini, M., Barker, N., Waterman, M., Bowerman, B., Clevers, H., Shibuya, H., Matsumoto, K. (1999). The TAK1-NLK-MAPK-related pathway antagonizes signalling between beta-catenin and transcription factor TCF. *Nature* 399, 798-802.

Jan, Y. N., and Jan, L. Y. (1998). Asymmetric cell division. *Nature* 392, 775-8.

Jiang, L. I., and Sternberg, P. W. (1998). Interactions of EGF, Wnt and HOM-C genes specify the P12 neuroectoblast fate in *C. elegans*. *Development* 125, 2337-47.

Kamb, A., Weir, M., Rudy, B., Varmus, H., and Kenyon C. (1989). Identification of genes from pattern formation, tyrosine kinase, and potassium channel families by DNA amplification. *Proc. Natl. Acad. Sci. USA* 86, 4372-4376.

Keino-Masu, K., Masu, M., Hinck, L., Leonardo, E. D., Chan, S. S., Culotti, J. G., and Tessier-Lavigne, M. (1996). Deleted in Colorectal Cancer (DCC) encodes a netrin receptor. *Cell* 87, 175-85.

Kenyon, C. J., Austin, J., Costa, M., Cowing, D. W., Harris, J. M., Honigberg, L., Hunter, C. P., Maloof, J. N., Muller-Immerglück, M. M., Salser, S. J., Waring, D. A., Wang, B. B., and Wrischnik, L. A. (1997). The dance of the Hox genes: patterning the anteroposterior body axis of *Caenorhabditis elegans*. *Cold Spring Harbor Symposia on Quantitative Biology* 62, 293-305.

Knoblich, J. A. (1997). Mechanisms of asymmetric cell division during animal development. *Current Opinion in Cell Biology* 9, 833-41.

Knoblich, J. A., Jan, L. Y., and Jan, Y. N. (1995). Asymmetric segregation of Numb and Prospero during cell division. *Nature* 377, 624-7.

Kraut, R., and Campos-Ortega, J. A. (1996). *inscuteable*, a neural precursor gene of *Drosophila*, encodes a candidate for a cytoskeleton adaptor protein. *Developmental Biology* 174, 65-81.

Kraut, R., Chia, W., Jan, L. Y., Jan, Y. N., and Knoblich, J. A. (1996). Role of *inscuteable* in orienting asymmetric cell divisions in *Drosophila*. *Nature* 383, 50-5.

Lauffenburger, D. A., and Horwitz, A. F. (1996). Cell migration: a physically integrated molecular process. *Cell* 84, 359-69.

Lawrence, P. A., and Morata, G. (1994). Homeobox genes: their function in *Drosophila* segmentation and pattern formation. *Cell* 78, 181-9.

Lecuit, T., and Cohen, S. M. (1997). Proximal-distal axis formation in the *Drosophila* leg. *Nature* 388, 139-45.

Leung-Hagesteijn, C., Spence, A. M., Stern, B. D., Zhou, Y., Su, M. W., Hedgecock, E. M., and Culotti, J. G. (1992). UNC-5, a transmembrane protein with immunoglobulin and thrombospondin type 1 domains, guides cell and pioneer axon migrations in *C. elegans*. *Cell* *71*, 289-99.

Lin, R., Thompson, S., and Priess, J. R. (1995). pop-1 encodes an HMG box protein required for the specification of a mesoderm precursor in early *C. elegans* embryos. *Cell* *83*, 599-609.

Lin, X. and Perrimon, N. (1999). Dally cooperates with *Drosophila* Frizzled2 to transduce Wingless signalling. *Nature* *400*, 281-284.

Maloof, J. N., and Kenyon, C. (1998). The Hox gene *lin-39* is required during *C. elegans* vulval induction to select the outcome of Ras signaling. *Development* *125*, 181-90.

Maloof, J. N., Whangbo, J., Harris, J. M., Jongeward, G. D., and Kenyon, C. (1999). A Wnt signaling pathway controls hox gene expression and neuroblast migration in *C. elegans*. *Development* *126*, 37-49.

McGinnis, W., and Krumlauf, R. (1992). Homeobox genes and axial patterning. *Cell* *68*, 283-302.

Meneghini, M.D., Ishitani, T., Carter, J.C., Hisamoto, N., Ninomiya-Tsuji, J., Thorpe, C.J., Hamill, D.R., Matsumoto, K., Bowerman, B. (1999). MAP kinase and Wnt pathways converge to downregulate an HMG-domain repressor in *Caenorhabditis elegans*. *Nature* *399*, 793-7.

Montell, D. J. (1994). Moving right along: regulation of cell migration during *Drosophila* development. *Trends in Genetics* *10*, 59-62.

Montell, D. J., Rorth, P., and Spradling, A. C. (1992). slow border cells, a locus required for a developmentally regulated cell migration during oogenesis, encodes *Drosophila* C/EBP. *Cell* 71, 51-62.

Moore, L. A., Broihier, H. T., Van Doren, M., Lunsford, L. B., and Lehmann, R. (1998). Identification of genes controlling germ cell migration and embryonic gonad formation in *Drosophila*. *Development* 125, 667-78.

Murphy, A. M., Lee, T., Andrews, C. M., Shilo, B. Z., and Montell, D. J. (1995). The breathless FGF receptor homolog, a downstream target of *Drosophila* C/EBP in the developmental control of cell migration. *Development* 121, 2255-63.

Neumann, C. J., and Cohen, S. M. (1997). Long-range action of Wingless organizes the dorsal-ventral axis of the *Drosophila* wing. *Development* 124, 871-80.

Nusse, R., and Varmus, H. E. (1992). Wnt genes. *Cell* 69, 1073-87.

Park, W. J., Liu, J., and Adler, P. N. (1994). The frizzled gene of *Drosophila* encodes a membrane protein with an odd number of transmembrane domains. *Mechanisms of Development* 45, 127-37.

Perris, R. (1997). The extracellular matrix in neural crest-cell migration. *Trends in Neurosciences* 20, 23-31.

Rhyu, M. S., Jan, L. Y., and Jan, Y. N. (1994). Asymmetric distribution of numb protein during division of the sensory organ precursor cell confers distinct fates to daughter cells [see comments]. *Cell* 76, 477-91.

Rocheleau, C. E., Downs, W. D., Lin, R., Wittmann, C., Bei, Y., Cha, Y. H., Ali, M., Priess, J. R., and Mello, C. C. (1997). Wnt signaling and an APC-related gene specify endoderm in early *C. elegans* embryos [see comments]. *Cell* 90, 707-16.

Ruvkun, G., and Hobert, O. (1998). The taxonomy of developmental control in *Caenorhabditis elegans* [see comments]. *Science* 282, 2033-41.

Salser, S. J., and Kenyon, C. (1992). Activation of a *C. elegans* Antennapedia homologue in migrating cells controls their direction of migration. *Nature* 355, 255-8.

Salser, S. J., and Kenyon, C. (1996). A *C. elegans* Hox gene switches on, off, on and off again to regulate proliferation, differentiation and morphogenesis. *Development* 122, 1651-61.

Salser, S. J., and Kenyon, C. (1994). Patterning *C. elegans*: homeotic cluster genes, cell fates and cell migrations. *Trends Genet* 10, 159-64.

Sawa, H., Lobel, L., and Horvitz, H. R. (1996). The *Caenorhabditis elegans* gene *lin-17*, which is required for certain asymmetric cell divisions, encodes a putative seven-transmembrane protein similar to the *Drosophila* frizzled protein. *Genes and Development* 10, 2189-97.

Seeger, M. and Beattie, C. (1999). Attraction versus repulsion: modular receptors make the difference in axon guidance. *Cell* 97, 821-824.

Shackleford, G. M., Shivakumar, S., Shiue, L., Mason, J., Kenyon, C., and Varmus, H. E. (1993). Two *wnt* genes in *Caenorhabditis elegans*. *Oncogene* 8, 1857-64.

Shen, C. P., Knoblich, J. A., Chan, Y. M., Jiang, M. M., Jan, L. Y., and Jan, Y. N. (1998). Miranda as a multidomain adapter linking apically localized Inscuteable and basally localized Staufin and Prospero during asymmetric cell division in *Drosophila*. *Genes and Development* 12, 1837-46.

Shivakumar, S. (1996). Wnt genes and their role in *Caenorhabditis elegans* development. Ph.D. Thesis, University of California-San Francisco.

Shulman, J. M., Perrimon, N., and Axelrod, J. D. (1998). Frizzled signaling and the developmental control of cell polarity. *Trends in Genetics* 14, 452-8.

Sil, A., and Herskowitz, I. (1996). Identification of asymmetrically localized determinant, Ash1p, required for lineage-specific transcription of the yeast HO gene [see comments]. *Cell* 84, 711-22.

Song, H., Ming, G., He, Z., Lehmann, M., Tessier-Lavigne, M., and Poo, M. (1998). Conversion of neuronal growth cone responses from repulsion to attraction by cyclic nucleotides [see comments]. *Science* 281, 1515-8.

Spana, E. P., Kopczynski, C., Goodman, C. S., and Doe, C. Q. (1995). Asymmetric localization of numb autonomously determines sibling neuron identity in the *Drosophila* CNS. *Development* 121, 3489-94.

Sternberg, P. W., and Horvitz, H. R. (1988). lin-17 mutations of *Caenorhabditis elegans* disrupt certain asymmetric cell divisions. *Developmental Biology* 130, 67-73.

Strutt, D. I., Weber, U., and Mlodzik, M. (1997). The role of RhoA in tissue polarity and Frizzled signalling. *Nature* 387, 292-5.

Sutherland, D., Samakovlis, C., and Krasnow, M. A. (1996). branchless encodes a *Drosophila* FGF homolog that controls tracheal cell migration and the pattern of branching. *Cell* 87, 1091-101.

Sym, M., Robinson, N., and Kenyon, C. (1999). MIG-13 positions migrating cells along the anteroposterior body axis of *C. elegans*. *Cell* 98, 25-36.

Takizawa, P. A., Sil, A., Swedlow, J. R., Herskowitz, I., and Vale, R. D. (1997). Actin-dependent localization of an RNA encoding a cell-fate determinant in yeast. *Nature* 389, 90-3.

Tear, G. (1999). Neuronal guidance. A genetic perspective. *Trends in Genetics* 15, 113-8.

Tessier-Lavigne, M., and Goodman, C. S. (1996). The molecular biology of axon guidance. *Science* 274, 1123-33.

Thorpe, C. J., Schlesinger, A., Carter, J. C., and Bowerman, B. (1997). Wnt signaling polarizes an early *C. elegans* blastomere to distinguish endoderm from mesoderm [see comments]. *Cell* 90, 695-705.

Uemura, T., Shepherd, S., Ackerman, L., Jan, L. Y., and Jan, Y. N. (1989). numb, a gene required in determination of cell fate during sensory organ formation in *Drosophila* embryos. *Cell* 58, 349-60.

Vaessin, H., Grell, E., Wolff, E., Bier, E., Jan, L. Y., and Jan, Y. N. (1991). prospero is expressed in neuronal precursors and encodes a nuclear protein that is involved in the control of axonal outgrowth in *Drosophila*. *Cell* 67, 941-53.

van den Heuvel, M., Nusse, R., Johnston, P., and Lawrence, P. A. (1989). Distribution of the wingless gene product in *Drosophila* embryos: a protein involved in cell-cell communication. *Cell* 59, 739-49.

Van Doren, M., Broihier, H. T., Moore, L. A., and Lehmann, R. (1998). HMG-CoA reductase guides migrating primordial germ cells [see comments]. *Nature* 396, 466-9.

Wang, B. B., Muller, I. M., Austin, J., Robinson, N. T., Chisholm, A., and Kenyon, C. (1993). A homeotic gene cluster patterns the anteroposterior body axis of *C. elegans*. *Cell* 74, 29-42.

LIBRARY  
UNIVERSITY OF  
MICHIGAN



Wolf, F. W., Hung, M. S., Wightman, B., Way, J., and Garriga, G. (1998). *vab-8* is a key regulator of posteriorly directed migrations in *C. elegans* and encodes a novel protein with kinesin motor similarity. *Neuron* 20, 655-66.

Yu, X., Riese, J., Eresh, S., and Bienz, M. (1998). Transcriptional repression due to high levels of Wingless signalling. *Embo Journal* 17, 7021-32.

Zecca, M., Basler, K., and Struhl, G. (1996). Direct and long-range action of a wingless morphogen gradient. *Cell* 87, 833-44.

## **Chapter 2: *egl-20*, a Gene Involved in Anteroposterior Patterning, Encodes a Wnt Homolog**

### **SUMMARY**

The *egl-20* gene functions in diverse anteroposterior (A/P) migration and patterning events during the postembryonic development of *C. elegans*. *egl-20* activity is required to activate expression of the Hox gene *mab-5* within the QL neuroblast, which in turn programs the posterior migrations of the QL descendants. *egl-20* activity is also required for anterior migrations of the QR. Furthermore, *egl-20* is involved in the orientation of asymmetric cell divisions in the epidermal V cell lineages. To begin understanding the molecular function of EGL-20, we cloned the *egl-20* gene. Together with Jeanne Harris and Gregg Jongeward, I have determined that *egl-20* encodes a member of the Wnt family of secreted glycoproteins. In addition, I have identified the molecular lesions associated with several alleles of *egl-20*.

### **INTRODUCTION**

The first *egl-20* mutant was isolated in a screen for egg-laying defective mutants that were altered in the functioning or development of the neural components of the egg-laying system (Trent et al., 1983). *egl-20* was shown to affect migration of the hermaphrodite-specific neurons (HSNs), which provide direct synaptic inputs to the vulval and uterine muscles (Desai et al., 1988). Several years later, our lab isolated *egl-20* in a screen using Nomarski optics to visualize animals with misplaced Q descendants (Harris et al., 1996). Subsequently, Jeanne Harris characterized the migration defects of

the QL and QR descendants in *egl-20* animals. She showed that the QL descendants migrate anteriorly rather than posteriorly in *egl-20* mutants because of a failure to activate the Hox gene *mab-5* in QL and its descendants. In addition, she observed that *egl-20* mutants are defective in the anterior migration of the QR descendants: these cells stop prematurely and are found in positions posterior to the wild-type stopping points. Analysis of *egl-20* in combination with other mutations indicated that this phenotype was not due to a defect in motility, but rather a defect in guidance. Jeanne Harris also observed that *egl-20* mutants are defective in the orientation of the asymmetric V5 cell divisions along the A/P body axis. To understand the molecular basis for these defects in *egl-20* mutants, Jeanne Harris initiated the cloning of the *egl-20* gene. Gregg Jongeward narrowed down the *egl-20* rescuing activity to a region of LG IV spanned by three cosmids. Here I report that the *egl-20* gene encodes a member of the Wnt family of secreted signaling molecules. In addition, I have identified new *egl-20* alleles from a screen for mutants with defective Q cell migrations carried out by Mary Sym and Queelim Ch'ng (unpublished results). I have determined the molecular lesions associated with 7 of the 18 known *egl-20* alleles.

## RESULTS

### ***egl-20* encodes a Wnt family member**

We cloned the *egl-20* gene by positional mapping and transformation rescue (see Materials and Methods). A single cosmid, W08D2, was found to rescue the *egl-20(n585)* egg-laying and Q cell migration defects. This cosmid was located in a sequenced region of the genome, and was found to contain an open reading frame (ORF) predicted to

RESEARCH ARTICLE

encode a Wnt family member. We found that several W08D2 subclones, including a 6.3 kb HindIII fragment containing this Wnt gene as the only complete ORF, also rescued the *egl-20(n585)* mutant phenotypes (Figure 2.1).

Wnt genes encode secreted signaling molecules that regulate diverse developmental processes in a wide range of species (Cadigan and Nusse, 1997). Like other Wnt family members, EGL-20 possesses a hydrophobic region at the N-terminus that could serve as a signal sequence (von Heijne, 1986). In addition, the predicted EGL-20 protein has three potential sites for N-linked glycosylation and contains 24 highly conserved cysteine residues (Figure 2.2a). Comparison of the predicted EGL-20 protein sequence with other members of the Wnt family shows that EGL-20 shares the greatest identity with mouse Wnt-7B (47% amino acid identity) and mouse Wnt-7A (35% amino acid identity) (Gavin et al., 1990) (Figure 2.2b).

### **Isolation of new *egl-20* alleles**

Additional *egl-20* mutations were isolated in a screen for misplaced Q cell descendants using a *mec-7::gfp* fusion, which labels a number of neurons including the two Q cell descendants AVM (QR.paa) and PVM (QL.paa) (Mary Sym et al., unpublished data). Candidate *egl-20* alleles were identified initially by the presence of V5 polarity reversals or by the presence of QR descendants whose final positions were shifted posteriorly relative to wild type (Table 2.1). These candidate alleles were then tested for noncomplementation to *egl-20(n585)* (see Materials and Methods).

W08D2

## Molecular lesions associated with *egl-20* alleles

To identify molecular lesions in 7 of 18 existing *egl-20* alleles, I amplified genomic DNA from mutant animals by PCR and determined the sequences of the coding regions and the splice junctions (Table 2.1). The *mu320* allele contains an opal mutation located in the second exon of *egl-20*. The predicted *mu320* protein product has only 48 amino acids in addition to the presumptive signal sequence and thus may be a null allele. The *mu241* allele changes an invariant splice-donor GT sequence to AT in the second intron. The strong reduction-of-function allele, *n585*, is associated with a T-to-A transversion at nucleotide 295, changing a highly conserved cysteine at position 99 to a serine. The less severe allele, *mu25*, is associated with a G-to-A transition at nucleotide 329, changing a highly conserved cysteine at position 110 to tyrosine. Similarly, the weak hypomorphic allele, *mu39*, is associated with a G-to-A transition at nucleotide 497, which changes a highly conserved cysteine at position 166 to tyrosine. The *mu234* allele is associated with A-to-G transition at nucleotide 100, changing an asparagine at position 34 to aspartate. I could not amplify the complete genomic sequence from *egl-20(n1437)* animals. However, I obtained the *n1437* cDNA by RT-PCR using *egl-20* specific primers. The predicted *n1437* protein product contains a deletion of amino acids 287 to 323 near the carboxy terminus of EGL-20. It will be necessary to perform Southern blot analysis to determine the nature of this deletion.

## DISCUSSION

Previous work from our laboratory showed that the *egl-20/Wnt*, *lin-17/frizzled* (Sawa et al., 1996) and *bar-1/armadillo* (Eisenmann et al., 1998) genes are required to activate *mab-5* expression in QL (Harris et al., 1996; Maloof et al., 1999). In addition, the *mig-5* gene has been reported to encode a homolog of the Wnt pathway member *dishevelled*, and to have a QL migration defect similar to that of *mab-5* mutants (Guo, 1995). These findings indicate that a Wnt signaling pathway, with components conserved from the Wnt signal to an *armadillo*-related transactivator, functions to control the direction of Q cell migration by regulating *mab-5* expression.

*egl-20*, *lin-17* and *bar-1* mutants have some phenotypes in common, but they do not overlap completely. For example, *egl-20* and *lin-17* mutants are defective in the migration of the HSN neuron, whereas *bar-1* mutants are wild-type for this migration (Harris et al., 1996; data not shown). This observation raises the possibility that *egl-20* may use different signal transduction pathways for its functions in different cell types. Interestingly, the different functions of *egl-20* can be mutated separately (Table 2.1). Thus the EGL-20 protein might interact with multiple downstream components via different domains. In support of this concept, analyses of *wingless* alleles in *Drosophila* have suggested the presence of functional domains in the Wg protein that have different signaling activities (Bejsovec and Wieschaus, 1995).

The cloning of *egl-20* enabled me to proceed with a molecular analysis of how the Q descendants direct their migrations and how the V5 cell orients its division along the A/P axis. The next two chapters describe progress toward understanding how the EGL-

20/Wnt protein controls neuronal migrations and the polarity of an asymmetric cell division.

## MATERIALS AND METHODS

### General Methods and Strains

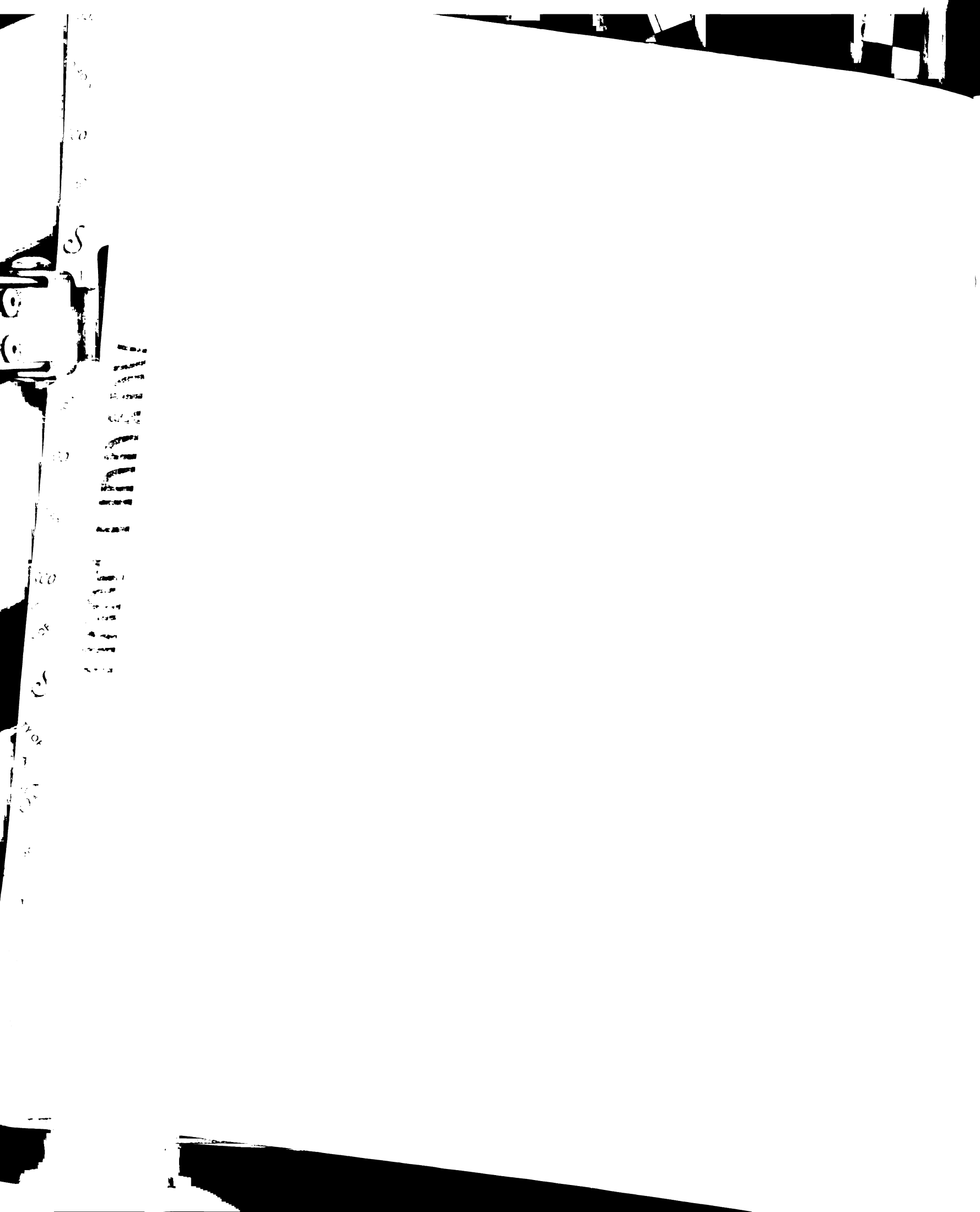
Strains were maintained using standard methods (Brenner, 1974; Wood, 1988). Unless otherwise noted, strains were maintained and analyzed at 25°C. The mutant alleles used are either described by this paper, described by Wood (1988), or referenced below.

Mutations used:

LGIV: *egl-20(n585)*, *egl-20(n1437)*, *egl-20(mu27)*, *egl-20(mu25)*, *egl-20(mu39)* (Trent et al., 1983; Harris et al., 1996), *egl-20(mu241)*, *egl-20(mu320)*.

### Cloning of *egl-20*

The *egl-20* gene was previously localized to the gene cluster on Linkage Group IV between the cloned genes *fem-3* and *mec-3* (Trent et al., 1983; Harris et al., 1996). Using restriction fragment length polymorphisms in the region between *fem-3* and *mec-3*, we mapped *egl-20* to an interval covered by the cosmids from C28D4 to ZZH8. We generated transgenic lines of these candidate cosmids by germline transformation using pPD10.46 (*unc-22* anti-sense) as the coinjection marker (Mello et al., 1991) and scored the lines for their ability to rescue both the QL migration and egg-laying defects caused by the *egl-20(n585)* mutation. A single cosmid located in this interval, W07H7, rescued the *egl-20(n585)* mutant phenotypes. Subsequently, the cosmid W07H7 was found to be

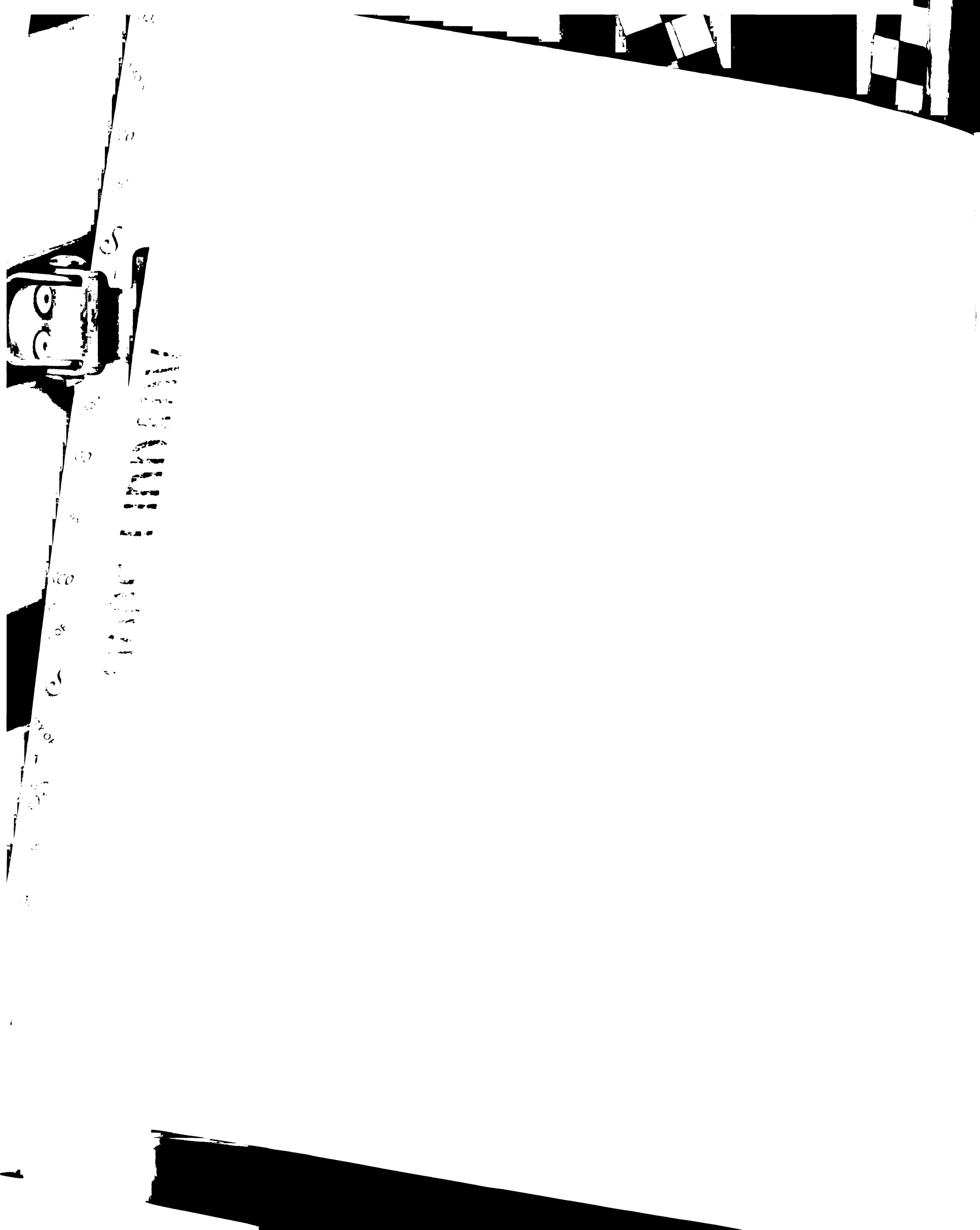




identical by restriction digest pattern to the cosmid W08D2, which had been sequenced by the *C. elegans* Genome Sequencing Project. One of the predicted open reading frames (ORFs) on the cosmid W08D2 (W08D2.1) was homologous to the Wnt family of signaling molecules. A 6.3 kb HindIII fragment of the cosmid W08D2 (pJW12), containing the entire predicted *Wnt* gene, was subcloned into the LITMUS38 vector (New England Biolabs). Transgenic lines carrying pJW12 in an *egl-20(n585)* background exhibited wild-type egg-laying and QL migration. We subsequently obtained the *egl-20* cDNA by RT-PCR from mixed-stage N2 RNA. We first synthesized cDNA templates using an oligo dT primer, Q<sub>T</sub> (Frohman, 1993). We then amplified the *egl-20* cDNA by using the *egl-20* specific primers, JW28: 5'-CCGGGGCCCCGCTAGCATGCAATTTTTCATTTGC-3' and JW29: 5'-CCGGAGCTCCTGCAGTTTGCATGTATGTACTGC-3'. We obtained a single 1.2 kb product, which was subcloned into the pCRII vector (Invitrogen) and sequenced. My sequence analysis showed that Genefinder mispredicted the 5' splice site of the 7<sup>th</sup> intron. The actual splice site occurs at nucleotide 1512 of the *egl-20* genomic DNA sequence instead of nucleotide 1527. This difference shortens the predicted EGL-20 protein by five amino acids.

### **Complementation tests to identify new *egl-20* alleles**

Candidate *egl-20* alleles were first mated with *dpy-20(e1282); him-5(e1490)* males. The *dpy-20* mutation serves as a linked marker for *egl-20*. The male progeny from this cross, which were heterozygous for the putative *egl-20* mutation, were then mated with *egl-*

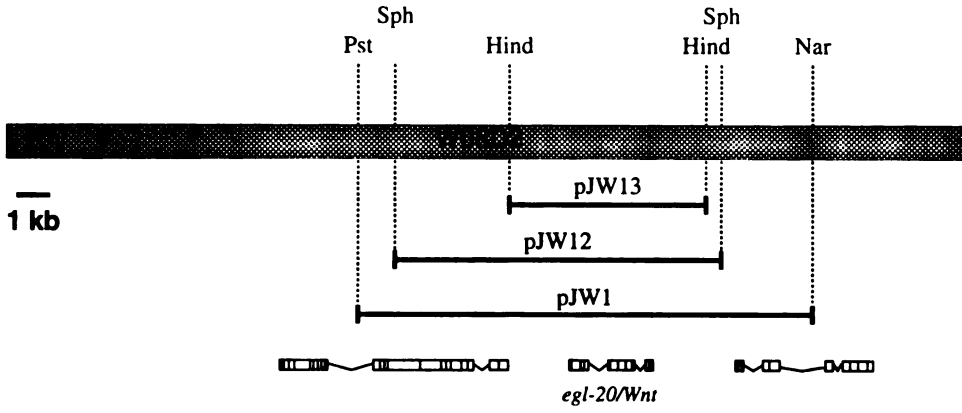


*20(n585) dpy-20(e1282)* hermaphrodites. To assay for complementation, the final positions of the Q descendants were determined in the non-Dpy progeny of this cross.

### Sequencing *egl-20* alleles

Two regions of the predicted *Wnt* gene were PCR amplified from seven *egl-20* mutant alleles: *n585*, *n1437*, *mu320*, *mu241*, *mu27*, *mu25* and *mu39*. Exons 1-4 were amplified with JW1: 5'-CTTAACCAGGCAAATCGGAA-3' and JW5: 5'-CACACATAAGACAACACCTG-3'; exons 5-10 were amplified with JW3: 5'-CGTGTCGTTATGAAATACGC-3' and JW4: 5'-TCTTGTTTTGCTAGGTCCCG-3'. These amplified regions included the entire coding region and all intron/exon boundaries of the predicted *Wnt* gene. Fragments were cloned and sequenced, as described above, from two independent PCR reactions. *egl-20(mu27)* was isolated in a non-complementation screen using *egl-20(n585)*, as previously reported in Harris et al. (1996). Sequence of the *Wnt* gene from this allele revealed that the molecular lesion is identical to that of the *egl-20(n585)* allele. Thus this "allele" was most likely a re-isolation of the original *egl-20(n585)* mutation.





ACCEPTED MANUSCRIPT

**Figure 2.1.** The cosmid W08D2 contains *egl-20* rescuing activity.

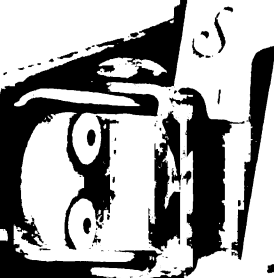
Three subclones of W08D2 that were able to rescue the *egl-20* mutant phenotypes are shown. All three subclones rescued *egl-20(n585)* animals to a similar extent (data not shown).



**Figure 2.2.** *egl-20* encodes a Wnt homolog.

(A) The predicted EGL-20 protein based on the 1182 bp *egl-20* cDNA sequence. The positions and natures of six *egl-20* mutations are indicated. The potential signal sequence (von Heijne, 1986) is highlighted with gray shading, and three potential N-linked glycosylation sites are underlined with dotted lines. Conserved cysteines are highlighted with black squares.

(B) Alignment of the EGL-20 protein sequence with mouse Wnt7a and Wnt7b (Gavin et al., 1990), *Drosophila* Wingless (Rijsewijk et al., 1987), and *C. elegans* LIN-44 (Herman and Horvitz, 1994). EGL-20 shares closest homology to the mouse Wnt7b and Wnt7a. Identical and similar residues are indicated by black and gray boxes, respectively. Highly conserved cysteines are indicated by asterisks. The GenBank accession number for the *egl-20* gene is AF103732.



1940

1941

1942

1943

1944

1945

1946

1947

1948

1949

1950

1951

1952

1953

1954

1955

1956

1957

1958

1959

1960

1961

1962

1963

1964

1965

1966

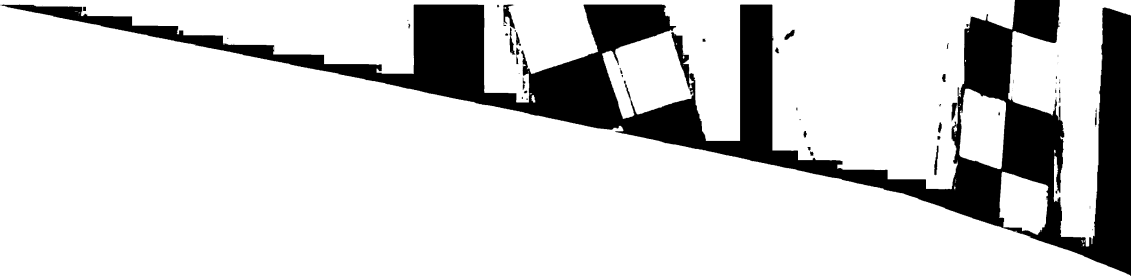
1967

1968

1969

1970

Vertical text on the left margin, including numbers and possibly names, partially obscured by the fastener.







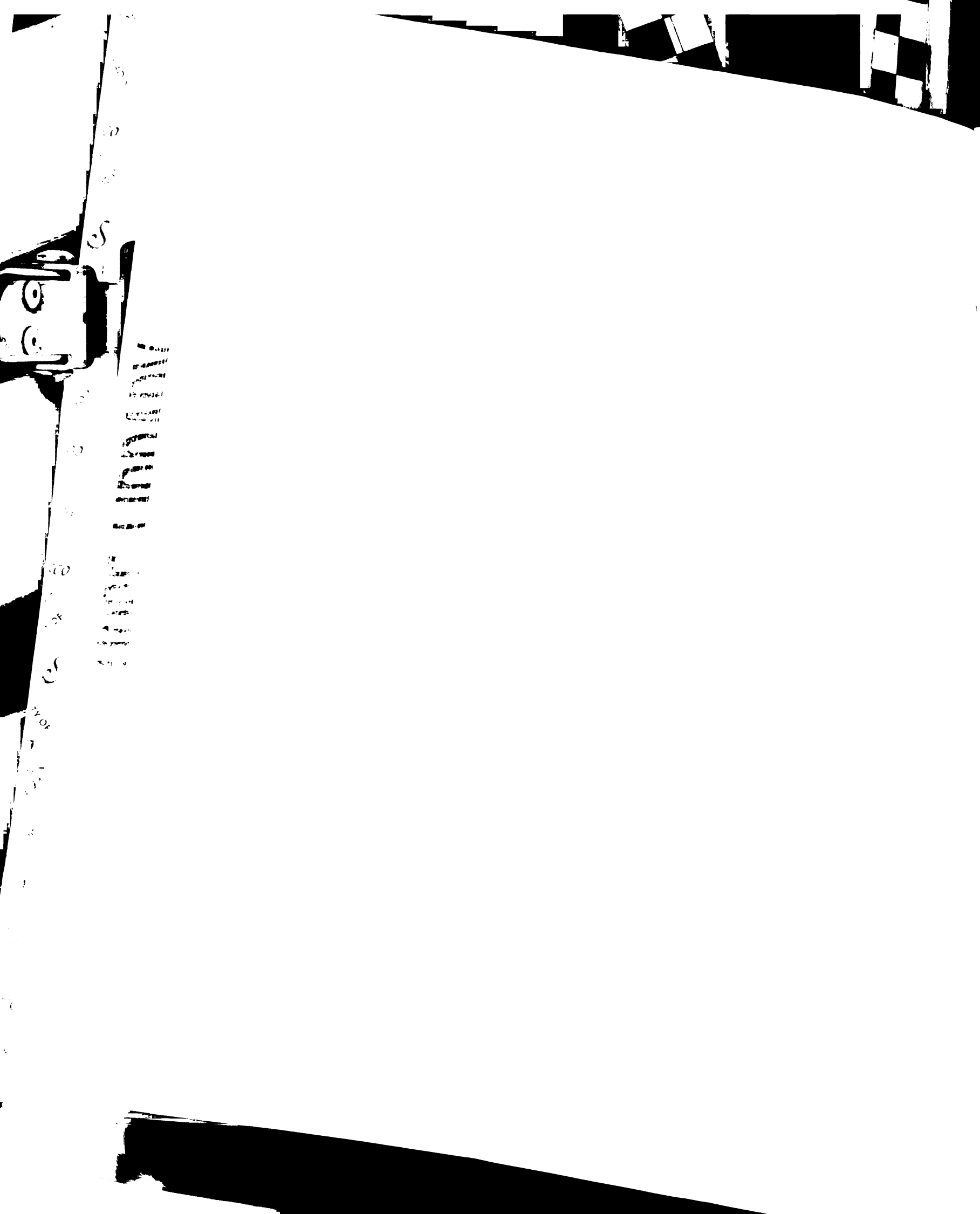
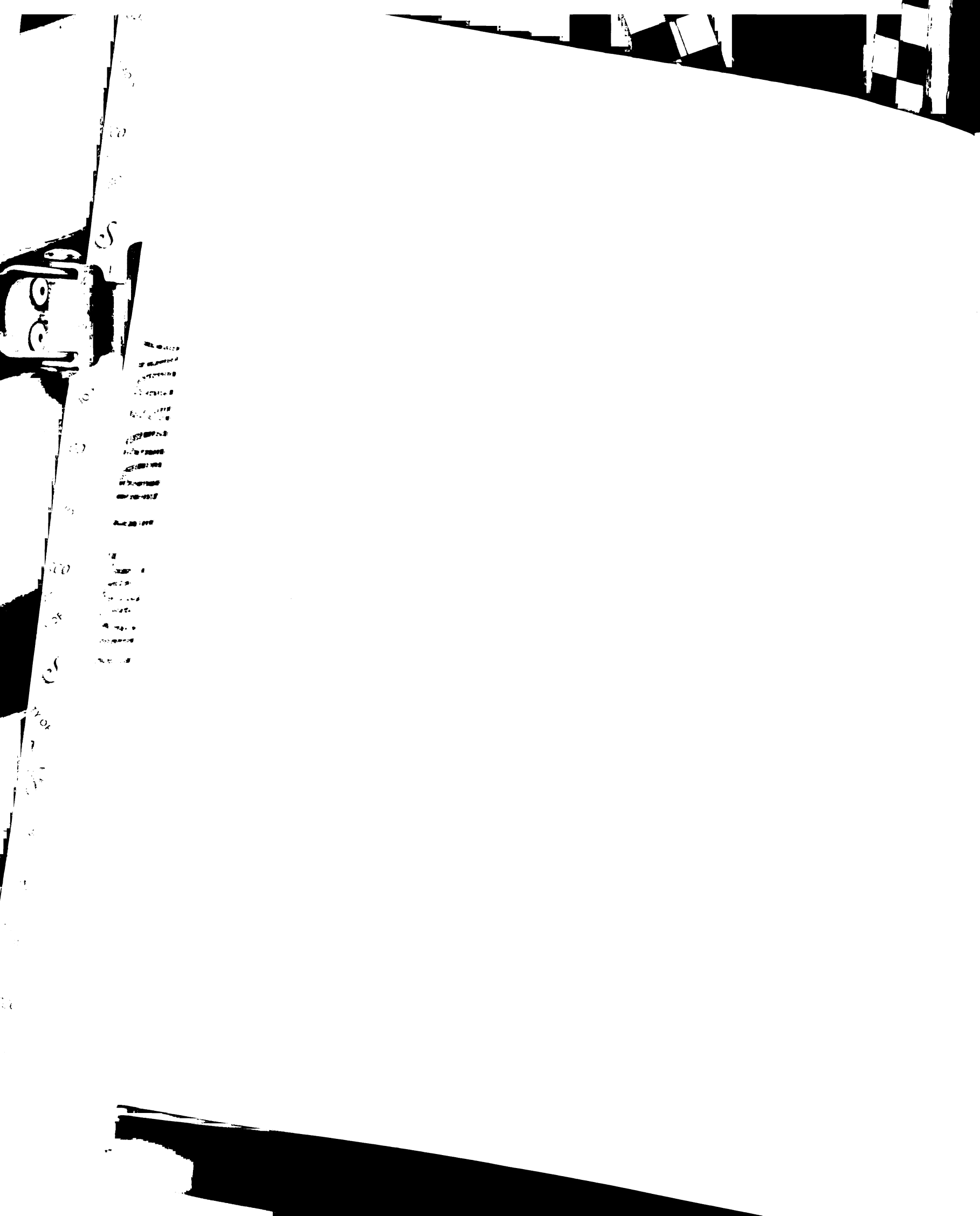


**Table 2.1 Phenotypes and molecular lesions of *egl-20* alleles**

Allele	QL descendants anterior	QR descendants posterior	V5 polarity reversals	Molecular lesion
<i>n585</i>	+	+	+	Cys → Ser 99
<i>n1437</i>	+	+	+	deletion: Val → Glu 287 323
<i>mu25</i>	+	+	+	Cys → Tyr 110
<i>mu39</i>	+	+	-	Cys → Tyr 166
<i>mu320</i>	+	+	+	Arg → opal 49
<i>mu241</i>	+	+	+	splice donor GT → AT intron 2
<i>mu234</i>	+	+	+	Asn → Asp 34
<i>mu253</i>	+	+	+	n.d.
<i>mu254</i>	+	+	+	n.d.
<i>mu259</i>	+	-	-	n.d.
<i>mu309</i>	+	-	-	n.d.
<i>mu311</i>	+	-	+	n.d.
<i>mu314</i>	+	-	+	n.d.
<i>mu323</i>	+	+	-	n.d.
<i>mu332</i>	+	+	+	n.d.
<i>mu333</i>	+	+	-	n.d.
<i>mu341</i>	+	+	-	n.d.
<i>mu344</i>	+	+	+	n.d.

n.d. = not determined



## REFERENCES

Bejsovec, A., and Wieschaus, E. (1995). Signaling activities of the *Drosophila* wingless gene are separately mutable and appear to be transduced at the cell surface. *Genetics* *139*, 309-20.

Cadigan, K. M., and Nusse, R. (1997). Wnt signaling: a common theme in animal development. *Genes and Development* *11*, 3286-305.

Desai, C., Garriga, G., McIntire, S. L., and Horvitz, H. R. (1988). A genetic pathway for the development of the *Caenorhabditis elegans* HSN motor neurons. *Nature* *336*, 638-46.

Eisenmann, D. M., Maloof, J. N., Simske, J. S., Kenyon, C., and Kim, S. K. (1998). The beta-catenin homolog BAR-1 and LET-60 Ras coordinately regulate the Hox gene *lin-39* during *Caenorhabditis elegans* vulval development. *Development* *125*, 3667-80.

Gavin, B. J., McMahon, J. A., and McMahon, A. P. (1990). Expression of multiple novel Wnt-1/int-1-related genes during fetal and adult mouse development. *Genes and Development* *4*, 2319-32.

Harris, J., Honigberg, L., Robinson, N., and Kenyon, C. (1996). Neuronal cell migration in *C. elegans*: regulation of Hox gene expression and cell position. *Development* *122*, 3117-31.

Herman, M. A., and Horvitz, H. R. (1994). The *Caenorhabditis elegans* gene *lin-44* controls the polarity of asymmetric cell divisions. *Development* *120*, 1035-47.

Maloof, J. N., Whangbo, J., Harris, J. M., Jongeward, G. D., and Kenyon, C. (1999). A Wnt signaling pathway controls hox gene expression and neuroblast migration in *C. elegans*. *Development* *126*, 37-49.



Rijsewijk, F., Schuermann, M., Wagenaar, E., Parren, P., Weigel, D., and Nusse, R. (1987). The *Drosophila* homolog of the mouse mammary oncogene *int-1* is identical to the segment polarity gene *wingless*. *Cell* *50*, 649-57.

Sawa, H., Lobel, L., and Horvitz, H. R. (1996). The *Caenorhabditis elegans* gene *lin-17*, which is required for certain asymmetric cell divisions, encodes a putative seven-transmembrane protein similar to the *Drosophila* *frizzled* protein. *Genes and Development* *10*, 2189-97.

Trent, C., Tsung, N. and Horvitz, H.R. (1983). Egg-laying defective mutants of the nematode *Caenorhabditis elegans*. *Genetics* *104*, 619-647.

von Heijne, G. (1986). A new method for predicting signal sequence cleavage sites. *Nucleic Acids Research* *14*, 4683-90.



122  
123  
124  
125  
126  
127  
128  
129  
130  
131  
132  
133  
134  
135  
136  
137  
138  
139  
140  
141  
142  
143  
144  
145  
146  
147  
148  
149  
150  
151  
152  
153  
154  
155  
156  
157  
158  
159  
160  
161  
162  
163  
164  
165  
166  
167  
168  
169  
170  
171  
172  
173  
174  
175  
176  
177  
178  
179  
180  
181  
182  
183  
184  
185  
186  
187  
188  
189  
190  
191  
192  
193  
194  
195  
196  
197  
198  
199  
200



## **Chapter 3: A Wnt Signaling System that Specifies Two Patterns of Cell Migration in *C. elegans***

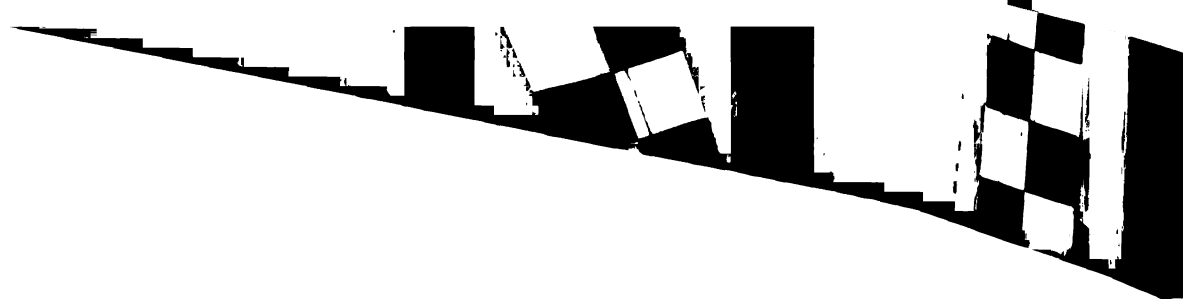
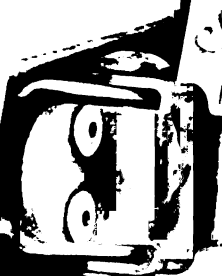
### **SUMMARY**

In *C. elegans*, a bilateral pair of neuroblasts, QL and QR, give rise to cells that migrate in opposite directions along the anteroposterior (A/P) body axis. QL and its descendants migrate posteriorly whereas QR and its descendants migrate anteriorly. We find that a Wnt family member, EGL-20, acts in a dose-dependent manner to specify these opposite migratory behaviors. High levels of EGL-20 promote posterior migration by activating a canonical Wnt signal-transduction pathway, whereas low levels promote anterior migration by activating a separate, undefined pathway. We find that the two Q cells respond differently to EGL-20 because they have different response thresholds. Thus, in this system two distinct dose-dependent responses are specified not by graded levels of the Wnt signal, but instead by left-right asymmetrical differences in the cellular responsiveness to Wnt signaling.

### **INTRODUCTION**

Secreted signaling molecules of the Wnt, Hedgehog and TGF- $\beta$  families are known to mediate a number of long-range patterning events during tissue development (Neumann and Cohen, 1997a). In many cases, these signals generate patterns within fields of cells by acting as graded morphogens that specify cell fates in a concentration-dependent fashion. For example, in the *Drosophila* leg, distinct expression domains of several transcription factors are defined by gradients of both Wingless (Wg), a Wnt

102  
101  
100  
99  
98  
97  
96  
95  
94  
93  
92  
91  
90  
89  
88  
87  
86  
85  
84  
83  
82  
81  
80  
79  
78  
77  
76  
75  
74  
73  
72  
71  
70  
69  
68  
67  
66  
65  
64  
63  
62  
61  
60  
59  
58  
57  
56  
55  
54  
53  
52  
51  
50  
49  
48  
47  
46  
45  
44  
43  
42  
41  
40  
39  
38  
37  
36  
35  
34  
33  
32  
31  
30  
29  
28  
27  
26  
25  
24  
23  
22  
21  
20  
19  
18  
17  
16  
15  
14  
13  
12  
11  
10  
9  
8  
7  
6  
5  
4  
3  
2  
1



family member, and Decapentaplegic (Dpp), a TGF- $\beta$  family member (Lecuit and Cohen, 1997). In this study, we demonstrate that a Wnt signaling system in *C. elegans* uses a different strategy to establish two distinct patterns of cell migration.

The QL and QR neuroblasts are born in equivalent A/P positions on the left and right sides of the animal. Both neuroblasts give rise to cells that migrate to distinct positions along the A/P axis and differentiate into sensory neurons (Chalfie and Sulston, 1981; Sulston and Horvitz, 1977). QL and QR undergo identical patterns of division, yet their descendants exhibit opposite migratory behaviors in response to EGL-20/Wnt signaling (Harris et al., 1996; Maloof et al., 1999; Sulston and Horvitz, 1977) (Figures 3.1A and 3.1B). EGL-20 causes QL to switch on expression of the Hox gene *mab-5* (Salser and Kenyon, 1992), which, in turn, causes the descendants of QL either to remain stationary (the QL.p descendants) or to migrate posteriorly (QL.ap) (Figure 3.1B). In *egl-20(-)* animals, *mab-5* is not expressed in QL and the descendants of both QR and QL migrate anteriorly (Figure 3.1B). EGL-20 activity is also required for certain cells in the QR lineage to migrate anteriorly (Harris et al., 1996). In *egl-20(-)* mutants, the QR.p descendants stop at positions located posterior to their wild-type stopping points. In addition, the QL.p descendants, which migrate anteriorly because they fail to express *mab-5*, stop at positions located posterior to the positions that they would adopt in *mab-5(-)* mutants. Thus, in the wild type, EGL-20 plays two essentially opposite roles in Q cell migration. In the QL lineage it promotes posterior migration, whereas in the QR lineage it promotes anterior migration. In this study, we have asked how EGL-20 triggers these two different responses in a reproducible, left-right asymmetrical fashion.

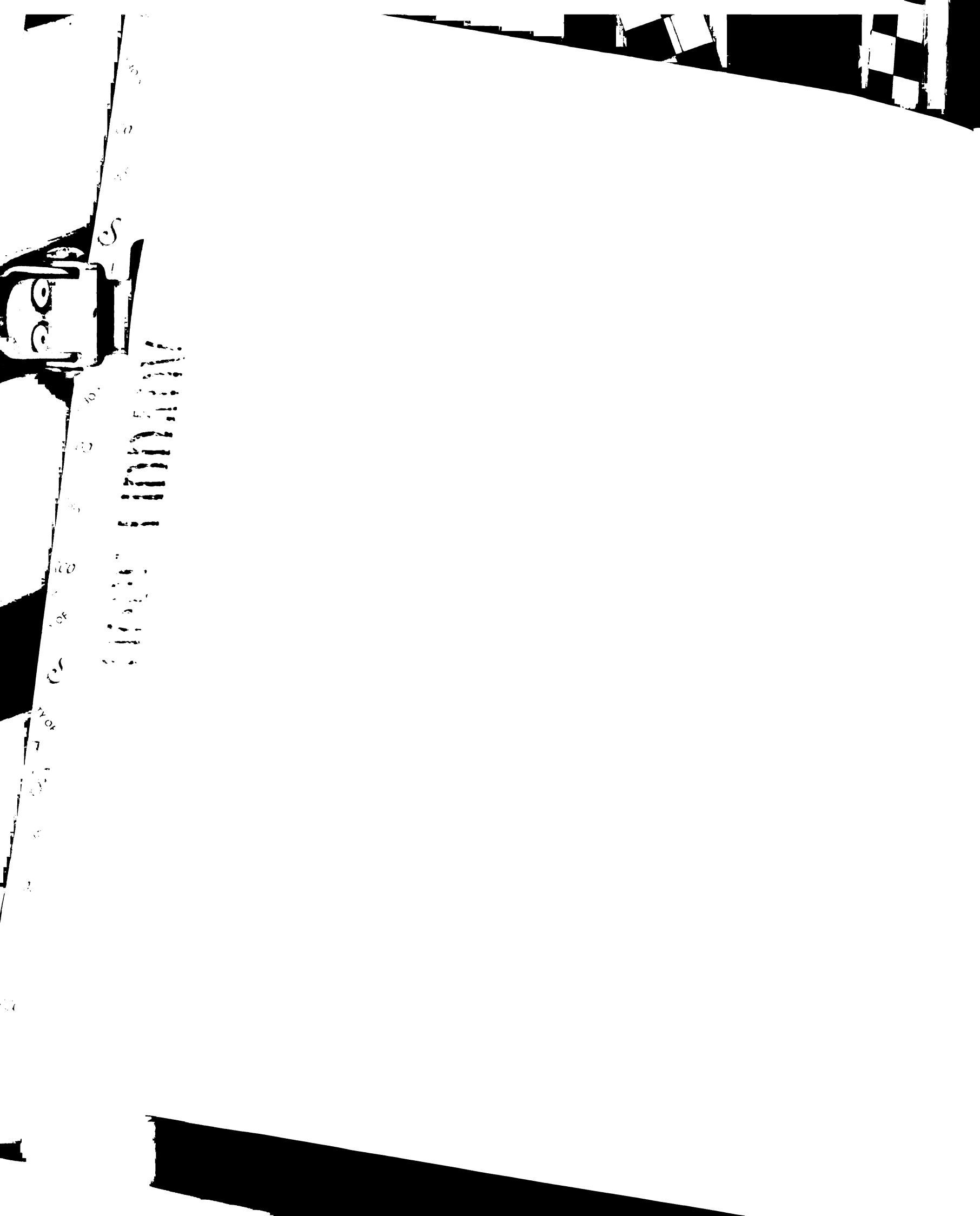
## RESULTS

### Expression of *egl-20* is not left-right asymmetrical

To begin to investigate how EGL-20 might activate *mab-5* expression in QL but not QR, we first determined the *egl-20* expression pattern. We tagged a genomic *egl-20* transgene with *gfp* (Chalfie et al., 1994) and introduced it into *egl-20(-)* animals. Multiple transgenic lines showed full rescue of the *egl-20* mutant phenotypes, suggesting that the fusion protein was expressed in the cells that require *egl-20* activity. At hatching and during the time of Q cell migration, we found that *egl-20::GFP* was expressed exclusively within a group of epidermal and muscle cells located in the posterior of the animal near the anus (Figures 3.1C and 3.1D). These cells are equidistant from either Q cell at hatching and are symmetrically distributed on the left and right sides of the animal. Both the level and the distribution of EGL-20::GFP appeared to be similar on the left and right sides of the animal. Thus the left-right asymmetry of *mab-5* activation does not appear to be caused by left-right asymmetrical expression of *egl-20*.

### The EGL-20/Wnt protein does not act as a positional signal for *mab-5* activation

Studies in *Drosophila* have shown that the concentration of secreted Wingless (Wg) protein can provide cells with positional information, allowing them to adopt different fates that depend on their distance from the Wg source (Lecuit and Cohen, 1997; Neumann and Cohen, 1997b; Struhl and Basler, 1993; Zecca et al., 1996). The localized expression of *egl-20::gfp* suggested a similar mechanism for establishing the asymmetric pattern of *mab-5* expression in the Q cells (Figure 3.1E). Before QL turns on



*mab-5*, it migrates a short distance posteriorly (Salser and Kenyon, 1992). At the same time, QR migrates a short distance anteriorly. This early migration shifts QL closer to the source of EGL-20, whereas it shifts QR further from the source of EGL-20. As a consequence, it seemed possible that only QL might receive a sufficient level of EGL-20 to activate *mab-5* expression. To test this possibility, we expressed EGL-20 in the head instead of the tail by placing the *egl-20::gfp* fusion gene under the control of the *myo-2* promoter (Fire et al., 1990), which drives expression only in the anteriorly-located pharynx (Figures 3.2A and 3.2B). If EGL-20 acted in a spatially-graded manner to provide positional information along the A/P axis, then expressing EGL-20 in the anterior should cause *mab-5* to be expressed in QR but not QL. However, we found that moving the source of EGL-20 from posterior to anterior did not reverse the pattern of Q cell migration. Instead, many of the animals carrying the *myo-2-egl-20::gfp* fusion were rescued for the *egl-20* mutant phenotype (Figure 3.2C). In these animals, only the QL descendants were able to exhibit the *mab-5*-dependent migratory fate and remain in the wild-type posterior positions (Figure 3.2C, lower left panel). Also, in *egl-20(-)* animals carrying the *myo-2-egl-20::gfp* fusion, many of the QR.p descendants migrated far into the anterior (Figure 3.2C, lower right panels). Thus we infer that the posterior localization of EGL-20 is not required either for the left-right asymmetry of *mab-5* activation or for the correct execution of the anterior migration program in the QR lineage.

## The Q cells respond to EGL-20 in a dose-dependent manner

In one transgenic line, in which *myo-2-egl-20::gfp* was expressed at relatively low levels, the QL descendants were not located in the posterior. Instead, the descendants of both QL and QR migrated far into the anterior (Figure 3.2C third row). Thus in these animals, the anterior migration phenotype, but not the *mab-5* expression phenotype, appeared to be rescued. Because this line produced a relatively low level of EGL-20::GFP, these results suggested that the response to EGL-20 might be dose dependent. To test this hypothesis directly, we carried out a dose-response analysis of EGL-20 activity. We placed the *egl-20* cDNA under the control of a heat shock (hs) promoter (Stringham et al., 1992) and introduced this fusion into *egl-20(-)* animals. We then provided different levels of hs-EGL-20 by varying the duration of heat shock. Following heat shock, we monitored *mab-5::lacZ* (Salser and Kenyon, 1992) expression in the Q cells as well as the final positions of the Q descendants.

We found that the response to EGL-20 was dose-dependent. As expected, in the absence of heat shock, the descendants of both QL.p and QR.p behaved as they do in *egl-20(-)* mutants: neither the QL nor the QR descendants expressed *mab-5::lacZ* (Figures 3.3A and 3.3B) and both the QL.p and QR.p descendants migrated anteriorly, but stopped short of the normal QR.p positions (Figure 3.3C). At low levels of heat shock (7 and 10 min. pulses), both the QL.p and QR.p descendants exhibited a response to hs-EGL-20; however their responses were different. The QR.p descendants migrated further anteriorly in response to hs-EGL-20, as did some of the QL.p descendants. However, the remaining QL.p descendants stayed in the posterior, near their locations in the wild type. At high levels of heat shock (20 and 30 min. pulses), the descendants of both cells

remained in the posterior (Figure 3.3C). Together with the experiments described above, these findings suggested the model that the response to EGL-20 was dose dependent, with low EGL-20 levels triggering anterior migration and high EGL-20 levels triggering posterior migration by activating *mab-5* expression. Moreover, they also suggested that cells in the QL lineage were more sensitive to the EGL-20 signal than were cells in the QR lineage. To test this model, we examined the two EGL-20-dependent responses independently of one another.

**Both QL and QR can activate *mab-5* expression in response to EGL-20, but QL is more sensitive to EGL-20 than is QR.**

We assayed *mab-5* activation by examining the expression of a *mab-5::lacZ* construct in response to timed pulses of hs-EGL-20. We found that when the animals were exposed to relatively long pulses of *hs-egl-20*, cells in both the QL and QR lineages expressed *mab-5* (Figures 3.3A and 3.3B). This indicated that QR, like QL, has the potential to express *mab-5::lacZ* in response to EGL-20 signaling. However, as predicted, we found that relatively low levels of hs-EGL-20 induced different responses in the QL and QR lineages. The QL descendants began to express *mab-5::lacZ* at relatively low doses of *hs-egl-20* (5-7 min.) whereas the QR descendants began to express *mab-5::lacZ* at higher doses (10 min.) (Figure 3.3A). Following a 10 minute heat pulse, all of the QL descendants expressed *mab-5::lacZ* whereas many of the QR descendants still did not (Figures 3.3A and 3.3B). This finding indicates that although both QL and QR are capable of turning on *mab-5* expression in response to Wnt signaling, QL requires lower levels of EGL-20 than QR requires to trigger this response.



Under the conditions we used, we did not find a dose of *hs-egl-20* in which all the QL descendants but none of the QR descendants turned on *mab-5*. This may be due to heterogeneity in the responses of individual animals to the heat shock, differences in the ages of the animals at the time of heat shock (which ranged between 0 and 30 minutes after hatching) or to the operation of an additional regulatory mechanism in the animal that also biases QL toward *mab-5* activation.

### **Low levels of EGL-20 promote anterior migration**

To investigate the anterior migration response without the complication of *mab-5* expression, we provided various doses of hs-EGL-20 in *mab-5(-); egl-20(-)* double mutants and assayed the extent of anterior migration. We found that levels of hs-EGL-20 that had been insufficient to activate *mab-5* in QR were able to promote anterior cell migration in both the QR and QL lineages (Figure 3.4A). We also observed that low doses of hs-EGL-20 in wild-type animals caused the anteriorly-migrating QR descendants to overshoot their normal stopping points and migrate too far anteriorly (data not shown). This finding suggests that the anterior migration program does not operate in an all-or-nothing fashion. Instead, the level of EGL-20 in the animal may help to determine the extent of anterior cell migration.

### **Different signal transduction pathways mediate the two responses to EGL-20**

In principle, different levels of EGL-20 could trigger distinct cellular responses by stimulating the same signal transduction pathway to different degrees. This type of situation appears to exist in the *Drosophila* wing, where the downstream components for

Wg signal transduction, *dishevelled* and *armadillo*, are required for both the high and low-threshold responses to Wg signaling (Neumann and Cohen, 1997b). Alternatively, different levels of EGL-20 could trigger different responses by activating distinct signal transduction pathways.

EGL-20 appears to turn on *mab-5* expression by activating a classical Wnt signal transduction pathway (Harris et al., 1996; Maloof et al., 1999). *mab-5* activation requires *lin-17* (Harris et al., 1996), a *frizzled* homolog (Sawa et al., 1996) that may function as an EGL-20 receptor, as well as *bar-1* (Maloof et al., 1999), a  $\beta$ -catenin/*armadillo* homolog (Eisenmann et al., 1998) and possibly *mig-5*, a *dishevelled* homolog (Guo, 1995).

Previous experiments have suggested that *lin-17* is not required for the QR descendants to migrate anteriorly, because *lin-17* loss-of-function mutations do not shorten the migrations of cells in the QR lineage (Harris et al., 1996) (Figure 3.4C). We found that the same was true for *bar-1* loss-of-function mutations (Figure 3.4C, QueeLim Ch'ng and C.K.). This indicates that EGL-20 does not induce the anterior-migration response by activating these two proteins. Curiously, in both *lin-17(-)* and *bar-1(-)* mutants, the QR.p descendants migrated a small but statistically significant distance further anteriorly than in the wild type ( $p = 0.014$  and  $p = 0.021$ , respectively). This suggested the possibility that EGL-20 might promote anterior migration, at least in part, by repressing the activity of LIN-17 and BAR-1. To test this, we asked whether these mutations might be epistatic to *egl-20* mutations. Instead, we found that in both double mutants, the final positions of the QR.p descendants were intermediate between the final positions of the two single mutants (Figure 3.4C). Because the double mutants did not resemble the *lin-17* or *bar-1* single mutants, it seems unlikely that EGL-20 promotes anterior migration by inhibiting

the activities of these two proteins. Instead, the result suggests that LIN-17 and BAR-1 might act independently of EGL-20 to position the QR.p descendants along the A/P axis. We conclude that EGL-20 does not trigger the two dose-dependent responses by activating the same signal transduction pathway to different extents. Instead, high levels of EGL-20 appear to activate one response pathway, while low levels activate another.

## DISCUSSION

In this study, we have asked how the EGL-20 protein regulates left-right asymmetric patterns of migration in the Q cell lineages. During normal development, EGL-20 activates *mab-5* expression and thereby promotes posterior migration in the QL lineage. However, it triggers a different response, anterior cell migration, in the QR lineage. Our findings show that both QL and QR are capable of exhibiting either of the two migratory responses to EGL-20. Moreover, both Q cells respond in a dose-dependent manner to EGL-20: relatively low levels of EGL-20 promote anterior cell migration whereas relatively high levels trigger *mab-5* expression and posterior migration. Surprisingly, despite its localized expression in the animal, EGL-20 does not act as a spatially-graded morphogen to specify these distinct migratory fates. Instead, QL and QR exhibit different responses because they have different response thresholds to EGL-20 signaling: QL requires a lower concentration of EGL-20 activity to express the high-threshold fate. We propose that physiological levels of EGL-20 are high enough to activate *mab-5* expression in QL but not QR (Figure 3.4B). Cells in the QR lineage adopt the less stringent EGL-20-dependent fate, and migrate anteriorly.

The mechanism that creates left-right differences in the responsiveness of QL and QR to Wnt signaling is not known. It is possible that this differential sensitivity to EGL-20 arises because one or more components of the *mab-5* activation pathway are expressed at higher levels in QL than QR. Alternatively, a left-right asymmetric cell or factor could act outside of the Q cells in a local way to influence EGL-20 signaling. Local cell-extrinsic signals that are thought to involve direct cell-cell contact are known to prevent EGL-20 from activating *mab-5* in certain posterior epidermal cells (Austin and Kenyon, 1994; Hunter et al., 1999; Sulston and White, 1980).

In *Drosophila*, Dpp has been shown to increase the sensitivity of certain cells to the Wg signal (Lecuit and Cohen, 1997). These observations raised the possibility that a TGF- $\beta$  signaling pathway might make QL more sensitive than QR to EGL-20. Therefore, we examined the positions of the Q descendants in several strains containing mutations in the *C. elegans* homologs of TGF- $\beta$  pathway signaling components. We examined mutations in two of the four reported TGF- $\beta$  signaling molecules (Colavita et al., 1998; Ren et al., 1996; Ruvkun and Hobert, 1998), a type I receptor for TGF- $\beta$  (Georgi et al., 1990), the only reported type II receptor (Estevez et al., 1993) and two of the six reported SMAD transducing molecules (Savage et al., 1996) (see Experimental Procedures). These mutants represent disruptions in the known TGF- $\beta$  signaling pathways, which regulate dauer formation, body size and axon guidance. We did not observe any defects in the migrations of the QL or QR descendants within this group of mutants. Our results imply that these TGF- $\beta$  pathways do not pre-pattern the Q cells to respond differently to EGL-20.

High levels of EGL-20 promote posterior migration by activating *mab-5* expression. How might low levels of EGL-20 trigger anterior cell migration? Because the QR descendants do not require a localized source of EGL-20 to migrate anteriorly, EGL-20 cannot act as a repulsive guidance cue. One possibility is that EGL-20 causes cells in the QR lineage to express a gene analogous to *mab-5* that promotes anterior migration. Alternatively, EGL-20 could affect anterior migration by modifying an extracellular chemoattractant or repellent.

Unlike previous dose-dependent Wnt response pathways that have been investigated, our genetic analysis indicates that the signal transduction pathways that specify the two dose-dependent responses to EGL-20 are not the same. High levels of EGL-20 appear to activate a canonical Wnt signal transduction pathway that turns on *mab-5* (Harris et al., 1996; Maloof et al., 1999), whereas low levels of EGL-20 activate a different, poorly defined, pathway that promotes anterior cell migration. Since QL and QR can each exhibit both responses to EGL-20, it appears that the anterior migration pathway is overridden when EGL-20 levels are high and the *mab-5*-activation pathway is stimulated.

In summary, we have shown that three features of this system allow the QL and QR descendants to respond differently to EGL-20. First, EGL-20 specifies cellular responses in a dose-dependent fashion. Second, QL and QR have different EGL-20 response thresholds; QL is more sensitive to EGL-20 than is QR. Third, the endogenous level of EGL-20 falls between these two response thresholds (see Figure 3.4B). Together these regulatory features allow EGL-20 to diversify patterns of cell migration in *C. elegans*. Without EGL-20 activity, all the descendants of QL and QR would migrate

anteriorly, and the QL.p and QR.p descendants would move a relatively short distance. Instead, the operation of this signaling system allows the QL and QR descendants to migrate in a left-right asymmetric fashion to positions that span the entire A/P body axis.

## **MATERIALS AND METHODS**

### ***egl-20* Reporter Genes and Transgenic Arrays**

The rescuing *egl-20::gfp* translational fusion (pJW31) was made by inserting a XmaI-digested fragment of *gfp* coding sequences (pPD113.37, a F64L S65T variant from A. Fire) into an AgeI site engineered after the last codon of *egl-20*. In addition to the entire *egl-20* genomic sequence, this construct contains 6.8 kb upstream of the *egl-20* start site and 1.9 kb downstream of the stop codon. *muIs49* was made by integrating an extrachromosomal array containing pJW31 injected at 25 ng/μl and pPD10.46, a plasmid carrying *unc-22* anti-sense, co-injected at 125 ng/μl. To make the *myo-2::egl-20-gfp* fusion (pJW33), a PCR fragment containing *gfp* coding sequences and an engineered stop codon was inserted in frame at the 3' end of the *egl-20* cDNA. The *gfp* coding sequence was amplified using the primer pair JW30 (5'-CCGCTGCAGATGAGTAAAGGAGAAGAAGT-3') and JW31 (5'-CCGGAGCTCTTATTTGTATAGTTCATCCAT-3'). The *gfp*-tagged *egl-20* cDNA was then inserted into NheI-SacI digested pPD30.69, a plasmid containing *myo-2* promoter sequences (from A. Fire) (Fire et al., 1990). The extrachromosomal array *muEx68* was generated by injecting pJW33 at 20 ng/μl and pPD10.46 at 125 ng/μl into *egl-20(n585)*

animals. The extrachromosomal array *muEx79* contains pJW33 injected at 10 ng/ $\mu$ l and pPD10.46 co-injected at 125 ng/ $\mu$ l.

### **Heat Shock Constructs and Conditions**

The *hs-egl-20* fusion (pJW30) was generated by inserting a PCR-amplified *egl-20* cDNA fragment with an engineered stop codon into NheI-SacI digested pPD49.78 (*hsp 16-2*, from A. Fire) (Stringham et al., 1992). The *egl-20* cDNA was amplified using the primer pair JW28 (5'-CCGGGGCCCGCTAGCATGCAATTTTTCATTTGC-3') and JW29 (5'-CCGGAGCTCCTGCAGTTTGCATGTATGTACTGC-3'). *muIs53* was made by integrating an extrachromosomal array containing pJW30 injected at 20 ng/ $\mu$ l and pPD10.46 co-injected at 125 ng/ $\mu$ l. Staged populations of larvae grown at 20°C were collected at 0 to 30 minutes after hatching and were subjected to heat shock for various lengths of time on an aluminum block that was maintained at 33°C. Immediately after heat shock, the animals were placed at 20°C and allowed to grow until the migrations of the Q cell descendants were complete (end of L1 larval stage).

### **$\beta$ -galactosidase Detection**

Staged populations of *egl-20(n585) unc-31(e169) muIs2 [mab-5::lacZ, unc-31(+)]*; *muIs53 [hs-egl-20, unc-22 anti-sense]* animals were grown at 20°C. Larvae were collected at 0 to 30 minutes after hatching and heat shocked at 33°C for various lengths of time. Following heat shock, the animals were allowed to grow at 20°C until the Q cells had divided once (approximately 2.5 hours after hatching). The animals were then

fixed on slides and stained as described by Maloof et al. (1999). Statview 5.0 (SAS) software was used to carry out data analysis.

### **Examination of TGF- $\beta$ Pathway Mutants**

The mutations used are derived from wild-type Bristol N2 and are listed by linkage group (LG). LGIII: *sma-2(e502)* (SMAD), *sma-3(e491)* (SMAD) (Savage et al., 1996), *daf-4(e1364)* (Type II receptor) (Estevez et al., 1993), *daf-7(e1372)* (TGF- $\beta$ ) (Ren et al., 1996). LGIV: *daf-1(m40)* (Type I receptor) (Georgi et al., 1990), *unc-129(ev554)*, *unc-129(ev557)* (TGF- $\beta$ ) (Colavita et al., 1998). Final positions of the QL.p and QR.p descendants were determined late in the L1 larval stage. More than 20 animals were examined on both the left and right sides for each strain except for *unc-129(ev557)* (n=15). *daf-1(m40)* and *daf-4(e1364)* were scored at 15°C and 25°C. *daf-7(e1372)* was scored only at 15°C. All other strains were examined at 20°C.

### **ACKNOWLEDGEMENTS**

We thank Tim Yu for expert assistance with confocal microscopy, Jeanne Harris for construction and examination of the *lin-17(n671); egl-20(n585)* double mutant, QueeLim Ch'ng for examination of *bar-1(ga80)*, the Bargmann lab for strains, Andrew Fire for reporter gene vectors and Javier Apfeld, Scott Alper, Joy Alcedo, Lucie Yang and other members of the Kenyon lab for many helpful discussions and comments on the manuscript. J.W. is supported by a NSF Predoctoral Fellowship. C.K. is the Herbert Boyer Professor of Biochemistry and Biophysics. This work was supported by NIH grant GM37053 to C.K.



**Figure 3.1.** *egl-20* regulates Q cell migration and is expressed in the posterior.

(A) Q neuroblast lineage. The left and right Q cells (QL and QR, large circles) generate identical cell lineages to produce three neurons (diamond and two small squares) and cells that undergo apoptosis (crosses).

(B) Migrations of the QL and QR descendants in the wild type and representative *egl-20* mutants. Positions of the cells in the Q lineage are shown relative to lateral epidermal cells called the V cells (gray ovals). At hatching, QL and QR are located in approximately the same anteroposterior position. A few hours after hatching, the QL cell migrates posteriorly a short distance and then begins to express the Hox gene *mab-5*. The QL cell then divides and both descendants continue to express *mab-5* (filled square and filled triangle). The QL.ap descendant migrates into the tail (filled diamond), but the two descendants of the QL.pa cell (filled small squares) do not migrate substantially. Similarly, soon after hatching, the QR cell migrates anteriorly a short distance and divides. Its descendants, which do not express *mab-5*, continue to migrate anteriorly. In *egl-20* mutants, the QL cell still migrates posteriorly, but does not express *mab-5*. Consequently, its descendants migrate into the anterior. In addition, the QR.p descendants stop migrating prematurely and are located in positions posterior to the wild-type final positions. Confocal image of a wild-type L1 larva carrying the integrated array *muIs49(egl-20::gfp)*. The earliest expression of *egl-20::gfp* is detected in the tail region of the embryo at pretzel stage (around 600 min.). At the time of the Q lineage migrations, *egl-20::gfp* is expressed in the anal depressor muscle (*mu anal*) and in the postembryonic blast cells P9/10, K, F, U and B. *muIs49* rescues cell migration defects (QL, QR and HSN) and the egg-laying

defect of *egl-20(n585)* animals. The *egl-20(n585)* allele contains a mutation in a highly conserved cysteine and behaves as a strong reduction-of-function mutation by genetic criteria (Harris et al., 1996). An identical expression pattern and rescued phenotype were produced by a second independent integrated array carrying *egl-20::gfp*. Dorsal is up and anterior is left. Scale bar is 10  $\mu\text{m}$ .

(D) Diagram of the cells expressing *egl-20::gfp* during the L1 larval stage.

(E) Positional model for the asymmetric activation of *mab-5* expression (blue shading) in the Q lineage (see text).

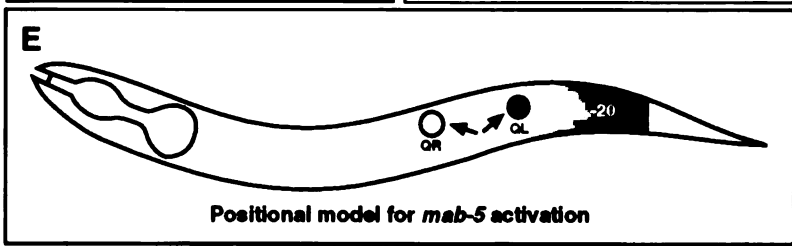
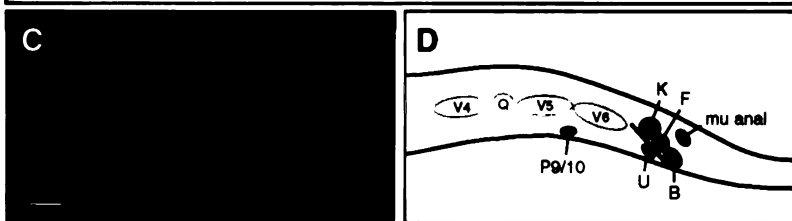
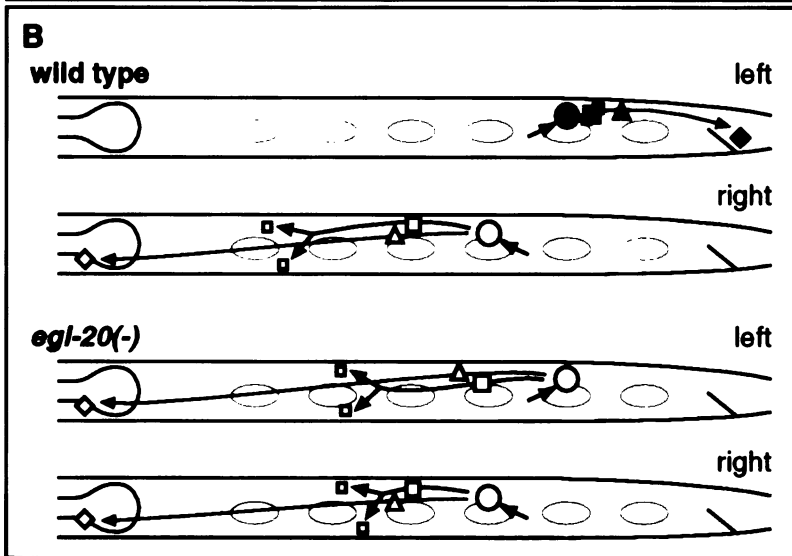
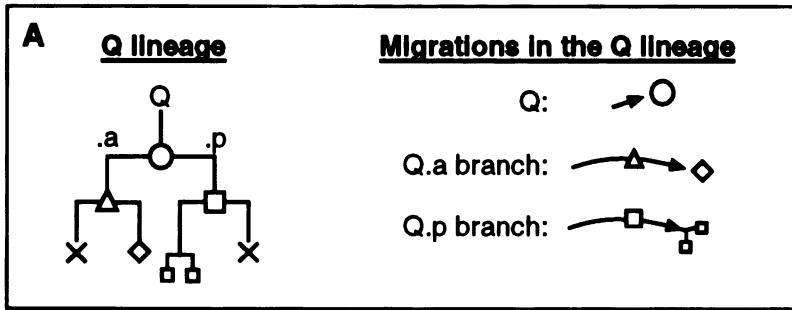


**Figure 3.2.** EGL-20 does not act as a positional signal.

- (A) Confocal image of *muEx68* (*myo-2-egl-20::gfp*) expression in the pharynx of an *egl-20(n585)* animal at the L1 larval stage. *gfp* expression in the pharynx is present from the late embryo throughout. (Scale bar = 10  $\mu$ m).
- (B) Test of the positional model for *mab-5* activation. Expressing *egl-20* in the head instead of the tail should cause QR but not QL to express *mab-5* and exhibit the posterior migration phenotype (see text).
- (C) The final positions of the QL.p and QR.p descendants (small squares in Figure 3.1A) in wild type, *egl-20(n585)*, *egl-20(n585)* animals carrying *muEx79* (*myo-2-egl-20::gfp* injected at 10ng/ $\mu$ l) and *egl-20(n585)* animals carrying *muEx68* (*myo-2-egl-20::gfp* injected at 20ng/ $\mu$ l) are shown relative to the positions of the epidermal V cell descendants after approximately 10 hrs of development at 15°C. The Q.ap cells (diamond in Figure 3.1A) were not assayed because they are often located in neuron-rich regions, making them difficult to identify. *n*, total number of cells observed. *p*, *p*-value determined using Fisher's exact test. In wild-type animals, the QL.p descendants remain in the posterior whereas the QR.p descendants migrate to positions in the anterior, *n* > 200. In *egl-20(n585)* animals, the QL.p descendants migrate anteriorly because they fail to express *mab-5*, *n* = 72. In addition, the final positions of the QR.p descendants are shifted posteriorly relative to wild type in *egl-20(n585)* animals, *n* = 83. In *egl-20(n585)* animals bearing *muEx79*, which expresses relatively low levels of EGL-20::GFP, both the QL.p and QR.p descendants migrate to more anterior positions than they do in *egl-20(n585)* mutants, *n* = 40 and *n* = 48, respectively; *p* < 0.0001 for both. In contrast, the *muEx68* array, which expresses

higher levels of EGL-20::GFP, rescues the migrations of some of the QL.p descendants in *egl-20(n585)* animals,  $n = 64$ ,  $p < 0.0001$ . In addition, many of the QR.p descendants in *egl-20(n585); muEx68* animals are shifted anteriorly,  $n=43$ ,  $p = 0.016$  relative to the *egl-20(n585)* positions. At least two independent lines carrying the extrachromosomal *myo-2-egl-20::gfp* fusion were analyzed and shown to behave similarly for both injection concentrations. The migrations of the QL and QR cells themselves are normal in *egl-20(n585); muEx79* and *egl-20(n585); muEx68* animals ( $n \geq 10$  for each side). In this and other figures, the vertical dashed line serves as a common reference point for visual comparison and statistical analysis of the various histograms.  $p$  values represent the probability that the fraction of cells anterior to the reference line in the transgenic lines is equal to that of *egl-20(n585)* animals. For comparison of *egl-20(n585); muEx79* and *egl-20(n585)* on the left side, the reference line was set in front of V2.p.

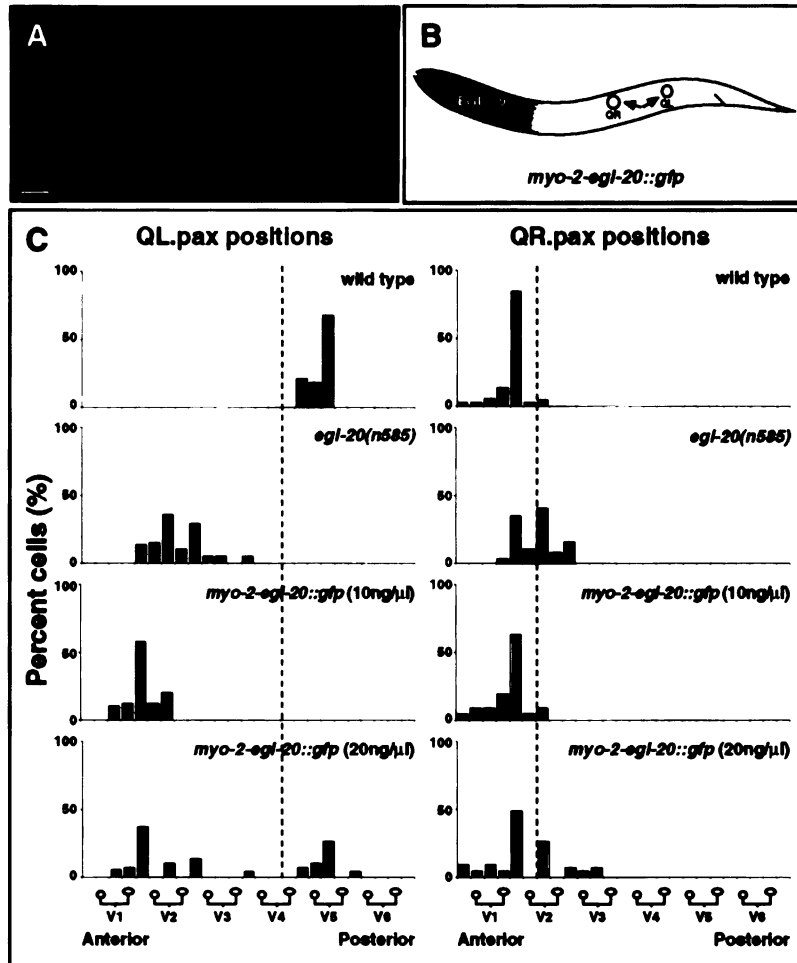


**Figure 3.3.** Cells in the QL and QR lineages have different response thresholds to the EGL-20 signal.

(A) Dose-response curve showing *mab-5::lacZ* expression in response to different doses of *hs-egl-20* in the QL (closed circles) and QR (open triangles) descendants. *egl-20(n585)* animals carrying integrated arrays containing the *mab-5::lacZ* reporter gene and *hs-egl-20* were collected at 0 to 30 minutes after hatching and heat shocked at 33°C for up to 30 minutes. Following heat shock, the animals were recovered at 20°C and fixed for  $\beta$ -galactosidase detection following the first division of the Q cells. The QL descendants were able to express *mab-5::lacZ* at lower doses of *hs-egl-20* than were the QR descendants ( $n > 50$  for each time point except for QL descendants at 7 min.,  $n = 43$ ).

(B) Nomarski photographs of *mab-5::lacZ* expression in the Q cell descendants in *egl-20(n585)* animals following different doses of *hs-egl-20*. The black arrowheads indicate the QL and QR descendants. In the absence of any *hs-egl-20*, the QL and QR descendants are unable to express *mab-5::lacZ* in *egl-20(n585)* animals (top panels). After an intermediate dose of *hs-egl-20* (10 min.), the QL descendants have turned on *mab-5::lacZ* expression, whereas many of the QR descendants have not (middle panels). We never observed animals in which *mab-5::lacZ* was expressed in the QR but not QL descendants. At high doses of *hs-egl-20* (30 min.), *mab-5::lacZ* is expressed in both QL and QR descendants (bottom panels). This *mab-5::lacZ* fusion is expressed in all cells in which *mab-5* is predicted to function genetically (Salser and Kenyon, 1992). In the L1 larval stage, *egl-20* mutations appear to affect *mab-5* expression only in the Q lineage.

(C) The final positions of the QL.p and QR.p descendants in *egl-20(n585)* animals

following different doses of *hs-egl-20*,  $n \geq 50$  for each dose. p values were derived

using the Fisher exact test and represent the probability that the fraction of cells

posterior to the reference line in heat-shocked animals is equal to that of the non-heat

shocked control animals. The final positions of the Q descendants in heat-shocked

*egl-20(n585)* animals not carrying the *hs-egl-20* array were not different from those in

non-heat shocked control animals,  $n = 50$ .



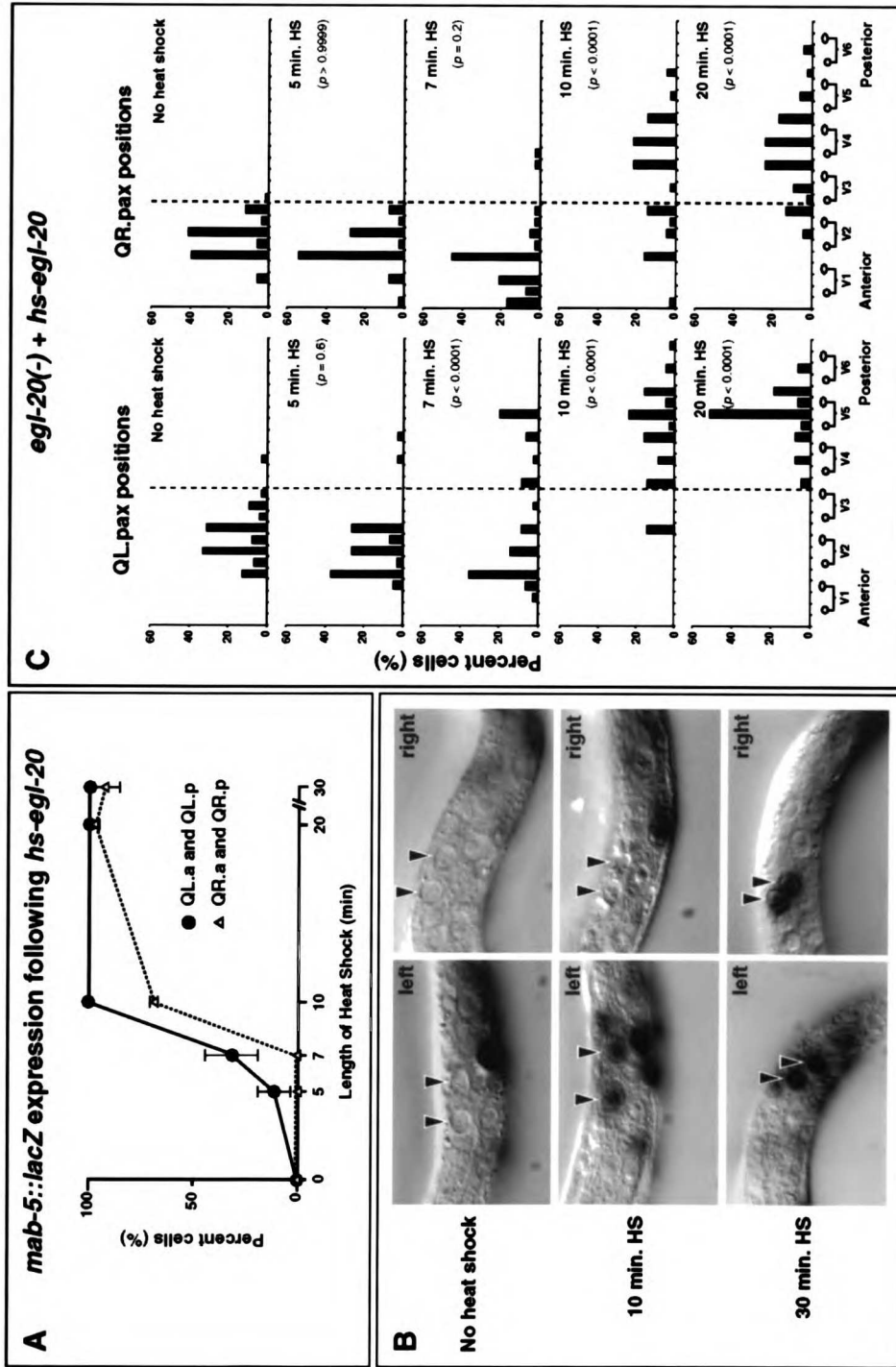
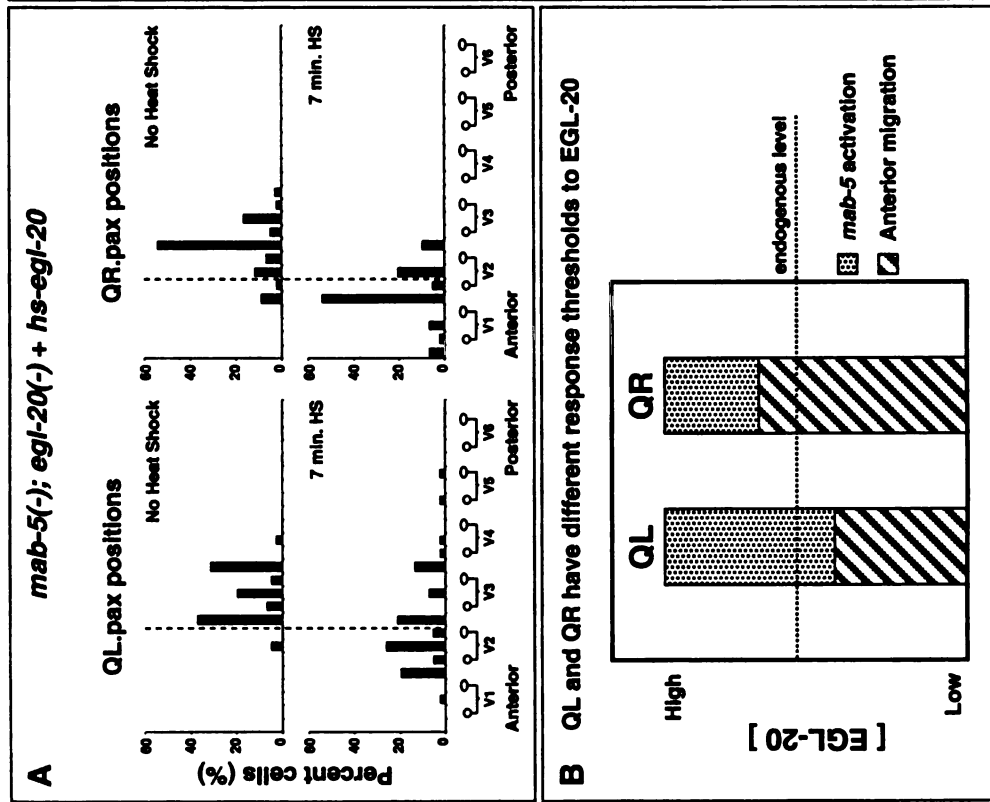
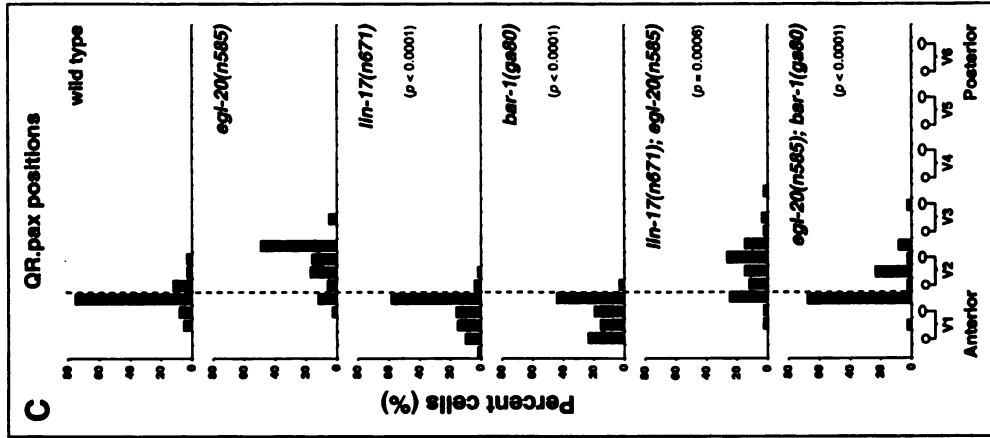


**Figure 3.4.** The threshold for anterior migration is lower than the threshold for *mab-5* expression in both Q cells.

(A) The final positions of the QL.p and QR.p descendants in *mab-5(e2088); egl-20(n585)* animals following a low dose of *hs-egl-20*,  $n > 50$  for each panel. In the absence of *mab-5*, QL and QR respond similarly to *hs-egl-20*. A dose of *hs-egl-20* which is normally unable to activate *mab-5* expression (7 min. pulse) in QR can promote anterior migration of both the QR and QL descendants,  $p < 0.0001$ . We observed that very high doses of *hs-egl-20* (20 min. and 30 min. pulses) caused both the QL and QR descendants to migrate to positions along the entire A/P body axis even in the absence of *mab-5* (data not shown). It is possible that high levels of EGL-20 interfere with the ability of the cells to distinguish anterior from posterior. Alternatively, this response may be a non-specific effect of high, non-physiological levels of EGL-20.  $p$  values relative to the non-heat shocked control animals were determined using Fisher's exact test.

(B) Model to explain how EGL-20 elicits different responses in the QL and QR lineages during normal development. Both QL and QR can exhibit both migratory behaviors in response to EGL-20. In addition, the threshold for anterior migration (hashed shading) is lower than the threshold for *mab-5* expression (dotted shading) in both Q cells. However, the thresholds of the two Q cells are set differently: QL has a lower threshold for *mab-5* expression than does QR. Thus, the QL cell responds to the endogenous level of EGL-20 (dotted line) by expressing *mab-5*, whereas the QR cell responds to the endogenous level of EGL-20 by migrating into the anterior body region.

(C) The final positions of the QR.p descendants in wild type (Harris et al., 1996) and *egl-20(n585)*, *lin-17(n671)*, *bar-1(ga80)*, *lin-17(n671); egl-20(n585)* and *egl-20(n585); bar-1(ga80)* mutants. All strains were examined at 25°C. *n* = 100 for all strains except for *bar-1(ga80)*, *n* = 50. *p* values relative to *egl-20(n585)* were determined using Fisher's exact test. The *lin-17(n671)* and *lin-17(n671); egl-20(n585)* data are from Jeanne Harris and C.K. The *bar-1(ga80)* data are from QueeLim Ch'ng and C.K.



## REFERENCES

- Austin, J., and Kenyon, C. (1994). Cell contact regulates neuroblast formation in the *Caenorhabditis elegans* lateral epidermis. *Development* *120*, 313-23.
- Cadigan, K. M., and Nusse, R. (1997). Wnt signaling: a common theme in animal development. *Genes and Development* *11*, 3286-305.
- Chalfie, M., and Sulston, J. (1981). Developmental genetics of the mechanosensory neurons of *Caenorhabditis elegans*. *Developmental Biology* *82*, 358-70.
- Chalfie, M., Tu, Y., Euskirchen, G., Ward, W. W., and Prasher, D. C. (1994). Green fluorescent protein as a marker for gene expression. *Science* *263*, 802-5.
- Colavita, A., and Culotti, J. G. (1998). Suppressors of ectopic UNC-5 growth cone steering identify eight genes involved in axon guidance in *Caenorhabditis elegans*. *Developmental Biology* *194*, 72-85.
- Eisenmann, D. M., Maloof, J. N., Simske, J. S., Kenyon, C., and Kim, S. K. (1998). The beta-catenin homolog BAR-1 and LET-60 Ras coordinately regulate the Hox gene *lin-39* during *Caenorhabditis elegans* vulval development. *Development* *125*, 3667-80.
- Estevez, M., Attisano, L., Wrana, J. L., Albert, P. S., Massagué, J., and Riddle, D. L. (1993). The *daf-4* gene encodes a bone morphogenetic protein receptor controlling *C. elegans* dauer larva development. *Nature* *365*, 644-9.
- Fire, A., Harrison, S. W., and Dixon, D. (1990). A modular set of lacZ fusion vectors for studying gene expression in *Caenorhabditis elegans*. *Gene* *93*, 189-98.
- Georgi, L. L., Albert, P. S., and Riddle, D. L. (1990). *daf-1*, a *C. elegans* gene controlling dauer larva development, encodes a novel receptor protein kinase. *Cell* *61*, 635-45.

Guo, C. (1995). *mig-5*, a gene that controls cell fate determination and cell migration in *C. elegans*, is a member of the *dsh* family. PhD Thesis, The Johns Hopkins University.

Harris, J., Honigberg, L., Robinson, N., and Kenyon, C. (1996). Neuronal cell migration in *C. elegans*: regulation of Hox gene expression and cell position. *Development* 122, 3117-31.

Hunter, C. P., Harris, J. M., Maloof, J. N., and Kenyon, C. (1999). Hox gene expression in a single *Caenorhabditis elegans* cell is regulated by a caudal homolog and intercellular signals that inhibit Wnt signaling. *Development* 126, 805-814.

Hunter, C. P., and Kenyon, C. (1995). Specification of anteroposterior cell fates in *Caenorhabditis elegans* by *Drosophila* Hox proteins. *Nature* 377, 229-32.

Lecuit, T., and Cohen, S. M. (1997). Proximal-distal axis formation in the *Drosophila* leg. *Nature* 388, 139-45.

Maloof, J. N., Whangbo, J., Harris, J. M., Jongeward, G. D., and Kenyon, C. (1999). A Wnt signaling pathway controls hox gene expression and neuroblast migration in *C. elegans*. *Development* 126, 37-49.

Neumann, C., and Cohen, S. (1997a). Morphogens and pattern formation. *Bioessays* 19, 721-9.

Neumann, C. J., and Cohen, S. M. (1997b). Long-range action of Wingless organizes the dorsal-ventral axis of the *Drosophila* wing. *Development* 124, 871-80.

Ren, P., Lim, C. S., Johnsen, R., Albert, P. S., Pilgrim, D., and Riddle, D. L. (1996). Control of *C. elegans* larval development by neuronal expression of a TGF-beta homolog. *Science* 274, 1389-91.

Salser, S. J., and Kenyon, C. (1992). Activation of a *C. elegans* Antennapedia homologue in migrating cells controls their direction of migration. *Nature* 355, 255-8.

Savage, C., Das, P., Finelli, A. L., Townsend, S. R., Sun, C. Y., Baird, S. E., and Padgett, R. W. (1996). *Caenorhabditis elegans* genes *sma-2*, *sma-3*, and *sma-4* define a conserved family of transforming growth factor beta pathway components. *Proceedings of the National Academy of Sciences of the United States of America* 93, 790-4.

Sawa, H., Lobel, L., and Horvitz, H. R. (1996). The *Caenorhabditis elegans* gene *lin-17*, which is required for certain asymmetric cell divisions, encodes a putative seven-transmembrane protein similar to the *Drosophila* frizzled protein. *Genes and Development* 10, 2189-97.

Stringham, E. G., Dixon, D. K., Jones, D., and Candido, E. P. (1992). Temporal and spatial expression patterns of the small heat shock (*hsp16*) genes in transgenic *Caenorhabditis elegans*. *Molecular Biology of the Cell* 3, 221-33.

Struhl, G., and Basler, K. (1993). Organizing activity of wingless protein in *Drosophila*. *Cell* 72, 527-40.

Sulston, J., and Horvitz, H. (1977). Post-embryonic cell lineages of the nematode, *C. elegans*. *Developmental Biology* 56, 110-156.

Sulston, J. E., and White, J. G. (1980). Regulation and cell autonomy during postembryonic development of *Caenorhabditis elegans*. *Dev Biol* 78, 577-97.

Sym, M., Robinson, N., and Kenyon, C. (1999). MIG-13 positions migrating cells along the anteroposterior body axis of *C. elegans*. *Cell* 98, 25-36.

Zecca, M., Basler, K., and Struhl, G. (1996). Direct and long-range action of a wingless morphogen gradient. *Cell* 87, 833-44.

Zipkin, I. D., Kindt, R. M., and Kenyon, C. J. (1997). Role of a new Rho family member in cell migration and axon guidance in *C. elegans*. *Cell* 90, 883-94.

UNIVERSITY OF MICHIGAN LIBRARY



## **Chapter 4: Multiple layers of signaling regulate the polarity of an asymmetric cell division**

### **SUMMARY**

In the previous chapter, I described the role of the *egl-20/Wnt* gene in regulating migrations of the QL and QR descendants along the anteroposterior (A/P) axis. Here I describe the requirement for *egl-20* in establishing the correct A/P polarity of the asymmetric V5-cell division. Jeanne Harris initially observed the V5 polarity defect in *egl-20* mutants. Together, we showed that signals from adjacent seam cells are responsible for the V5 polarity reversals in *egl-20* mutants, but do not influence polarity in wild-type animals. Using *egl-20* reporter genes, I showed that EGL-20 does not provide direct polarity information to the V5 cell. Our analysis demonstrates complex regulation of a single cell division by cell signaling.

### **INTRODUCTION**

The generation of diverse cell types in a multicellular organism relies on the process of asymmetric cell division: the ability of a single cell to give rise to daughter cells with different fates (Horvitz and Herskowitz, 1992; Jan and Jan, 1998). An important feature of many asymmetric cell divisions is the spatial orientation of the daughter cells relative to each other and to the body axis. The Wnt signaling pathway has been implicated in the polarization of a number of asymmetric cell divisions in a variety of organisms.

In *C. elegans* the Wnt signaling pathway regulates asymmetric cell divisions that occur during embryogenesis and post-embryonic development. In the 4-cell embryo, the EMS blastomere receives a polarizing signal from its neighbor, the P2 germline precursor (Goldstein, 1992). The MOM-5/Fz receptor acts in the EMS blastomere to receive the MOM-2/Wnt signal from the P2 cell (Rocheleau et al., 1997; Thorpe et al., 1997). This

signaling event polarizes the EMS to divide asymmetrically such that the anterior daughter adopts the mesodermal fate and the posterior daughter adopts the endodermal fate.

During post-embryonic development, LIN-44/Wnt and LIN-17/Frizzled regulate the asymmetric divisions of epidermal cells in the tail including B, F, U and T (Herman and Horvitz, 1994; Herman et al., 1995; Sawa et al., 1996; Sternberg and Horvitz, 1988). Interestingly, *lin-44* activity is required for the polarity of these asymmetric divisions, whereas *lin-17* activity is required to generate the asymmetry. LIN-17 also plays a role in the P7.p vulval precursor cell lineage, where it is required for both polarity and asymmetry of the cell division (Sternberg and Horvitz, 1988).

We have shown previously that the EGL-20/Wnt protein regulates Hox gene expression and patterns neuronal migrations along the A/P body axis (Harris et al., 1996; Maloof et al., 1999). Here we show that the *egl-20/Wnt* gene is also required to establish the polarity of asymmetric cell divisions in the lateral epidermis of *C. elegans*. The six epidermal V cells (V1-V6), which give rise to cuticular and sensory structures, divide in a polarized pattern along the A/P axis during the postembryonic larval stages. In wild-type animals, the first division of each V cell is an oriented asymmetric division: the posterior daughters (Vn.p cells) become seam cells that continue to divide, whereas the anterior daughters (Vn.a cells) become epidermal cells that fuse with the epidermal syncytium called *hyp7* (Sulston and Horvitz, 1977). Loss-of-function mutations in *egl-20* cause reversals in the polarity of the V5 daughter cell fates. In *egl-20* mutants, V5.a often becomes a seam cell while V5.p fuses with *hyp7*. Thus, *egl-20* mutants continue to display asymmetry in the V5 division, but are defective in the relative orientation of these two fates along the A/P axis.

Our findings show that multiple signaling systems control the polarity of the V5-cell division. First, in wild-type animals, EGL-20 plays a permissive role in establishing polarity. *egl-20* is expressed in the posterior body region; however, reversing the spatial location of EGL-20 relative to the V5 cell completely rescues the polarity defect in *egl-20(-)*

animals. While EGL-20 signals through a canonical Wnt signal transduction pathway for Hox gene activation, it appears to signal through a different, unidentified pathway to establish polarity in the V5 division. Second, in the absence of *egl-20* activity, signals from posterior seam cells appear to cause polarity reversals in the V5 division, since ablation of these cells in an *egl-20* mutant background completely suppresses the V5 polarity defect. Two genes, *lin-17* and *pry-1*, can influence the orientation of the V5-cell division in *egl-20* mutants, suggesting that they may play a role in this intercellular signaling pathway. In addition, our findings suggest that *lin-44/Wnt* may play a role in spatially restricting the activity of the signals from the posterior seam cells. In the absence of both EGL-20 and posterior neighbors, the V5-cell division polarizes normally. This suggests that the EGL-20/Wnt system plays a role of repressing or overriding a local perturbation in polarity signals, but does not provide essential polarizing information to the V5-cell division.

## RESULTS

### **Mutations in *egl-20* reverse the polarity of the asymmetric V5-cell division**

In wild-type animals, the first division of the epidermal V cells generates a polarized pattern of seam cells and syncytial nuclei along the A/P axis of the worm. These two cell types can be visualized using Nomarski optics and distinguished by differences in the morphology of their nuclei and by the distinctive eye-shaped outline of the seam cells (Figure 4.1A). The seam and syncytial fates also can be distinguished by using the monoclonal antibody MH27, which stains the apical junctions between epithelial cells. Immediately after the V cells divide, MH27 staining reveals the outlines of both daughter cells. However, the outlines of the syncytial daughter cells disappear as they fuse with *hyp7* and lose their cell-cell junctions (Figure 4.1C).

In approximately 50% of *egl-20(n585)* animals, we observed that this alternating pattern of seam and syncytial fates often was disrupted by reversals in the relative positions of the V5 daughter cells. In these animals, the V5.a cell exhibited the morphology of a seam cell and the V5.p cell exhibited the morphology of a syncytial nucleus (Figure 4.1B). Consistent with this observation, the V5.p cell fused with *hyp7* in 27/63 *egl-20(n585)* animals stained with the MH27 antibody (Figure 4.1D). The *n585* mutation behaves as a strong reduction-of-function mutation in genetic tests (Harris et al., 1996). Thus we infer that wild-type *egl-20* activity is required to establish the proper A/P polarity of the asymmetric V5 daughter fates.

The reversals in the relative positions of V5.a and V5.p could arise either because of a polarity reversal within the V5-cell division, or because of migration of the daughters after their birth. For example, the head seam cell (H1) normally undergoes a polarity reversal following its first division in wild-type animals: the seam and syncytial daughter cells move past each other to switch their A/P positions (Sulston and Horvitz, 1977). To distinguish these, we observed the V5-cell division in 14 *egl-20(n585)* animals until the daughter cell fates could be determined unambiguously. In six of these animals, the fates of V5.a and V5.p were reversed, and in eight animals the fates were in the wild-type orientation. The V5 daughters remained stationary in all cases. This finding indicates that the mispositioning of the V5 daughters in *egl-20* mutants arises from reversals in the polarity of asymmetric cell fate specification in the V5-cell division.

The V cells have a polarized asymmetry that can be observed by MH27 staining long before the cells divide (Austin and Kenyon, 1994). In wild-type animals, the V(2-6) cells each have a ventral projection that extends from the anterior half of the cell to the ventral midline. Only the anterior daughters inherit this projection following V-cell division. To determine whether mutations in *egl-20* reversed the asymmetry of the V5 cell itself, we examined *egl-20(n585)* animals stained with MH27. We found that all V-cell morphologies were indistinguishable from wild type, indicating that the initial asymmetry

of V5 itself was normal in *egl-20* mutants (Figure 4.1E). Thus mutations in *egl-20* appear to disrupt the polarity of the V5-cell division rather than that of V5 itself. For simplicity, in this study, we refer to this phenotype as the “V5 polarity” phenotype.

We examined the V5 polarity phenotype in three other *egl-20* alleles. The *egl-20(n1437)* and *egl-20(mu25)* alleles also caused cell fate reversals of the V5 daughters, whereas the weak loss-of-function allele *egl-20(mu39)* allele did not (Table 4.1). None of these mutations affected the divisions of V1-V4, V6 or T, a seam cell located in the tail. The establishment of V5 polarity in *egl-20* mutants appeared to be a temperature-sensitive process since all of the *egl-20* alleles that exhibit V5 polarity reversals were temperature-sensitive for the phenotype (Table 4.1). Therefore an *egl-20*-independent system can polarize the V5-cell division correctly at low temperatures, but not at high temperatures.

*egl-20* activity is also required to specify the correct polarity of later asymmetric divisions in the V5 lineage. We examined the positions and morphologies of the V5 descendants in *egl-20(n585)* animals at the end of the L2 larval stage and observed additional polarity reversals in the second and third divisions of the V5 lineage. In addition, occasional polarity reversals occurred in the third division of the V3, V4, and V6 cell lineages (the second division of these V cells is symmetric and cannot be examined for polarity reversals). Since the frequency of polarity reversals in later V-cell divisions is relatively low (see Table 4.1 legend), we have focused our studies on the V5-cell division in *egl-20(n585)* mutants.

### **Establishment of asymmetry does not appear to require lateral signaling between the V5 daughter cells**

How are the asymmetric cell fates in the V5 division established? One possibility is that intrinsic cell fate determinants are segregated unequally within the V5 cell prior to division. Alternatively, the V5 daughter cells may be equivalent at birth and differentiate later as a result of lateral signaling between the daughter cells or as a result of signaling

from neighboring cells. We tested whether lateral signaling between the V5 daughters was required for cell fate determination in either wild-type or *egl-20(-)* animals. Using a laser microbeam, we ablated one of the V5 daughters shortly after the V5-cell division and then examined the fate adopted by the remaining daughter. Following V5.a ablation in wild-type animals, V5.p always adopted the seam fate (n = 5). Conversely when V5.p was ablated, V5.a always adopted the syncytial fate (n = 8). In *egl-20(n585)* animals, each V5 daughter was able to adopt either the seam or syncytial fate in the absence of the other daughter. Following V5.a ablation, V5.p adopted the seam fate in 5/7 animals and adopted the syncytial fate in 2/7 animals. Similarly when V5.p was ablated, V5.a adopted the seam fate in 5/8 animals and adopted the syncytial fate in 3/8 animals. Together these results suggested that the fate of each daughter is established independently of its sister cell. Thus, ablations in both wild-type and *egl-20(n585)* animals did not reveal evidence for lateral signaling between the V5 daughters.

We determined the temperature-sensitive period (TSP) for V5 polarity determination in *egl-20(n585)* animals (data not shown). Shifting *egl-20(n585)* animals from the restrictive temperature (25°C) to the permissive temperature (15°C) prior to the time of V5 division suppressed the polarity reversal defect, whereas the reciprocal shift resulted in frequent V5 polarity reversals. Animals that were shifted after the time of V5 division exhibited the polarity phenotype characteristic of the original temperature. Thus, in *egl-20* mutants, it appears that polarity is established within the V5 cell and not in the V5 daughters.

### **Genes that act with *egl-20* to activate *mab-5* expression do not influence the polarity of the V5-cell division**

The *egl-20/Wnt* gene is required to activate expression of the Hox gene *mab-5* in the migratory neuroblast QL (Harris et al., 1996; Maloof et al., 1999). Mutations in a number of other genes, including *lin-17/frizzled* (Sawa et al., 1996), *bar-1/β-*

*catenin/armadillo* (Eisenmann et al., 1998), *mig-1*, and *mig-14*, also disrupt *mab-5* expression in these cells (Harris et al., 1996; Maloof et al., 1999). We examined mutations in all of these genes for their effects on V5 polarity, and found that, with one exception, V5 developed normally. Only *mig-14(k124)* animals exhibited V5 polarity reversals at a low frequency (Table 4.2). The *pry-1(mu38)* mutation, a negative regulator of the *mab-5* activation pathway (Maloof et al., 1999), also did not exhibit polarity defects in the V5-cell division. If EGL-20 polarized the V5-cell division by activating this canonical Wnt pathway, then mutations in *lin-17*, *bar-1* and *mig-1* should also have caused polarity reversals. Conversely, if EGL-20 polarized the V5-cell division by repressing this same pathway, then *pry-1* mutations should have caused V5 polarity reversals. Since none of these mutations affected V5 polarity, we infer that EGL-20 exerts its effect on V5 polarity through another, undefined pathway.

We also examined mutations in two genes that affect the polarity of other asymmetric cell fate decisions in *C. elegans*: *lin-44*, a *Wnt* homolog required for normal polarity of the T seam cell lineage (Herman and Horvitz, 1994; Herman et al., 1995) and *lin-18*, which regulates the polarity of two vulval precursor cell lineages (Ferguson et al., 1987). These mutants were not defective in the polarity of the V5 or other V-cell divisions (Table 4.2).

### **The polarity of the V5-cell division is not determined by the spatial pattern of *egl-20* expression in the animal**

How does *egl-20* activity orient the V5-cell division? Previously we showed that a rescuing *egl-20::gfp* transgene is expressed exclusively within a group of epidermal and muscle cells located in the tail region, posterior to V5 (Whangbo and Kenyon, submitted). This suggested a model in which the asymmetric expression of EGL-20 along the A/P axis could provide the spatial information required to orient the V5-cell division. Specifically, because of its expression pattern in the animal, the level of EGL-20 on the posterior side of

the V5 cell would be higher than its level on the anterior side. This, in turn, could impart polarity information to the V5 cell; for example, by biasing receptor activation to one side of the cell. To test this model, we examined the polarity of the V5-cell division in animals in which the source of EGL-20 was moved from the posterior to the anterior (Figure 4.2A). The *myo-2-egl-20::gfp* fusion gene, which is expressed only in the pharynx, is able to rescue the Q cell migration defects of *egl-20* mutants (Whangbo and Kenyon, submitted). When we examined the *egl-20(-)* animals carrying the *myo-2-egl-20::gfp* fusion in which the QL descendants were restored to their normal positions, we found that the polarity of the V5-cell divisions was also wild type (Figure 4.2B). Therefore the polarity of the V5 division is not dependent upon the posterior localization of EGL-20.

### **Overexpression of EGL-20 causes ectopic polarity reversals in the V cells**

Next, we tested whether the level of EGL-20 could influence the polarity of the V5-cell division. We provided different doses of hs-EGL-20 by varying the duration of heat shock in *egl-20(-)* animals carrying a *hs-egl-20* fusion gene (Whangbo and Kenyon, submitted). In the absence of heat shock, the V5 cell divided with reversed polarity at the expected frequency for *egl-20(n585)* animals at 20°C (Fig. 2C). We observed that a 5-minute pulse of *hs-egl-20* significantly suppressed the frequency of polarity reversals (Figure 4.2C). Surprisingly, we found that higher levels of hs-EGL-20 could disrupt the polarities of all the V-cell divisions (Figure 4.2C). Thus, although these other V cells normally do not require *egl-20* activity to establish their polarities, they are capable of responding to the EGL-20 signal.

What genes are required for high levels of hs-EGL-20 to cause these ectopic V-cell polarity reversals? We provided hs-EGL-20 in various strains carrying mutations in known components of the EGL-20 signal transduction pathway for *mab-5* activation. We observed that a mutation in the *mig-14* gene was able to suppress the ectopic polarity reversals (Table 3). To ask whether *mig-14* might affect the production of EGL-20, we



looked at the distribution of EGL-20::GFP in *mig-14(k124)* animals. We detected the EGL-20::GFP fusion protein using polyclonal antibodies specific for GFP. In wild-type animals, we observed that the EGL-20::GFP was present outside of the expressing cells (Figure 4.3A). However, in *mig-14(k124)* animals, the EGL-20::GFP did not appear to travel as far as in wild type (Figure 4.3B). Thus *mig-14* appears to be required for the normal secretion or distribution of EGL-20. We found that mutations in *lin-17* and *bar-1* did not have an effect did not alter the response of the V cells to hs-EGL-20. Therefore, like the response pathway required for EGL-20 to polarize the V5 division, the signal transduction pathway through which hs-EGL-20 polarizes the other V-cell divisions is unknown.

### **Signals from neighboring cells orient the V5-cell division in *egl-20* mutants, but not in wild-type animals**

Previous studies have shown that in the wild type, contact-dependent signaling between V cells can influence the fates of cells in the V5 lineage at later developmental stages (Austin and Kenyon, 1994; Sulston and White, 1980; Waring et al., 1992). Therefore, we asked whether signals from neighboring V cells might influence the polarity of the V5-cell division in wild-type or in *egl-20(n585)* animals.

To address this question, we used a laser microbeam to ablate seam cells adjacent to V5 in wild-type animals and subsequently examined the polarity of the V5-cell division (Table 4.4). We found that V5 divided with wild-type polarity after ablation of either its anterior (V1-V4) or posterior (V6 and T) neighbors. V5 also divided correctly after ablation of all the seam cell neighbors (V1-V4, V6 and T). Thus, signals between V cells were not required for correct polarity of the V5-cell division in the wild type.

Surprisingly, we found that ablation of neighboring cells was able to influence the polarity of the V5-cell division in *egl-20* mutants (Table 4.4). V5 always divided with wild-type polarity in *egl-20* mutants in which V6 and T were ablated. Thus, ablation of

posterior neighbors in an *egl-20* mutant appeared to suppress the V5 polarity reversal defect. To confirm that the V-cell descendants remained stationary under these conditions, we observed the V5 division in six *egl-20(n585)* animals in which V6 and T had been ablated until the fates of the daughter cells could be distinguished clearly. In all six animals, the V5 daughter cells remained stationary and adopted the wild-type fates. Thus, we conclude that removal of posterior seam-cell neighbors in *egl-20* mutants can restore wild-type polarity to the V5 division. These results implied that the polarity of the V5-cell division was reversed in *egl-20* mutants because V5 received “polarity-reversing” signals from the posterior seam cells.

Next, we tested whether ablation of both V6 and T was necessary for rescue of the V5 polarity reversals in *egl-20* mutants. We found that ablation of V6 alone was not sufficient for complete rescue of the V5 polarity reversals in *egl-20* mutants and that ablation of T alone had no rescuing activity (Table 4.4). These results suggested that the signaling between V5 and its posterior neighbors occurred through direct cell-cell contact or short-range signals.

The V5 cell appears to be unique in its ability to respond to the polarity-reversing signals in *egl-20(n585)* animals. Austin and Kenyon (1994) have shown that seam cells are capable of forming new contacts when their normal neighbors have been removed by cell ablation. To allow V4 to move closer to V6, we ablated the two intervening cells, Q and V5, at hatching. In all six ablated animals, V4 always divided with normal polarity.

Since signals from posterior seam cells influenced the polarity of the V5-cell division in *egl-20* mutants, we asked if anterior cells were also capable of signaling. Ablation of the anterior seam cells (V2-V4) did not significantly alter the frequency of V5 polarity reversals in *egl-20* mutants (Table 4.4). Ablation of both anterior and posterior neighbors completely rescued the V5 polarity reversals in *egl-20* mutants, as observed for posterior ablations alone (Table 4.4). Thus, the anterior seam-cell neighbors did not influence the polarity of the V5 division in *egl-20* mutants.

### ***lin-44* does not encode the polarity-reversing signal**

What is the pathway responsible for generating polarity reversals in *egl-20* mutants? One possibility was that in the absence of EGL-20, another Wnt signal is able to provide polarity information to the V5 cell. We tested whether this other Wnt signal might be encoded by *lin-44*, which is expressed in tail hypodermal cells and orients the asymmetric divisions of certain tail epidermal cells (Herman and Horvitz, 1994; Herman et al., 1995). If *lin-44* encoded the polarity-reversing signal, then removing *lin-44* activity should suppress the reversals in an *egl-20(-)* background. However when we constructed the *lin-44(n1792); egl-20(n585)* double mutant strain, we observed that the V5 cell continued to divide with reversed polarity at a high frequency (Table 4.2). These results are not consistent with the model that LIN-44 is the primary polarity-reversing signal in *egl-20* mutants. However, the polarity reversals in the double mutant occurred at a slightly lower frequency than in *egl-20(n585)* single mutants, thus LIN-44 might possibly make a minor contribution to the polarity-reversing signal.

### **Mutations in *lin-17/Frizzled* prevent V5 polarity reversals from occurring in *egl-20/Wnt* mutants**

To determine whether any of the *mab-5* activation pathway genes might act within the signaling system that generates polarity reversals in *egl-20* mutants, we constructed double mutant strains carrying mutations in these genes as well as *egl-20(n585)*. Most of the mutations we examined did not have a strong or consistent effect on the *egl-20(n585)* V5 polarity phenotype (Table 4.2). However, mutations in *lin-17/frizzled* completely suppressed the V5 polarity reversals observed in *egl-20(n585)*. In *lin-17(-); egl-20(n585)* double mutants containing either the *lin-17(n671)* or the *lin-17(n677)* allele, the V5 daughter cells almost always developed normally. Mutations in *lin-17* produced the same

effect as ablation of V6 and T in *egl-20* mutants: both suppressed the V5 polarity reversals. Thus LIN-17 might act in the signaling system between V cells.

In addition, mutations in both alleles of *lin-18* consistently were able to suppress the V5 polarity reversals in *egl-20(-)* mutants from 50% to 30% (Table 4.2). Like *lin-17*, *lin-18* is also required to orient asymmetric cell divisions in the vulval precursor lineages. Thus, they may be acting together to cause polarity reversals in *egl-20* mutants. We also examined mutations in *mig-1*, and found that they did not have a consistent effect on the polarity of the V5-cell division (Table 4.2). Therefore, it is not clear at this point whether *mig-1* has a role in this process.

### **Mutations in *pry-1* enhance the frequency of V5 polarity reversals in *egl-20* mutants**

The *pry-1* gene functions as a negative regulator downstream of *egl-20* and upstream of *bar-1/Armadillo* in the *mab-5* activation pathway. Mutations in *pry-1* activate *mab-5* expression in both QL and QR in an *egl-20*-independent but *bar-1*-dependent fashion (Malloof et al., 1999). We examined the polarity of the V5-cell division in *pry-1*; *egl-20* double mutants and found that V5 divided with reversed polarity in a clear majority of animals (80%) (Table 4.2). Thus *pry-1*, like *lin-17*, appears to function in the pathway that reverses the polarity of the V5-cell division in *egl-20* mutants. The *pry-1*; *lin-17* double is too unhealthy to examine; thus we could not order these two genes in a genetic epistasis pathway.

### **LIN-44 is not required in order for the ablation of V6 and T to rescue the V5 polarity defect in *egl-20* mutants**

In the absence of both *egl-20* and V5's posterior neighbors, the V5 cell always divides with normal polarity. Thus, there is another system that can polarize V5. What genes are involved in this polarization pathway? In *Drosophila* there is evidence that the

Patched transmembrane protein restricts movement of the Hedgehog secreted signal (Chen and Struhl, 1998). Similarly, it seemed possible that the LIN-17/Fz could bind and sequester a second Wnt signal that would otherwise orient V5 correctly in *egl-20* mutants. We tested the possibility that the *lin-44/Wnt* gene encoded such a rescuing signal, since this gene is also expressed in the posterior of the animal and affects the polarities of asymmetric cell divisions (Herman et al., 1995). We ablated V6 and T in *lin-44(n1792); egl-20(n585)* double mutants (Table 4.4). If *lin-44* encoded the rescuing signal, then ablation of the posterior neighbors in the double mutant background should not suppress the V5 polarity reversals. Our results were only partially consistent with this model. We did observe some suppression on the ablated side, but not complete suppression as in *egl-20* single mutants. Surprisingly, we also observed the same level of suppression on the unablated sides. Thus, in *lin-44* mutants, ablation of V cells on one side of the animal had an effect on the other side. One interpretation of this curious result is that *lin-44* is required to restrict the polarity-reversing signal to one side of the animal.

### ***egl-20* and *lin-44* can functionally replace each other**

Since both *egl-20* and *lin-44* encode Wnt proteins that influence cell polarity, we wondered whether the two Wnt genes were interchangeable. We first introduced an extrachromosomal array carrying *hs-lin-44* into *egl-20(n585)* animals. We found that a 30-minute pulse of heat shock at 33°C could cause both QL and QR descendants to remain in the posterior and also could cause ectopic polarity reversals (Table 4.5). Both effects are similar to the effects of *hs-egl-20*. We also introduced an integrated array carrying *hs-egl-20* into *lin-44(n1792)* animals. We found that a 30-minute heat pulse in this strain could significantly rescue the T polarity defect, as inferred from the number of animals whose phasmids filled with DiI (Table 4.5). Thus *egl-20* and *lin-44* may have overlapping biochemical properties, although they are divergent at the level of their primary sequences.

## DISCUSSION

In this study, we have examined the effects of Wnt pathway family members and cell-cell interactions on the polarity of the V5-cell division. We find that in the wild type, the EGL-20/Wnt protein is required in order for the V5-cell division to polarize correctly. In the absence of EGL-20, signals from neighboring seam cells appear to reverse the polarity of the V5-cell division. When these signals are removed (by ablation of posterior neighbors), V5 can divide correctly again. Thus this system appears to involve three interrelated pathways: first, an EGL-20-dependent pathway that can override the effects of posterior seam cells; second, the cell-cell interaction pathway that can reverse the polarity of the V5-cell division in the absence of EGL-20, and third, an underlying polarity determining system that operates independently of both EGL-20 and signals from neighboring cells. We now discuss each of these three pathways in turn.

### **The role of EGL-20 in the polarization of the V5-cell division.**

In the wild type, *egl-20* function is required to polarize the V5-cell division correctly. One of the most surprising findings of this study is that despite its localized expression pattern in the animal, the EGL-20 protein appears to play a permissive rather than instructive role in cell polarization. If the spatial pattern of *egl-20* expression were important, then the ectopic expression of *egl-20* would be expected to completely reverse or else randomize V5 polarity. However, we found that expression of *egl-20* either in the head under the control of a pharyngeal promoter, or in a more global fashion under the control of a heat-shock promoter could rescue the V5 polarity defect in *egl-20(-)* mutants. This finding indicates that EGL-20 does not provide the spatial information required for cells to distinguish anterior from posterior. Instead, the cells receive this information from another source. EGL-20 appears to be required for V5 to respond to this information correctly.

Like *egl-20*, the *lin-44/Wnt* gene is also expressed in the tail region. Moreover, both genes are expressed and acting to influence epidermal cell polarity at the same time in development. The different functions of these two Wnt genes may be defined by their spatial restriction: *lin-44* is expressed in a group of hypodermal cells located in the tail whereas *egl-20* is expressed in a group of postembryonic blast cells located anteriorly to the site of *lin-44* expression. Each Wnt protein appears to pattern located just anterior to its site of expression. *lin-44* regulates the polarity of the epidermal T, B, F and U cell divisions whereas *egl-20* regulates polarity of the V5 division and cell migrations of the HSN neuron and Q descendants. Thus it is possible that other body region-specific Wnt proteins regulate the polarities of the other seam cell divisions in the animal.

Interestingly, like *egl-20*, *lin-44* may also act in a position-independent fashion, since hs-LIN-44 can rescue the T polarity defect seen in *lin-44(-)* mutants (Herman et al., 1995). Together these findings suggest that these Wnt proteins do not directly determine the polarities of the cell divisions they control. Instead, the polarities of these cells must be determined by another system of positional information that requires Wnt signaling in a permissive fashion to be expressed properly.

The LIN-17/Fz protein has been proposed to function as a receptor for LIN-44 in establishing polarity of the T cell division. Mutations in *lin-17* cause the T cell to divide symmetrically instead of asymmetrically, and *lin-17* mutations are epistatic to *lin-44* mutations (Sawa et al., 1996). Likewise, it is possible that LIN-17 functions as a receptor for EGL-20 to activate *mab-5* expression in the migrating QL neuroblast, since *lin-17* mutants also fail to activate *mab-5* expression correctly. Surprisingly, we find that LIN-17 is not likely to act as a receptor (at least as the sole receptor) for EGL-20 to polarize the V5-cell division, since *lin-17* mutations do not affect V5 polarity. In addition, none of the other mutations in genes known to function in the EGL-20-response pathway in the QL neuroblast affect the V5-cell division. These include mutations in genes thought to be activated by *egl-20* activity (such as *lin-17*, *mig-1* and *bar-1*) as well as genes thought to be

repressed by *egl-20* (*pry-1*). If EGL-20 functioned to activate this response pathway, then mutations in *lin-17*, *mig-1* and *bar-1* should produce polarity defects, and if EGL-20 functioned to inhibit this pathway, then *pry-1* mutations should produce polarity defects. Since none of these genes produce polarity defects, we conclude that EGL-20 does not affect V5 polarity by affecting this pathway. The identity of the EGL-20 response pathway for V5 polarity is not known.

Because LIN-44 and EGL-20 both affect cell polarity, we asked whether their functions might be interchangeable. Our findings suggest that EGL-20 can act through LIN-17 to polarize the T cell division. Conversely, LIN-44 can act through the EGL-20-response pathway to polarize the V5-cell division. The simplest way to explain these observations is to propose that a different *frizzled* homolog that can bind both EGL-20 and LIN-44 acts as the EGL-20 receptor in V5.

Like *egl-20*, the *mig-14* gene is also required to polarize V5 in the wild type. The *mig-14* gene is required for many if not all of the *egl-20* functions, including activation of *mab-5* expression, the anterior migration of the QR descendants and the polarization of the V5-cell division. We find that the localization of EGL-20 protein in *mig-14* mutants is limited to the cells that produce it and their immediate surroundings, suggesting that *mig-14* activity is required for establishing the correct distribution of EGL-20. In otherwise wild type animals, *mig-14* mutations produce only a minor V5 polarization phenotype, whereas *mig-14* is completely required for high levels of EGL-20 to produce widespread seam-cell polarity reversals in otherwise wild-type animals. Possibly this is because some EGL-20 protein can be processed or distributed normally in *mig-14* mutants, but not enough to trigger ectopic polarity reversals.

If the only role of *mig-14* were to process EGL-20, then one would predict that the double *mig-14; egl-20* mutant would have a phenotype similar to that of *egl-20* mutants alone. Instead, the phenotype of the double mutant is more severe than that of either single mutant. The *egl-20* mutations we examined are thought to reduce but not eliminate *egl-20*



activity. Thus one possibility is that *mig-14* mutations lower the small level of residual EGL-20 protein present in the *egl-20* mutants we examined. Alternatively, *mig-14* could be required for the processing of another Wnt protein that also influences V5 polarity.

### **Signals from posterior neighbors polarize the V5-cell division in *egl-20* mutants**

Our findings suggest that the apparently random polarization of the V5-cell division seen in *egl-20* mutants is actually caused by “polarity-reversing signals” that depend on the presence of posterior seam cells. When these posterior neighbors, V6 and T, are ablated, V5 divides correctly even in the absence of *egl-20* activity. Killing either V6 or T alone does not produce this effect, suggesting that the presence of either cell is sufficient to reverse the polarity of the V5-cell division in *egl-20* mutants. Ablating the anterior seam cells does not affect V5 polarity, suggesting that these cells do not produce the polarity-reversing signals. This finding suggests that the role of EGL-20 in the wild type is either to override or inhibit these “polarity-reversing” signals.

### ***lin-17* and *pry-1* influence the polarity of V5 in *egl-20* mutants.**

Our findings indicate that two genes, *lin-17* and *pry-1*, affect the polarity of the V5-cell division in *egl-20* mutants. *lin-17* activity is required for the polarity reversals seen in *egl-20* mutants, since *lin-17(-)* mutations prevent the polarity reversals. Conversely, the *pry-1* gene is required for the wild-type V5 polarization seen in many *egl-20(-)* animals, since *pry-1* mutations enhance the reversal frequency. Unfortunately, we were not able to determine whether these two genes act in a linear pathway to regulate V5 polarity, since the *lin-17 pry-1* double mutant is too unhealthy to analyze. One possibility is that the balance of *lin-17* and *pry-1* activities determines whether cells divide with a normal or reversed polarity. If these genes act in V5, then they could determine how V5 responds to polarity-

reversing signals from V5. If they act in V6 and T, then they could affect the production of polarity-reversing signals.

The fact that LIN-17 is a putative Wnt receptor suggests that another Wnt protein may function in the signalling pathway that reverses the polarity of the V5-cell division. If so, our findings rule out the possibility that the LIN-44/Wnt protein is the “reverse signal”, since *lin-44* mutations have only a minor effect on the polarity reversals seen in *egl-20* mutants. However, it is possible that a different Wnt signal may act in this pathway.

### **What orients the V5-cell division along the A/P body axis?**

In this study we have shown that although EGL-20 is located asymmetrically along the A/P body axis, it does not provide the V5 cell with the information it requires to distinguish anterior from posterior. In *egl-20* mutants, signals from posterior cells can reverse the polarity of V5, however once the posterior neighbors (or both posterior as well as anterior neighbors) are ablated, the V5 cell divides with normal polarity. Therefore a polarizing system that is independent of both *egl-20* as well as neighboring cells appears to orient the V5 cell along the A/P body axis. We propose that in the absence of *egl-20*, signals from neighboring cells can cause V5 to reverse its response to this polarizing information, and as a consequence, reverse the relative positions of its two daughter cells along the A/P body axis. In the wild type, *egl-20* acts through an unknown pathway to override or inhibit these polarity-reversing signals. Thus it appears that *egl-20* is required not to provide cells with fundamental polarizing information, but instead to prevent a local perturbation in polarizing information from arising. *lin-44* may play a similar role in the T cell, and perhaps other Wnt signals play similar roles in other seam cells. Why such a complex polarity-determining system should exist is not yet clear.

What is the system that provides the positional information necessary to allow the cells to distinguish anterior from posterior? It is possible that the actual polarizing signal acts in a global fashion. With few exceptions, the anterior daughters of each cell that

divides along the A/P axis expresses a single gene, the TCF homolog *pop-1* (Lin et al., 1998), suggesting the possibility of a globally-acting polarization activity. In the early embryo, the A/P localization of POP-1 is regulated by the MOM-2/Wnt protein which both orients and polarizes the EMS cell division (Rocheleau et al., 1997; Thorpe et al., 1997). Thus Wnt family members are capable of providing the spatial information that allows dividing cells to distinguish anterior from posterior. If a Wnt protein provides the V cells with spatial information required to orient correctly along the A/P axis, it may have escaped detection because it functions redundantly with other factors, or because it has an essential function in the animal. Alternatively, it is possible that this fundamental polarizing information is not provided by a Wnt signal, but instead by another type of signal. Our findings suggest that cells that divide asymmetrically have the potential to align themselves either “with” or “against” this field of polarizing activity, and that this orientation decision can be regulated by Wnt proteins such as EGL-20.

## **MATERIALS AND METHODS**

### **General Procedures, Nomenclature, and Strains**

Methods for routine culturing and genetic analysis are described by Brenner (1974) and Sulston and Hodgkin (1988). All experiments were performed at 25°C, unless otherwise noted. The wild-type strain N2 is the parent of all strains used with the exception of *egl-20(n1437)*, which was isolated in an MT2878 background.

### **Strains**

LG I: *lin-17(n671)*, *lin-17(n677)*, *lin-44(n1792)*, *mig-1(e1787)*, *pry-1(mu38)*

LG II: *mig-14(mu71)*, *mig-14(k124)*

LG III: *mul549[egl-20::gfp, pPD10.46 (unc-22 anti-sense)]*

LG IV: *egl-20(n585)*, *egl-20(n1437)*, *egl-20(mu25)*, *egl-20(mu39)*

LG V: *him-5(e1490)*, *mul553[hs-egl-20, pPD10.46]*

LGX: *bar-1(ga80)*, *lin-18(e620)*, *lin-18(n1051)*

### **Construction of double mutant strains**

To construct unlinked double mutants with *egl-20*, we first constructed a triple mutant strain containing the non-*egl-20* mutation and the *unc-24(e138)* and *dpy-20(e1282)* mutations. These triple mutant strains were then crossed as heterozygous males to *egl-20* hermaphrodites. The non-*egl-20* mutation was homozygosed first. Wherever possible, a phenotype other than a QL descendant or HSN migration (Mig) defect was used to determine the presence of the non-*egl-20* mutation. The *egl-20* mutation was homozygosed by chasing out the *unc-24(e138) dpy-20(e1282)*-marked chromosome IV.

***lin-17; egl-20***. Although approximately 48% of *mab-5(e2088)/+; egl-20(n585)/+* animals have a QL descendant Mig defect (Harris et al., 1996), *egl-20* does not have a transheterozygous interaction with *lin-17* mutations at 20°C (data not shown). The *lin-17(n671)* mutation suppressed the *egl-20* polarity reversal phenotype (Table 2) and partially suppressed the HSN and QL descendant Mig defects (data not shown). We therefore performed a complementation test to demonstrate the presence of an *egl-20* mutation in this strain (data not shown).

***egl-20; lin-18 and lin-44; egl-20***. Since *lin-44(n1792)* and *lin-18(e620)* do not affect QL descendant migrations (data not shown), we determined the presence of the *egl-20* mutation by scoring the Mig defect of the QL descendants. In addition, the phasmid neurons in *lin-44* mutants do not stain with the fluorescent dye, DiO (3,3'-dioctadecyloxycarbocyanine) (Herman and Horvitz, 1994), whereas the phasmid neurons in *egl-20* mutants fill normally (data not shown). This dye-filling phenotype was used to determine the presence of the *lin-44* mutation in the double mutant strain. The *lin-18* mutation was determined by the presence of a Bi-vulva phenotype (Ferguson and Horvitz, 1985).

### **Determining the fates of V5.a and V5.p**

The V5 daughter cell fates were identified directly by Nomarski differential interference contrast (DIC) microscopy. In wild-type animals, V5.a and V5.p adopt syncytial and seam cell fates, respectively. Along with differences in developmental potential, these two cell types differ in the morphology and placement of their nuclei (Sulston and Horvitz, 1977). The nucleus of V5.a is placed slightly ventral to the seam cell nucleus and has a granular nucleoplasm. In addition, V5.a fuses with the hyp7 syncytium and loses its cellular outline. The nucleus of the seam cell daughter (V5.p) is located laterally, in the focal plane directly below the alae (cuticular ridges). V5.p has a distinctive eye-shaped outline and a smooth nucleoplasm. Occasionally, in animals in which the fates of the V5 daughters were reversed, the seam cell nucleus was located ventrally rather than laterally.

In general, the above criteria remained applicable for determining the polarity of subsequent divisions in the V-cell lineages. Polarity was not determined for the second division of the V1-V4 and V6 lineages since all these divisions are symmetric (both daughters become seam cells). However, the second division of the V5 lineage remains asymmetric: the V5.p cell divides to generate a neuroblast (anterior daughter) and a seam cell (posterior daughter). The neuroblast has a grainy appearance under Nomarski optics, and continues to divide during the second larval stage (L2) to produce a neuronal structure called the postdeirid. The pattern of seam cell divisions in the third division is identical to that of the first division in all the V-cell lineages.

### **Immunofluorescence**

Animals were fixed and stained as described in Austin and Kenyon (1994) using the MH27 monoclonal antibody (provided by R. Barstead and R. Waterston.).

For anti-GFP staining, staged L1 larvae were fixed and stained as above. The rabbit polyclonal GFP antibody (Clontech) was used at a dilution of 1:1000. Rhodamine-conjugated goat anti-rabbit IgG (1:200) was used as the secondary antibody.

## **Cell Ablations**

Larvae were staged by collecting newly hatched animals at 30 minute intervals. The newly hatched animals were transferred to a fresh plate and allowed to feed for 30 minutes before mounting for ablation. Thus, the staged worms were 0.5 to 1 hour old at the start of ablations. Worms were ablated over the course of the next 30 minutes, so that all ablations were complete by 1.5 hours after hatching.

Individual cells were killed using a laser microbeam as described in Waring et al. (1992). Worms were immobilized for ablation on agarose pads containing 2-3 mM sodium azide. Operated worms were removed from the pad as soon as possible to minimize effects of the azide on development and viability, and then allowed to develop for 7-12 hours on a plate seeded with bacteria. Subsequently, the worms were remounted to confirm the absence of ablated cells and to determine the pattern of V5 daughter nuclei. The unablated sides of the experimental animals served as internal controls. In general, the ablation procedure produced only small developmental delays. Operated animals whose development appeared significantly retarded were discarded.

For lineaging after ablation, operated worms were allowed to recover for 3 hours on a seeded plate. The worms were then remounted and observed continuously until the V5 cell had divided and the fates of the daughters could be determined unambiguously based on nuclear morphology and position.

## **Temperature shift experiments**

Gravid hermaphrodites from populations cultured for at least two generations at either 15°C or 25°C were treated with alkaline hypochlorite to release their eggs (Sulston and Hodgkin, 1988). Larvae were staged by collecting newly hatched animals at 30 minute intervals and placing them on plates that had been preincubated at the initial temperature. To perform the "down-shift" experiment, staged animals on plates at 25°C were collected periodically in M9 media that had been preincubated at 15°C, pelleted briefly, and transferred to seeded

plates that also had been preincubated at 15°C. To perform the "up-shift" experiment, staged animals growing at 15°C were collected in M9 media that had been preincubated at 25°C and transferred to plates preincubated at 25°C. The shifted animals were allowed to continue developing at the new temperature. V5 polarity was determined after all V cells had divided once, and the P nuclei had descended into the ventral nerve cord.

### **Reporter Genes and Transgenic Arrays**

The rescuing *egl-20::gfp* translational fusion (pJW31), the *myo-2::egl-20-gfp* fusion (pJW33) and the *hs-egl-20* fusion (pJW30) were described previously (Whangbo and Kenyon, submitted). The extrachromosomal array *muEx68* was generated by injecting pJW33 at 20 ng/μl and pPD10.46 at 125 ng/μl into *egl-20(n585)* animals. The

extrachromosomal array *muEx88* contains pMHE19 injected at 20 ng/μl and pPD10.46 co-injected at 125 ng/μl.

### **Heat Shock Conditions**

Staged populations of larvae grown at 20°C were collected at 0 to 30 minutes after hatching and were subjected to heat shock for various lengths of time on an aluminum block that was maintained at 33°C. Immediately after heat shock, the animals were placed at 20°C and allowed to grow until the V-cell divisions were complete (end of L1 larval stage). Rescue of the phasmid defects in *lin-44* mutants was scored using a dye-filling assay, as described by Herman and Horvitz (1994).

### **ACKNOWLEDGEMENTS**

We would like to thank Lisa Williams for construction of the *pry-1(mu38); egl-20(n585)* double mutant, Mike Herman for pMHE19 (*hs-lin-44*), the Bargmann lab for anti-GFP antibodies and members of the Kenyon lab for extensive discussions. J.W. was supported

**Figure 4.1.** *egl-20* activity is required to orient the V5-cell division. Nomarski photomicrographs (A, B) of L1 larvae on agarose pads containing 100 mM azide, which enables visualization of the seam cell outlines. Fluorescence micrographs (C-F) of L1 larvae stained with monoclonal antibody MH27 to visualize outlines of the V cells. Tracings of the photographs are shown to the right. P cells are shaded in gray. Animals are oriented with anterior to the left. Scale bar is 10  $\mu$ m.

- (A) Wild-type. The posterior V5 daughter (V4.p) has adopted the seam cell fate and has a visible cell outline. The anterior V5 daughter (V5.a) has adopted the syncytial fate. Its nucleus is slightly ventral to the V5.p nucleus, and its nucleoplasm has a grainy texture.
- (B) *egl-20(n585)*. The polarity of the V5 division is reversed: V5.a has the morphology and position of a seam cell and V5.p has the morphology and position of a syncytial nucleus.
- (C) Wild-type animal, 2-4 hrs after hatching. The V2-V6 cells have a ventral projection from the anterior half of the cells that reaches to the ventral midline of the worm (n = 20).
- (D) Wild-type animal, 6-8 hrs after hatching. The anterior daughters of the V cells have fused with the *hyp7* syncytium and have lost their outlines (n = 26).
- (E) *egl-20(n585)* animal, 2-4 hrs after hatching. V-cell morphologies are normal (n = 20).
- (F) *egl-20(n585)* animal, 6-8 hrs after hatching. A polarity reversal in the V5-cell division resulted in the fusion of V5.p with the *hyp7* syncytium (47% of the animals examined showed a reversed fusion pattern in the V5 lineage, n = 55).



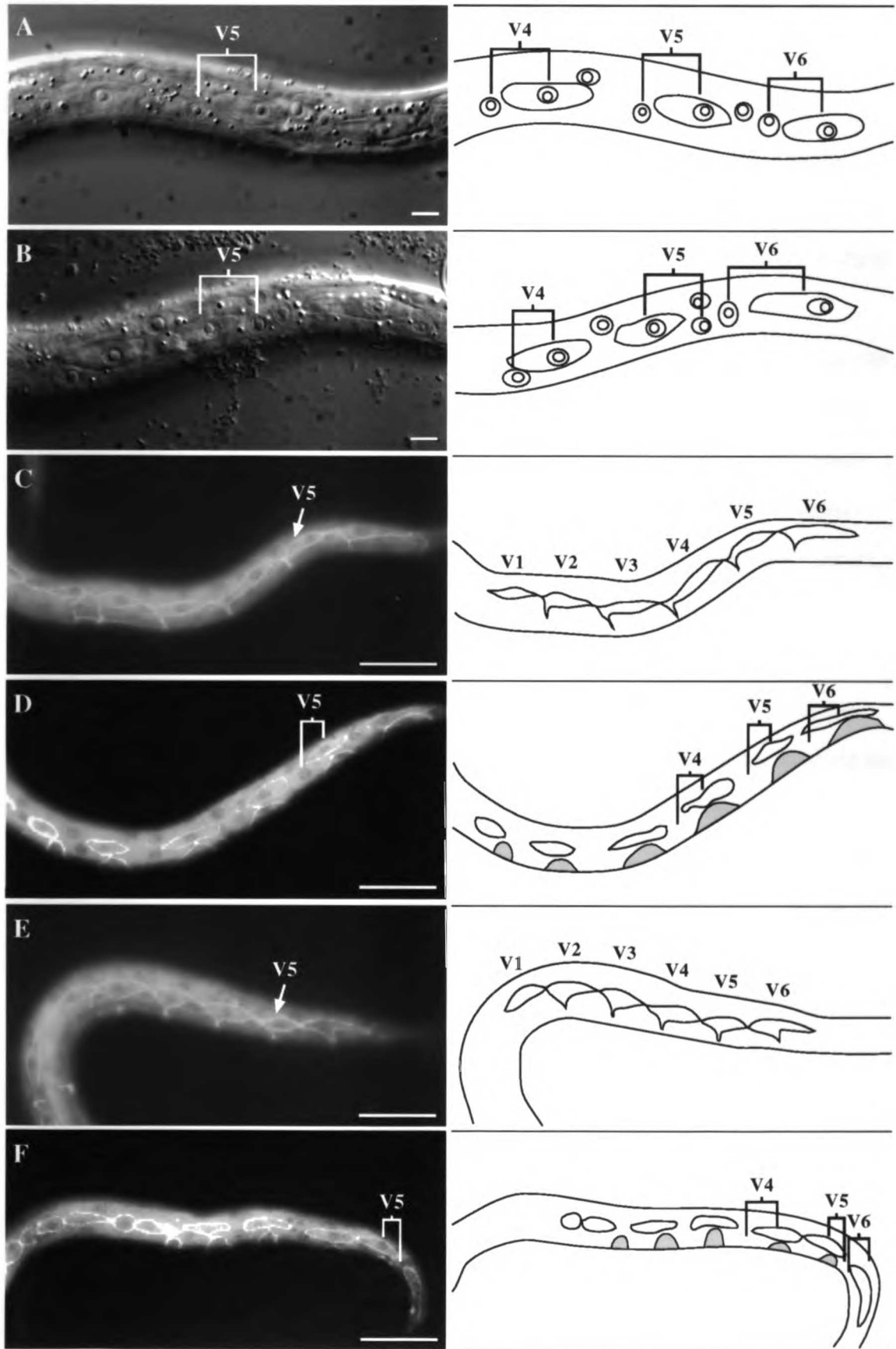
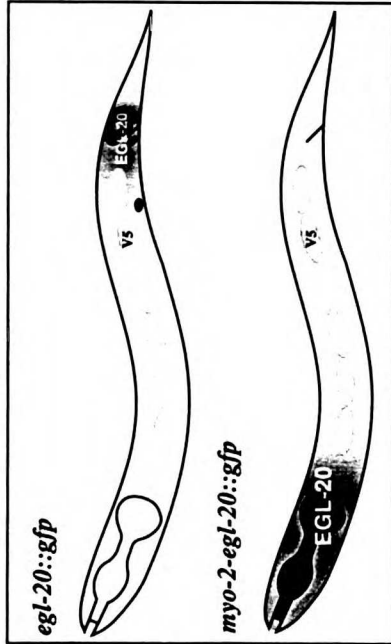


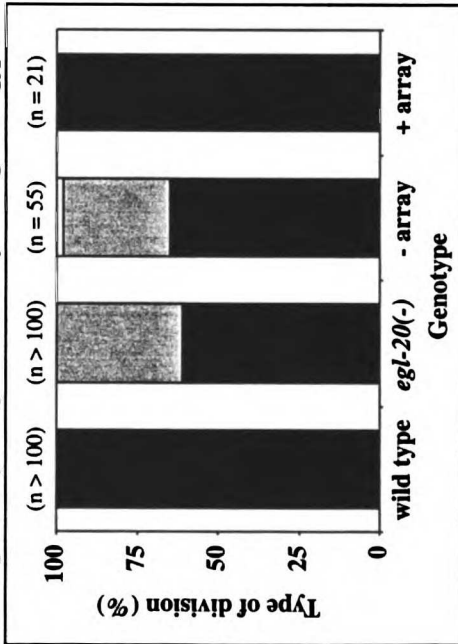
**Figure 4.2.** Posterior localization of EGL-20 is not required to orient the V5-cell division. All animals were examined at 20°C. (n) is the number of animals. p is the Fisher's exact p-value.

- (A) Schematic diagram of *egl-20* expression pattern in *egl-20(-)* L1 larvae carrying the following transgenes: *egl-20::gfp* (top) and *myo-2-egl-20::gfp* (bottom). Cells expressing the *egl-20* fusion genes are shaded in black. The putative EGL-20 gradient is represented by gray shading. The six V cells are represented by ovals.
- (B) Frequency of V5 reversals in *egl-20(n585)* animals that have lost (-) or retained (+) the *muEx68* (*myo-2-egl-20::gfp*) extrachromosomal array. Wild-type and *egl-20(n585)* data are shown for reference. We scored only *egl-20(-)* animals carrying the *myo-2-egl-20::gfp* in which the QL migration defects were rescued. *egl-20(n585)* animals carrying the *myo-2-egl-20::gfp* array are rescued for V5 polarity compared to animals that have lost the array (p = 0.0009). Solid black shading represents wild-type polarity. Dark gray shading represents reversed polarity. Light gray shading represents symmetric divisions in which both daughter cells adopt the syncytial fate.
- (C) Frequency of V-cell polarity defects in animals carrying integrated arrays containing *hs-egl-20* and *mab-5::lacZ*. The frequency of V5 reversals in animals following five minute heat shock is significantly suppressed compared to animals without heat shock (p = 0.0001). Surprisingly, a 10-minute heat pulse disrupts the polarities of all the V-cell divisions.

**A EGL-20 localization**



**B V5 polarity in *egl-20(-)* + *myo-2-egl-20::gfp***



**C *egl-20(-)* + *hs-egl-20***

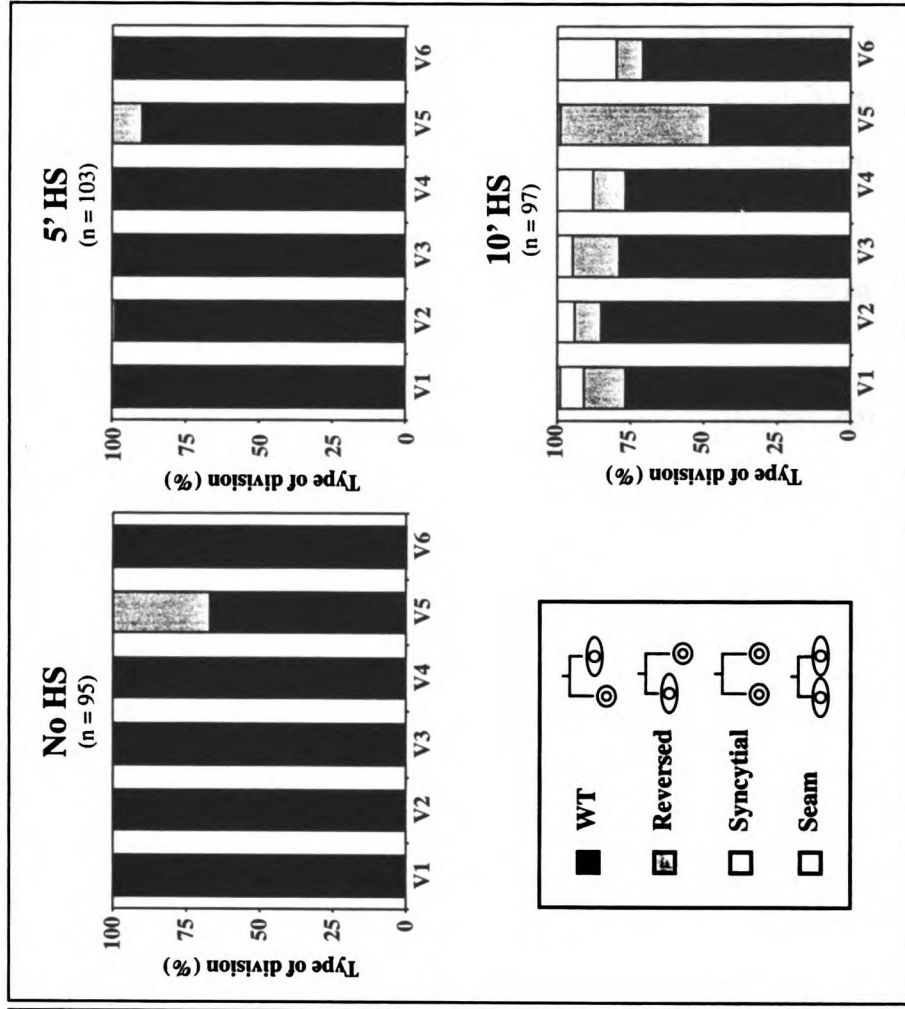


**Figure 4.3.** The EGL-20::GFP distribution is altered in a *mig-14(k124)* mutant background. Fluorescence micrographs of larvae 2-4 hrs after hatching stained with a polyclonal antibody against the GFP protein (Clontech) to visualize the *egl-20::gfp* expression pattern. Animals are oriented such that anterior is to the left and ventral is down. The tail region is shown.

(A) Wild-type animals carrying the integrated array *mulS49(egl-20::gfp)*. Exposure time = 300 ms.

(B) *mig-14(k124)* animals carrying the integrated array *mulS49(egl-20::gfp)*. Exposure time = 400 ms.

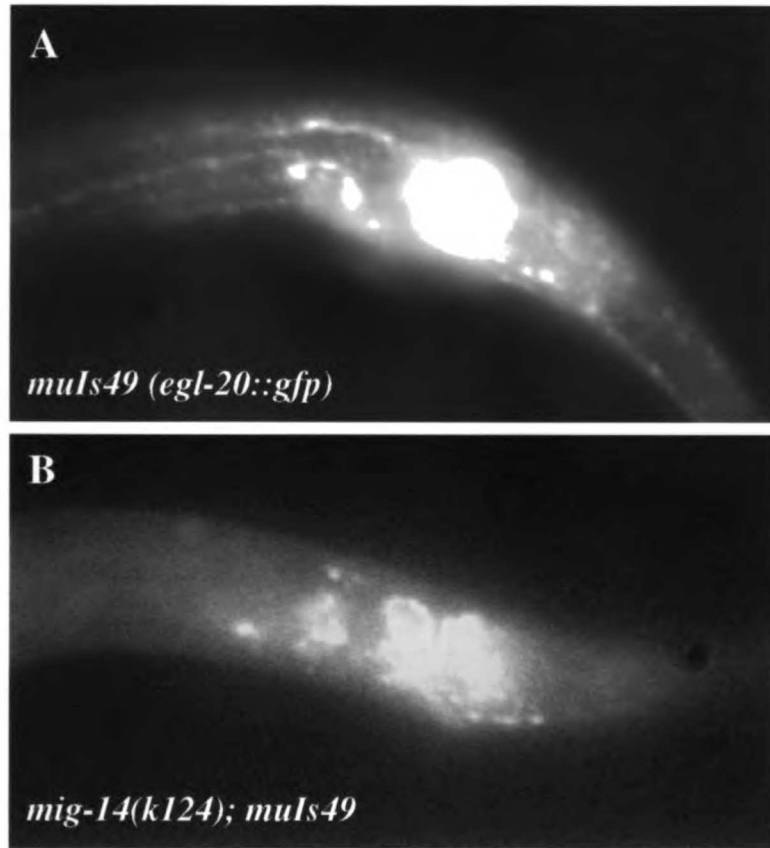


**Table 4.1. The polarity of the V5 cell division is reversed in *egl-20* mutants**

Genotype	% Reversed		
	25°C	20°C	15°C
wild type	0 (100)	0 (50)	0 (50)
<i>egl-20(n585)</i> *	50 (100)	39 (88)	6 (49)
<i>egl-20(n1437)</i>	49 (101)	4 (51)	10 (51)
<i>egl-20(mu25)</i>	36 (100)	12 (52)	8 (50)
<i>egl-20(mu39)</i>	0 (76)	0 (100)	0 (75)

The number of animals (n) examined at each temperature is shown in parentheses.

\* We also examined later divisions in the V5 lineage at 25°C. The seam cell daughter of V5 divided with reversed polarity in 42% of the animals scored (n=98). The seam cell daughter in the third division of the V5 lineage divided with reversed polarity in 30% of the animals scored (n=104). In addition, we observed polarity reversals in the division of the V6.pa cell (39%) and occasional reversals in the divisions of V3.pa, V4.pa and V4.pp ( $\leq 5\%$ ) (n=104).

**Table 4.2. V5 polarity phenotype of single and double mutants**

V5 polarity in single mutants		V5 polarity in double mutants		
Genotype	% Reversed	Genotype	% Reversed	p-value
wild type	0 (100)			
<i>egl-20(n585)</i>	50 (100)			
<i>mig-14(mu71)</i>	0 (79)	<i>mig-14(mu71); egl-20(n585)</i>	68 (102)	0.02
<i>mig-14(k124)</i>	7 (81)	<i>mig-14(k124); egl-20(n585)</i>	64 (90)	0.08
<i>lin-17(n671)</i>	0 (100)	<i>lin-17(n671); egl-20(n585)</i>	2 (100)	<0.0001
<i>lin-17(n677)</i>	0 (79)	<i>lin-17(n677); egl-20(n585)</i>	0 (90)	<0.0001
<i>mig-1(e1787)</i>	0 (100)	<i>mig-1(e1787); egl-20(n585)</i>	72 (100)	0.003
<i>mig-1(n687)</i>	0 (75)	<i>mig-1(n687); egl-20(n585)</i>	51 (152)	>0.9999
<i>mig-1(mu72)</i>	0 (61)	<i>mig-1(mu72); egl-20(n585)</i>	33 (147)	0.008
<i>pry-1(mu38)</i> <sup>a</sup>	0 (50)	<i>pry-1(mu38); egl-20(n585)</i> <sup>b</sup>	80 (100)	<0.0001
<i>bar-1(ga80)</i>	0 (100)	<i>egl-20(n585); bar-1(ga80)</i> <sup>c</sup>	36 (112)	0.09
<i>lin-44(n1792)</i> <sup>a</sup>	0 (100)	<i>lin-44(n1792); egl-20(n585)</i> <sup>d</sup>	40 (177)	0.01
<i>lin-18(e620)</i>	0 (80)	<i>egl-20(n585); lin-18(e620)</i>	30 (99)	0.0008
<i>lin-18(n1051)</i>	0 (68)	<i>egl-20(n585); lin-18(n1051)</i>	30 (108)	<0.0001

All animals were examined at 25°C.

The number of animals (n) examined for each strain is shown in parentheses.

The p-values were derived using the Fisher exact test. These values represent the probability that the frequency of V5 polarity reversals observed in the double mutant strains is a random sample of the frequency observed in *egl-20* mutants alone.

<sup>a</sup> These strains also contain the *him-5(e1490)* mutation, which causes a high incidence of males.

<sup>b</sup> The V6 cell divided symmetrically and yielded two syncytial daughters in two animals.

<sup>c</sup> We observed one animal in which the V5 cell divided symmetrically and gave rise to two syncytial daughters.

<sup>d</sup> Occasional polarity reversals (3% of the animals examined) and symmetric divisions (4%) occurred in the V6 cell division.

**Table 4.3. *hs-egl-20* causes polarity defects in all V cell divisions.**

Genotype	Type of division (%)	V1	V2	V3	V4	V5	V6
N2 (wild type) (n=51)	Reversed	0	0	0	0	0	0
	Symmetric	0	0	0	0	0	0
<i>mul53</i> ( <i>hs-egl-20</i> ) (n=84)	Reversed	20	8	30	33	37	5
	Symmetric	11	8	19	15	6	8
<i>lin-17</i> (n677); <i>mul53</i> (n=74)	Reversed	27	8	7	14	23	23
	Symmetric	22	7	18	9	20	38
<i>bar-1</i> ( <i>ga80</i> ); <i>mul53</i> (n=79)	Reversed	19	20	38	35	27	13
	Symmetric	9	3	16	22	3	13
<i>mig-14</i> ( <i>k124</i> ); <i>mul53</i> (n=75)	Reversed	0	0	0	0	0	0
	Symmetric	0	0	0	0	0	0



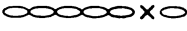













Newly hatched animals were heat shocked for 30 min. at 33°C and allowed to recover at 20°C. Polarity of the V cell divisions was determined after the V cell daughters had differentiated (approximately 8 hrs. following heat shock).

The number of animals (n) examined for each strain is shown in parentheses.

Animals carrying the *mul53* array without heat shock did not exhibit any V cell polarity defects (n>70 for each strain).



**Table 4.4. Polarity of the V5-cell division following ablations**

Genotype/Treatment	% reversed	p-value <sup>a</sup>
<b>wild type</b>		
 Control sides	0 (45)	
 V6, T ablated	0 (11)	
 V6 ablated	0 (15)	
 V2-V4 ablated	0 (10)	
 V1-V4, V6, T ablated	0 (11)	
<b><i>egl-20(n585)</i><sup>b</sup></b>		
 Control sides	47 (81)	
 V6, T ablated	0 (32)	< 0.0001
 T ablated	50 (10)	> 0.9999
 V6 ablated	10 (10)	0.04
 V1-V4 ablated	56 (27)	0.51
 V1-V4, V6, T ablated	0 (12)	0.0012
<b><i>lin-44(n1792); egl-20(n585)</i></b>		
 Unablated animals	40 (177)	
 V6, T ablated	13 (39)	0.0014
 Control sides/V6, T ablation	13 (38)	0.0013
 V1 ablated	42 (12)	> 0.9999
 Control sides/V1 ablation	31 (13)	> 0.9999

The number of animals (n) examined for each treatment is shown in parentheses.

The intact sides of the operated animals were used as controls.

<sup>a</sup>The p-values were derived using the Fisher exact test. For ablations in *egl-20(n585)*, these values represent the probability that the frequency of V5 polarity reversals observed in the ablated sides is a random sample of the frequency observed in the unablated control sides. For ablations in *lin-44(n1792); egl-20(n585)*, both the ablated and control sides were compared with animals that did not undergo operation. Thus, the p-values represent the probability that the frequency of V5 polarity reversals observed in the operated animals is a random sample of the frequency observed in the control animals which were not operated.

<sup>b</sup>We also performed the posterior ablations (V6 and T) in another allele, *egl-20(mu25)*. Of the ablated sides, V5 divided with reversed polarity 11% of the time (n=9). Of the unablated sides, V5 divided with reversed polarity 56% of the time (n=9). The Fisher exact p-value for this experiment was 0.07. Thus, posterior ablations in another allele of *egl-20* behave similarly.

1000

1000

**Table 4.5. *egl-20* and *lin-44* can substitute for each other.**

Assay	<i>lin-44</i> (n1792); <i>mul53</i> ( <i>hs-egl-20</i> )			p-value
	HS	-	+	
	Array	+	+	
Phasmids fill with DiI		11% (239)	42% (311)	<0.0001
Assay	<i>egl-20</i> (n585); <i>muEx88</i> ( <i>hs-lin-44</i> )			p-value
	HS	+	+	
	Array	-	+	
QL.pax are posterior <sup>a</sup>		0% (58)	79% (68)	<0.0001
QR.pax are posterior <sup>b</sup>		0% (58)	62% (72)	<0.0001
V5 polarity reversed <sup>c</sup>		40% (52)	23% (33)	0.1463

Newly hatched animals were heat shocked for 30 min. at 33°C and allowed to recover at 20°C. Final positions of the QL and QR descendants were determined approximately 8 hrs. following heat shock. Dye fill assays were performed on animals two days following heat shock.

The number of animals (n) examined for each strain is shown in parentheses.

The p-values were derived using the Fisher exact test. These values represent the probability that the frequency of phenotypes observed in the animals with heat shock is a random sample of the frequency observed in animals without heat shock.

<sup>a</sup> These numbers represent the fraction of QL.pax cells that were located posterior to V4.p.

<sup>b</sup> These numbers represent the fraction of QR.pax cells that were located posterior to V3.p.

<sup>c</sup> In animals carrying the *hs-lin44* array, ectopic polarity reversals were observed in V2, V3, V4 and V6.

1900

1901

## REFERENCES

Austin, J., and Kenyon, C. (1994). Cell contact regulates neuroblast formation in the *Caenorhabditis elegans* lateral epidermis. *Development* *120*, 313-23.

Chen, Y., and Struhl, G. (1998). In vivo evidence that Patched and Smoothed constitute distinct binding and transducing components of a Hedgehog receptor complex. *Development* *125*, 4943-8.

Eisenmann, D. M., Maloof, J. N., Simske, J. S., Kenyon, C., and Kim, S. K. (1998). The beta-catenin homolog BAR-1 and LET-60 Ras coordinately regulate the Hox gene *lin-39* during *Caenorhabditis elegans* vulval development. *Development* *125*, 3667-80.

Ferguson, E. L., and Horvitz, H. R. (1985). Identification and characterization of 22 genes that affect the vulval cell lineages of the nematode *Caenorhabditis elegans*. *Genetics* *110*, 17-72.

Ferguson, E. L., Sternberg, P. W., and Horvitz, H. R. (1987). A genetic pathway for the specification of the vulval cell lineages of *Caenorhabditis elegans* [published erratum appears in *Nature* 1987 May 7-13;327(6117):82]. *Nature* *326*, 259-67.

Goldstein, B. (1992). Induction of gut in *Caenorhabditis elegans* embryos. *Nature* *357*, 255-7.

Harris, J., Honigberg, L., Robinson, N., and Kenyon, C. (1996). Neuronal cell migration in *C. elegans*: regulation of Hox gene expression and cell position. *Development* *122*, 3117-31.

Herman, M. A., and Horvitz, H. R. (1994). The *Caenorhabditis elegans* gene *lin-44* controls the polarity of asymmetric cell divisions. *Development* *120*, 1035-47.

Herman, M. A., Vassilieva, L. L., Horvitz, H. R., Shaw, J. E., and Herman, R. K. (1995). The *C. elegans* gene *lin-44*, which controls the polarity of certain asymmetric cell divisions, encodes a Wnt protein and acts cell nonautonomously. *Cell* *83*, 101-10.

Horvitz, H. R., and Herskowitz, I. (1992). Mechanisms of asymmetric cell division: two Bs or not two Bs, that is the question. *Cell* *68*, 237-55.

1950

1951

Jan, Y. N., and Jan, L. Y. (1998). Asymmetric cell division. *Nature* 392, 775-8.

Lin, R., Hill, R. J., and Priess, J. R. (1998). POP-1 and anterior-posterior fate decisions in *C. elegans* embryos. *Cell* 92, 229-39.

Maloof, J. N., Whangbo, J., Harris, J. M., Jongeward, G. D., and Kenyon, C. (1999). A Wnt signaling pathway controls hox gene expression and neuroblast migration in *C. elegans*. *Development* 126, 37-49.

Rocheleau, C. E., Downs, W. D., Lin, R., Wittmann, C., Bei, Y., Cha, Y. H., Ali, M., Priess, J. R., and Mello, C. C. (1997). Wnt signaling and an APC-related gene specify endoderm in early *C. elegans* embryos [see comments]. *Cell* 90, 707-16.

Sawa, H., Lobel, L., and Horvitz, H. R. (1996). The *Caenorhabditis elegans* gene *lin-17*, which is required for certain asymmetric cell divisions, encodes a putative seven-transmembrane protein similar to the *Drosophila* frizzled protein. *Genes and Development* 10, 2189-97.

Sternberg, P. W., and Horvitz, H. R. (1988). *lin-17* mutations of *Caenorhabditis elegans* disrupt certain asymmetric cell divisions. *Developmental Biology* 130, 67-73.

Sulston, J., and Horvitz, H. (1977). Post-embryonic cell lineages of the nematode, *C. elegans*. *Developmental Biology* 56, 110-156.

Sulston, J. E., and White, J. G. (1980). Regulation and cell autonomy during postembryonic development of *Caenorhabditis elegans*. *Dev Biol* 78, 577-97.

Thorpe, C. J., Schlesinger, A., Carter, J. C., and Bowerman, B. (1997). Wnt signaling polarizes an early *C. elegans* blastomere to distinguish endoderm from mesoderm [see comments]. *Cell* 90, 695-705.

Waring, D. A., Wrischnik, L., and Kenyon, C. (1992). Cell signals allow the expression of a pre-existent neural pattern in *C. elegans*. *Development* 116, 457-66.

1950

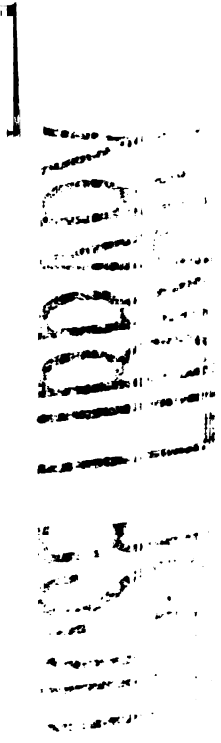
1951



## Chapter 5: Future directions

### SUMMARY

In this work, I have studied how the Wnt family member, *egl-20*, regulates migrations of the Q cells and the polarity of the asymmetric V5-cell division. In both cases, *egl-20* appears to function in a position-independent manner. The effects of EGL-20 on the QL and QR neuroblasts are dose-dependent. High levels of EGL-20 cause both Q cells to express the Hox gene *mab-5*, and consequently, migrate into the posterior. In contrast, low levels of EGL-20 cause both Q cells to migrate anteriorly. The division of the V5 cell is also sensitive to levels of EGL-20. Low (presumably endogenous) levels of EGL-20 can rescue the V5 polarity defect of *egl-20* mutants. However, higher levels of EGL-20 cause both polarity defects and loss of asymmetries in V5 and all the other V-cell divisions. These observations lead to many questions about the mechanism by which EGL-20 functions in these diverse processes. Phenotypic characterization of animals carrying mutations in genes encoding known Wnt signal transduction components indicate that *egl-20* interacts with different pathways for its effects in different tissues. In addition, the determination of polarity in the V5-cell division appears to be a complex process involving multiple layers of signaling. Thus in this chapter, I present several questions that arise from the work described in the previous chapters and I propose some future experiments to address these questions.



## I. *egl-20* and its role in Q cell migrations

### How does *egl-20* promote anterior migration in the QR lineage?

*egl-20* appears to cause activation of *mab-5* expression in the QL neuroblast through a canonical Wnt signal transduction pathway since mutations in *lin-17/frizzled* and *bar-1/armadillo* also disrupt this process. However, *egl-20* mutants differ from *lin-17* and *bar-1* mutants in the anterior migrations of the QR.p descendants. Mutations in *egl-20* cause the anteriorly migrating QR.p descendants to stop prematurely. In contrast, mutations in *lin-17* and *bar-1* cause the QR.p descendants to migrate too far anteriorly, i.e. they overshoot their wild-type stopping points. Thus for migrations in the QR lineage, *egl-20* acts in the opposite direction from the putative downstream signal transducing genes. It was possible that *egl-20* could negatively regulate this pathway on the right side. However, analysis of double mutants between *egl-20* and these genes did not reveal a clear epistasis. Other genes, including *mig-13* and *lin-39*, that are required for the anterior migrations of the QR descendants have been identified. Yet these genes also do not appear to act in a linear pathway with *egl-20*. Does *egl-20* lead to the expression of a transcription factor in QR and its descendants whose function is analogous to that of *mab-5* in the QL lineage? The Hox gene *lin-39* is expressed in QR and its descendants (also expressed initially in QL and its descendants) and is required cell autonomously for their anterior migration. However, *lin-39* expression is not dependent upon *egl-20* signaling. In order to understand how *egl-20* specifies anterior cell migration in the QR lineage, it will be necessary to carry out screens to identify the components that transduce the EGL-20 signal.

One approach to this problem is forward genetics. A possible screen to look for other genes that act with *egl-20* is to start with a *mab-5(-)* mutant strain. In *mab-5* mutants, both the QL and QR descendants migrate into the anterior. *egl-20* activity is required for both of these anterior migrations. *egl-20* mutations in a *mab-5(-)* background shift the final positions of both the QL and QR descendants posteriorly. Therefore, one can mutagenize a *mab-5(-)* mutant strain and look for animals in which the final positions of the Q descendants are shifted more posteriorly. An integrated *mec-7::gfp* array can be used to visualize the Q cells under a fluorescence dissecting microscope. Therefore, it is possible to examine a large number of mutagenized animals in a non-clonal screen. One advantage of screening in a *mab-5(-)* background over screening in a wild-type background is that descendants of both Q cells can be scored. In wild-type animals, the QL descendants are already in the posterior. Also in previous screens that started with a wild-type background, mutations affecting *mab-5* expression in the QL descendants were isolated at a much higher frequency than mutations specifically affecting the anterior migration of the QR descendants, since the latter phenotype is much more subtle. To avoid isolating additional *egl-20* mutations, one can provide multiple copies of the wild-type *egl-20* gene on an integrated array, which can be crossed into the *mab-5(-)* background.

In previous screens for mutations affecting the Q cell migrations, several mutants were isolated that exhibited defects in the anterior migration of the QR descendants (Mary Sym and Queelim Ch'ng, unpublished; Mary Sym, unpublished). Lucie Yang is currently characterizing two of these mutants, *mu290* and *mu232*. Double mutant analysis between these genes and *egl-20* indicate that *mu232*, but not *mu290*, may be in

1987

1988

the same pathway as *egl-20* for anterior migration of the QR descendants (Lucie Yang, unpublished). Interestingly, *mu232* also has defects in the seam cell lineages, indicating that it may be involved with *egl-20* in more than one process (Lucie Yang, unpublished). It will be interesting to know the molecular identity of *mu232*.

An alternative approach is to use reverse genetics. The *C. elegans* Sequencing Consortium has identified a number of Wnt signaling pathway components in the genome. Many of these have not yet been identified genetically. Since EGL-20 is a Wnt protein, it is reasonable to propose that the components of the signal transduction pathway that leads to anterior migration might be among this group of candidate genes. Thus it may be informative to inhibit the function of these candidate genes by RNA-mediated interference (RNAi).

### **What makes QL more sensitive than QR to levels of EGL-20?**

In Chapter 3, I demonstrated that both QL and QR can exhibit both the low and high dose responses to EGL-20. However, in the wild type, endogenous levels of EGL-20 trigger *mab-5* expression in QL (the high dose response) and promote anterior migration in QR (the low dose response). By providing varying levels of EGL-20 under the control of a heat shock promoter, I determined that QL and QR have different response thresholds to the same level of EGL-20. What is the mechanism underlying this left-right asymmetry of the Q cells? One possibility is that one or more components of the *mab-5* activation pathway are expressed at higher levels in QL than in QR. I have received a strain carrying the *lin-17::gfp* fusion gene from Hitoshi Sawa. However, expression of *lin-17::gfp* in this strain is widespread, and thus cannot distinguish this



possibility. The *bar-1::gfp* and BAR-1 anti-sera are currently available reagents and thus could be examined.

It is also possible to screen for mutations in genes that are involved in creating the differences in sensitivities between QL and QR to EGL-20. The starting strain would be an *egl-20(-)* mutant carrying integrated *hs-egl-20* and *mab-5::lacZ* arrays. Following mutagenesis, staged larvae (0-1 hour old) would be subjected to the low dose of heat shock and then assayed for *lacZ* expression. One could then look for mutants in which QR was altered to be as sensitive as QL. In that case, both Q cells would activate *mab-5::lacZ* in response to the low dose of hs-EGL-20. Conversely, one could look for mutants in which QL was altered to be less sensitive to EGL-20. In these mutants, both Q cells would be able to activate *mab-5::lacZ* expression only at the higher dose of hs-EGL-20. Since this screen involves a  $\beta$ -galactosidase detection assay, which requires killing the worm prior to its reproductive phase, it will be necessary to do this as a clonal screen.

In addition, one could examine mutants that have already been isolated in the previous screens. For example, a mutation in a gene that only affected the sensitivity of QL to EGL-20 would not exhibit any QR migration defects. On the left side, the QL descendants would migrate anteriorly due to a failure in activating *mab-5*. Several mutants with these phenotypes have been identified (Mary Sym and Queelim Ch'ng, unpublished). To test if the sensitivity of the Q cells is affected, it would be necessary to move this mutation into a *egl-20(-)* strain carrying integrated *hs-egl-20* and *mab-5::lacZ* arrays, and then provide *hs-egl-20*. The QL descendants should not be able to express



1941  
1942  
1943  
1944  
1945  
1946  
1947  
1948  
1949  
1950  
1951  
1952  
1953  
1954  
1955  
1956  
1957  
1958  
1959  
1960  
1961  
1962  
1963  
1964  
1965  
1966  
1967  
1968  
1969  
1970  
1971  
1972  
1973  
1974  
1975  
1976  
1977  
1978  
1979  
1980  
1981  
1982  
1983  
1984  
1985  
1986  
1987  
1988  
1989  
1990  
1991  
1992  
1993  
1994  
1995  
1996  
1997  
1998  
1999  
2000  
2001  
2002  
2003  
2004  
2005  
2006  
2007  
2008  
2009  
2010  
2011  
2012  
2013  
2014  
2015  
2016  
2017  
2018  
2019  
2020  
2021  
2022  
2023  
2024  
2025

*mab-5::lacZ* in response to a low dose of hs-EGL-20. QL and QR should respond the same way to all doses of hs-EGL-20.

Furthermore, one could screen for mutants defective in the anterior migration of the QR descendants. If QR was altered such that it had increased sensitivity to EGL-20, then it would activate *mab-5* expression and remain in the posterior. Thus, one would look for mutants in which the QL descendants were unaffected, but the QR descendants were located in the posterior. The posterior migration of the QR descendants in these mutants would have to be dependent on the presence of EGL-20 in order to eliminate mutations like *pry-1*, which activate *mab-5* expression independent of Wnt signaling.

#### **Where does the EGL-20 signal transduction pathway act?**

Although we have identified components that are likely to be part of the EGL-20 response pathway for *mab-5* activation, we do not know in which cells or tissues these components are acting. This pathway may or may not be acting directly in the QL cell. First, it will be necessary to demonstrate that components such as *lin-17* and *bar-1* are required for *mab-5::lacZ* activation in the Q cells in response to hs-EGL-20. Assuming these components are required for the response to EGL-20, one can proceed to carry out a mosaic analysis of these genes. If hs-EGL-20 can activate *mab-5* expression independently of *lin-17* and *bar-1*, then we must reevaluate our model for EGL-20 signal transduction.

I have constructed a *lin-17(n677); ncl-1(e1865)* strain for the purpose of performing mosaic analysis for the QL migration defect. I generated an extrachromosomal array containing pSH2(*lin-17+*), C33C3(*ncl-1+*) and pTG96(*sur-*

1981

1982

5::*gfp*, another cell autonomous marker). The QL anterior defect is not highly penetrant in *lin-17(-)* mutants, thus a large number of mosaics would have to be generated. In addition, I noticed ectopic phenotypes of the extrachromosomal array in the *lin-17(-)* strain (see Appendix I). Interestingly, these ectopic phenotypes resembled *egl-20(-)* mutants. Thus, *egl-20* might negatively regulate *lin-17* for some phenotypes, or excess LIN-17 might titrate away the endogenous EGL-20.

## II. EGL-20 and its role in establishing polarity of the V-cell divisions

### What is the *egl-20* signal transduction pathway for determining V5 polarity?

Identifying additional components that interact with EGL-20 is essential to understanding how polarity is established in the V-cell divisions. At this point, the only known mutations that cause reversals in the polarity of the V5-cell division are *egl-20* and *mig-14*. I found that the *mig-14* gene is required in order for hs-EGL-20 to affect V-cell polarity. In addition, EGL-20::GFP does not appear to diffuse as far in *mig-14(-)* animals. Does *mig-14* have a role in processing or producing EGL-20? To address this question, it will be necessary to clone the *mig-14* gene first. If *mig-14* is required for proper secretion of EGL-20, then it should be localized to the same cells that express *egl-20*.

When I began in the lab, I attempted a pilot screen to look directly for polarity mutants by using Nomarski optics. This screen did not yield any mutants. However, this type of screen is time-consuming because the L1 larvae must be loaded onto slides and viewed on high magnification. In addition, it is necessary to screen through many

animals if the phenotype is not completely penetrant. Recently, Scott Alper in the lab has developed a GFP fusion gene that is expressed at high levels specifically in the seam daughters of the V cells. Mutagenizing a strain carrying this fusion would accelerate the screening process. This fusion is bright enough that high magnification is not necessary to detect polarity reversals. Thus, animals can be examined on agarose pads at low magnification without coverslips.

For understanding how EGL-20 interacts with different downstream signal transducing proteins, sequence analysis of the different *egl-20* alleles may be informative. Currently, there are 18 existing alleles of *egl-20*. Some of the *egl-20* mutations are able to separate the different functions of *egl-20*. To identify molecules that directly interact with EGL-20, it is possible to carry out a screen for second-site suppressors of various *egl-20* mutations. Mutations in these genes should suppress the *egl-20(-)* phenotype, and when separated from *egl-20(-)*, these mutations should cause an *egl-20(-)* phenotype on their own.

### **What is the signal that causes V5 polarity reversals in *egl-20* mutants?**

The cell ablation experiments suggest that the “reverse signal” is produced or mediated by the V6 and T seam cells since killing these cells completely prevents polarity reversals in *egl-20* mutants. Screening for suppressors of the V5 polarity reversals in an *egl-20(-)* background may lead to the identification of this signal. To facilitate visualization of the V cells, the seam cell specific GFP fusion can be used (Scott Alper, unpublished).

Mutations in *lin-17* also suppress V5 polarity reversals in an *egl-20(-)* background. This finding suggests that *lin-17* may be required for the production of the reversing signal in the V6 and T cells. Alternatively, *lin-17* may act in the V5 cell to mediate the response to the polarity-reversing signal. Mosaic analysis of *lin-17* in an *egl-20(-)* background may be able to distinguish between these two possibilities. I have constructed a *lin-17(n677); ncl-1(e1865); egl-20(n585)* triple mutant strain for this purpose. In addition, I have introduced an extrachromosomal array containing pSH2(*lin-17+*), C33C3(*ncl-1+*) and pTG96(*sur-5::gfp*). Multiple *lin-17(n677); ncl-1(e1865); egl-20(n585)* strains carrying this extrachromosomal array behave as predicted. Animals that have completely lost the array do not exhibit any V5 polarity reversals, whereas animals carrying the array in all cells exhibit V5 polarity reversals at a high frequency.

The *pry-1(mu38)* mutation enhances the V5 polarity reversals in an *egl-20(-)* background. It will be helpful to know whether *pry-1* acts downstream of *lin-17* in the production of the reverse signal, or in the reception of the reverse signal. The *pry-1 lin-17* double mutant cannot be constructed because it is too unhealthy. However, it may be possible to perform RNAi of *egl-20* and *lin-17* in a *pry-1* mutant background to determine whether *pry-1* acts downstream of *lin-17* in the “reverse signal” pathway. In addition, to determine whether *pry-1* is involved in the production of the “reverse signal”, one can ablate the V6 and T seam cells in a *pry-1; egl-20* double mutant. If *pry-1* acts in these cells to generate the “reverse signal”, then ablation of these cells should completely abolish the V5 polarity reversals in an *egl-20* mutant.

Multiple systems appear to influence the polarity of the single V5-cell division. In the wild type, *egl-20* acts to override the polarity-reversing signals from the

neighboring seam cells. In the absence of *egl-20*, the neighbor seam cells can specify polarity of the V5 cell. When both *egl-20* activity and the neighbor seam cells are gone, there is yet another system that can correctly polarize the V5 division. To identify components of the latter system, one could screen for polarity reversals in a *lin-17; egl-20* mutant background, which exhibits wild-type polarity in all the V cells.

### **What signals polarize the other V-cell divisions?**

Mutations in the *egl-20/Wnt* gene primarily disrupt A/P polarity of the V5-cell division. Mutations in the *lin-44/Wnt* gene cause polarity reversals of several epidermal cells in the tail. Do other Wnt proteins polarize other cells in the epidermis? The *C. elegans* genome contains five predicted *Wnt*-like genes. The *Ce-Wnt-1* deletion mutant has an embryonic lethal phenotype and thus cannot be scored for polarity. I have scored some escapers from the embryonic-lethal *mom-2* strain, but did not observe any V-cell polarity defects. Mutations in *Ce-Wnt-2* have not been generated. To explore the possibility that these Wnt proteins play roles in post-embryonic development, one could perform in situ hybridizations of *mom-2*, *Ce-Wnt-1* and *Ce-Wnt-2* to determine when and where all they are expressed. Since hs-EGL-20 can disrupt the polarities of all the V-cell divisions, it is possible that a Wnt system is normally involved in polarizing these other V cells.

### **CONCLUSIONS**

In summary, the development of the Q cells and V cells in *C. elegans* involves many fundamental biological processes such as left-right asymmetry, Hox gene

regulation, cell migration and asymmetric cell fate determination. Several of these processes are controlled by the activity of a highly conserved signaling molecule, the EGL-20/Wnt protein. The findings of this work indicate that regulation of Q cell migration and V5 polarity by *egl-20* is complex and is likely to require multiple signal transduction pathways. Identifying additional components in the EGL-20 signal transduction pathway will allow a more detailed study of how Wnt proteins function at the molecular level. Once components required for the different functions of *egl-20* are identified, one can ask how this Wnt protein achieves signaling specificity. These studies, in turn, may establish new paradigms for the function of Wnt signaling pathways in other organisms.



**Appendix A: Final positions of the QL.pa and QR.pa descendants and polarity of the V5-cell division in *egl-20(mu241)* and *egl-20(mu320)* at 15°C, 20°C and 25°C**

*egl-20(mu241)* and *egl-20(mu320)* were isolated in a screen for mutants with misplaced Q cell descendants (Mary Sym et al., unpublished data). I have outcrossed both strains three times to wild type. *egl-20(mu241)* allele changes an invariant splice-donor GT sequence to AT in intron 2. *egl-20(mu320)* is associated with an opal mutation located in the second exon of *egl-20*. The predicted *mu320* protein product has only 48 amino acids in addition to the presumptive signal sequence and thus may be a null allele. The final positions of the QR.pa descendants in *egl-20(mu241)* and *egl-20(mu320)* are similar to that of other *egl-20* alleles in that they are shifted posteriorly relative to wild type. In addition, the QR.pa migration defect is temperature sensitive.

The positions of the QL.pa descendants differ slightly from that of *egl-20(n585)*, a strong reduction-of-function allele. In both *egl-20(mu241)* and *egl-20(mu320)*, there are some QL.pa descendants that remain in the posterior, and some are located in positions even more posterior than the wild-type positions. Similar distributions of the QL descendants are present in other alleles of *egl-20* including *mu39*, *mu25* and *n1437*. However, the QL phenotype in *mu241* and *mu320* appears to be temperature sensitive. It will be necessary to place both alleles over deficiency to determine whether they represent the null phenotype. In addition, making double mutant strains with a *mab-5(-)* allele will determine whether the posterior migrations of the QL.pa descendants require *mab-5* activity.

As in other alleles of *egl-20*, *mu241* and *mu320* exhibit polarity reversals in the V5-cell division in a temperature-sensitive manner. However, the frequency observed in these two alleles is lower than that observed for *egl-20*(*n585*).

Table A.1. Polarity of the V5-cell division in *mu241* and *mu320*

Genotype	% Reversed		
	25°C	20°C	15°C
wild type	0 (100)	0 (50)	0 (50)
<i>egl-20</i> ( <i>n585</i> )	50 (100)	39 (88)	6 (49)
<i>egl-20</i> ( <i>mu241</i> ) <sup>a</sup>	34 (150)	19 (150)	11 (103)
<i>egl-20</i> ( <i>mu320</i> ) <sup>b</sup>	33 (150)	5 (260)	8 (101)

The number of animals (n) examined at each temperature is shown in parentheses.

<sup>a</sup> Symmetric divisions in which V5 gave rise to two syncytial daughters were observed ( $\leq 2\%$  at 20°C and 25°C). In addition, occasional polarity reversals occurred in the V6 cell division ( $\leq 4\%$  at 20°C and 25°C).

<sup>b</sup> V6 divided symmetrically and gave rise to two syncytial daughters at a low frequency (5% at 20°C).

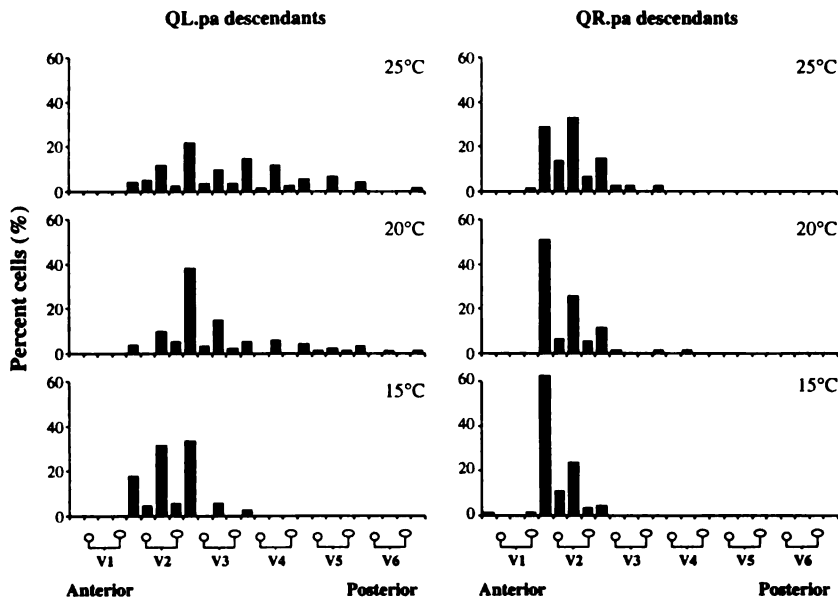


**Figure A.1.** Final positions of the QL.pa and QR.pa descendants in *egl-20(mu241)* at 15°C, 20°C and 25°C. (n > 100 cells for each temperature).

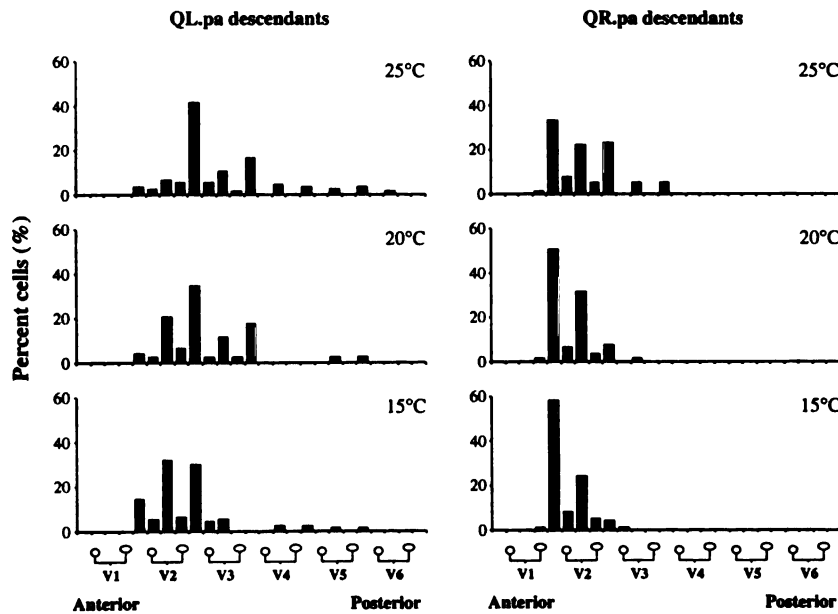


**Figure A.2.** Final positions of the QL.pa and QR.pa descendants in *egl-20(mu320)* at 15°C, 20°C and 25°C. (n > 100 cells for each temperature).

**Appendix B: The final positions of the QL.pa and QR.pa descendants in *egl-20(n585); bar-1(ga80)* double mutants**

Lisa Moore and I have re-built the *egl-20(n585); bar-1(ga80)* double mutant strain because the *egl-20* mutation was found to be absent from the first construction. The final positions of the QL.p descendants in the double mutant are different from either single mutant. I observed that some of the QL.p descendants migrated to posterior positions. These posterior migrations may be dependent upon *mab-5* or *egl-5* expression. Alternatively, they may be due to a yet unidentified Hox gene-independent mechanism.

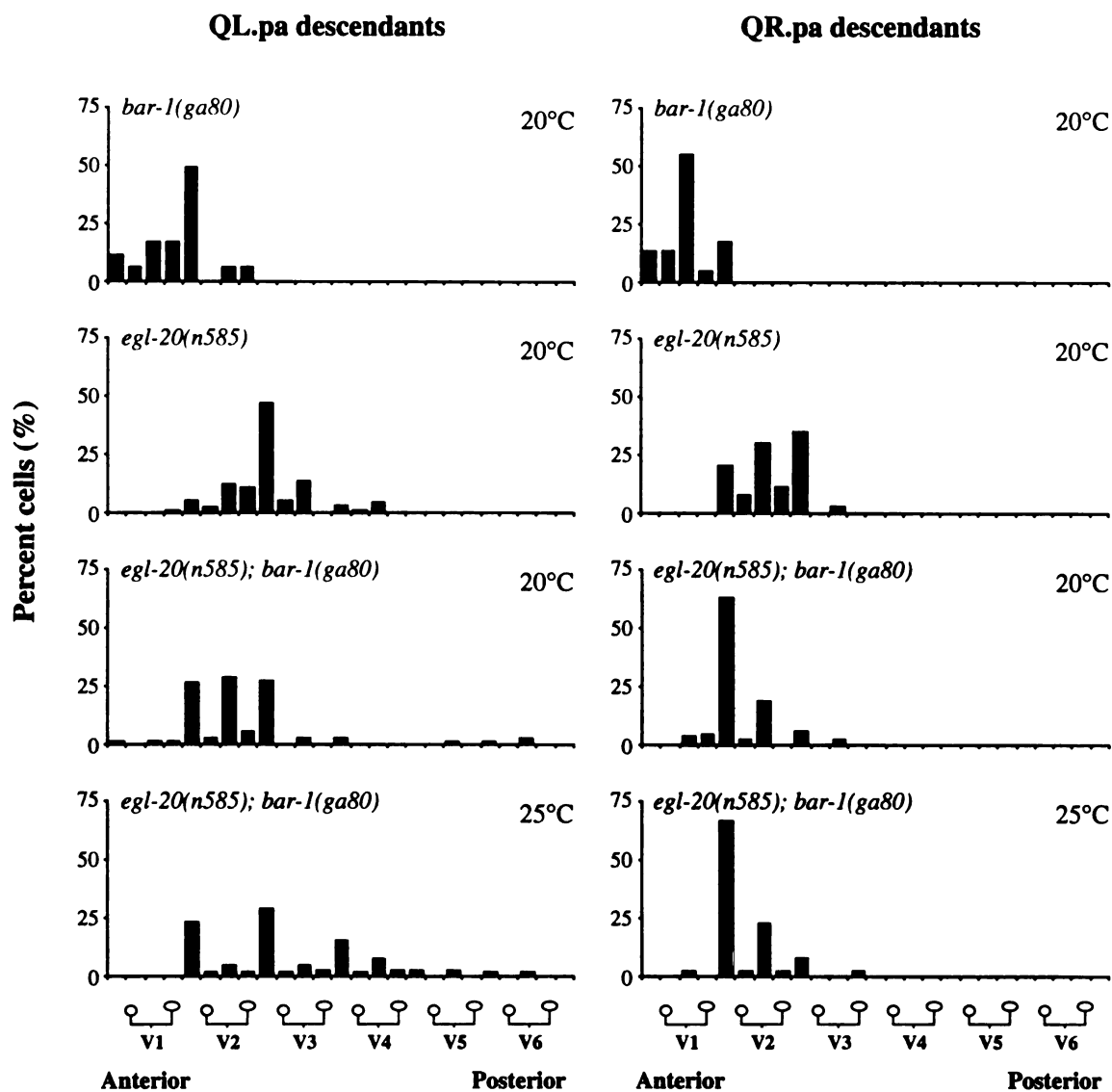


**Figure B.1.** Final positions of the QL.pa and QR.pa descendants in *egl-20(n585); bar-1(ga80)* double mutants at 20°C and 25°C. *bar-1(ga80)* and *egl-20(n585)* single mutants are shown for reference.  $n > 80$  cells for each strain, except for *bar-1(ga80)* ( $n \geq 20$  cells).

**Appendix C: A high dose of *hs-egl-20* causes posterior migration of the Q descendants in a *mab-5* and *egl-5*-independent manner**

I have found that a 30 minute pulse of *hs-egl-20* at 33°C can cause the QL and QR descendants to migrate posteriorly even in the absence of *mab-5*. How do high levels of EGL-20 specify posterior migration in a *mab-5*-independent manner? I tested the possibility that *hs-egl-20* might induce ectopic *egl-5* expression in the Q cells by providing a high dose of *hs-egl-20* in a *mab-5 egl-5* double mutant background. However, the Q descendants still migrate posteriorly in *the mab-5 egl-5* double mutants. Thus, the posterior migration in response to a high level of hs-EGL-20 is independent of both *mab-5* and *egl-5*.

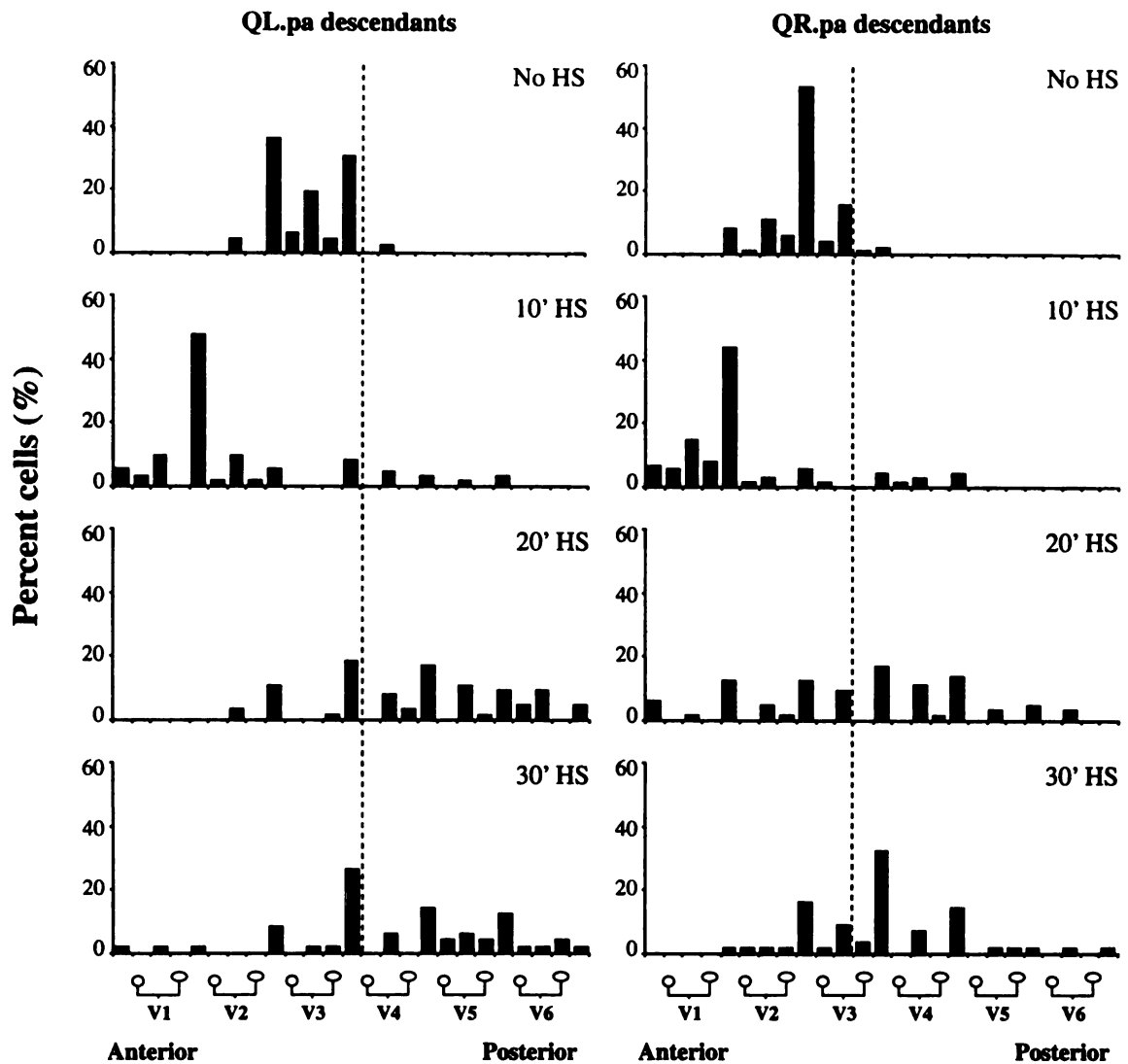


**Figure C.1.** Final positions of the QL.pa and QR.pa descendants in *mab-5(e2088); egl-20(n585); muIs53(hs-egl-20)* animals following 20 and 30 min. pulses of heat shock at 33°C. Animals were heat shocked as described in Chapter 3.  $n > 50$  cells for each time point. In this and other figures, the vertical dashed line serves as a common reference point for comparison of the various histograms.

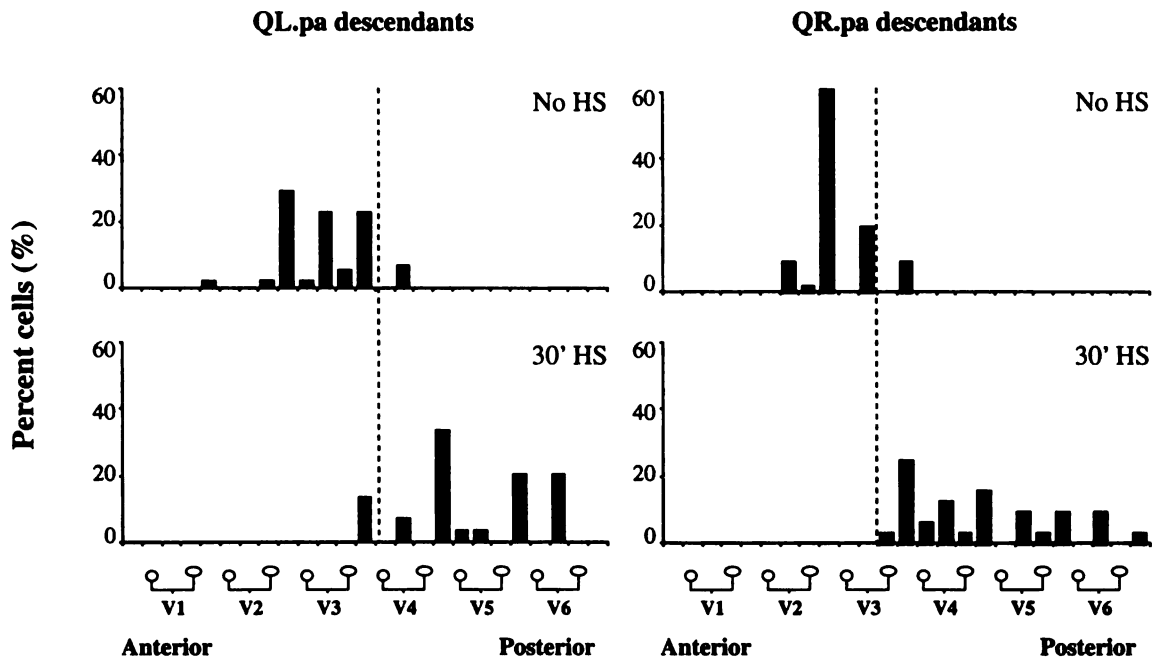


**Figure C.2.** Final positions of the QL.pa and QR.pa descendants in *mab-5(e1239) egl-5(n945); mul53(hs-egl-20)* animals following a 30 min. pulse of heat shock at 33°C. n = 56 cells for non-heat shocked control animals. n = 30 cells for heat shocked animals.



**Appendix D: *mig-14(mu71)* suppresses the *mab-5*-independent response to high levels of hs-EGL-20**

I tested whether *mig-14* was required for the *mab-5*-independent posterior migrations of the Q descendants in response to high levels of hs-EGL-20. I constructed the *mig-14(mu71); mab-5(e2088); muIs53(hs-egl-20)* triple mutant strain and provided various doses of heat shock at 33°C. The triple mutant strain does not exhibit the anterior migration response to a low dose of hs-EGL-20. The triple mutant strain also does not exhibit the posterior migration response to a high dose of hs-EGL-20. Interestingly, the Q descendants exhibit the low dose response when exposed to high levels of hs-EGL-20. This supports the model that *mig-14* is required for either the secretion or processing of the EGL-20 signal (see Chapter 4).

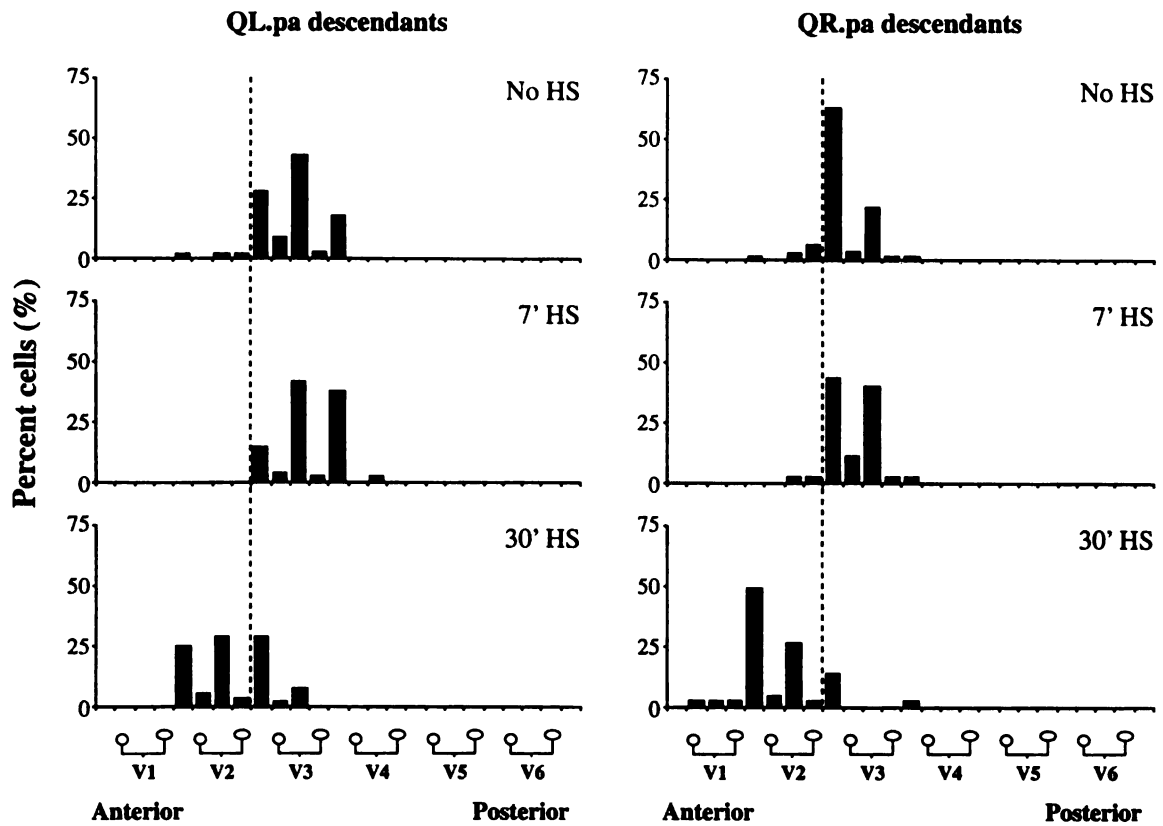


**Figure D.1.** Final positions of the QL.pa and QR.pa descendants in *mig-14(mu71); mab-5(e2088); muIs53(hs-egl-20)* animals following 7 and 30 min. pulses of heat shock at 33°C. n = 84 for the non-heat shocked control animals. n = 56 for the heat shocked animals.

**Appendix E: *mig-1* and *mig-13* mutants can exhibit the low dose response to *hs-egl-20***

The Q descendants migrate anteriorly in response to a low dose of *hs-egl-20*. I tested whether either the *mig-1* or *mig-13* genes were required for this anterior migration response by providing a low dose of *hs-egl-20* in these mutant backgrounds. Since *mab-5* was present in these strains, I only scored the positions of the QR.pa descendants. *mig-1* does not appear to be required for the anterior migration response of the QR descendants. In the *mig-13* mutant background, the QR descendants appear to be shifted more anteriorly. However, they do not migrate beyond the stopping points of the QR descendants in the *mig-13* background alone. Perhaps a low dose of *hs-egl-20* only allows the Q descendants to migrate a fixed distance from any starting point. Another possibility is simply that the QR descendants cannot migrate anteriorly beyond the V3.a cell without *mig-13* activity.

QR.pa descendants

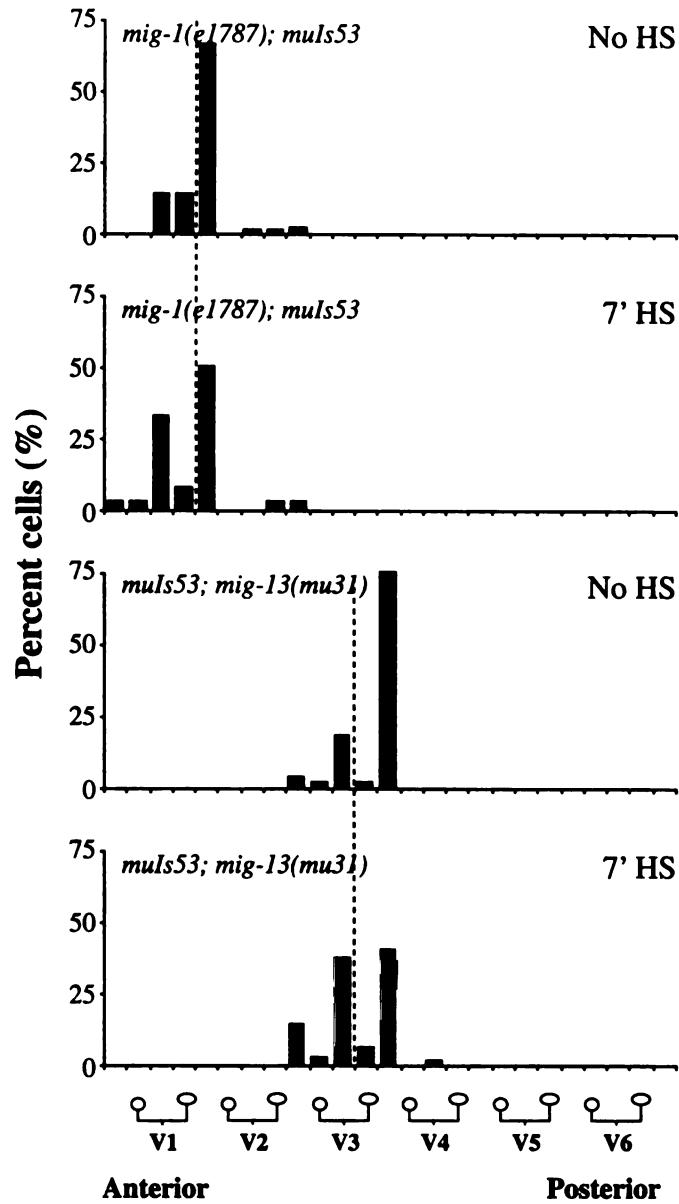


**Figure E.1.** Final positions of the QR.pa descendants in *mig-1(e1787); muls53(hs-egl-20)* and *muls53(hs-egl-20); mig-13(mu31)* animals following a low dose of heat shock at 33°C. n > 80 cells for non-heat shocked control animals. n > 40 for heat shocked animals.

## **Appendix F: Later polarity reversals in the V cell lineages of *egl-20(n585)* animals**

Since *egl-20* was required for correct polarity of the V5 cell division, we asked whether it was required for the polarity of other divisions in the V5 lineage. We examined the positions and morphologies of the V5 descendants at the end of the L2 larval stage, and observed additional polarity reversals later in the V5 lineage. We also noticed polarity reversals later in the V3, V4, and V6 cell lineages of *egl-20* mutants.

**Figure F.1.** Polarity reversals also occur later in the V-cell lineages of *egl-20(-)* mutants.

(A) Wild-type V-cell lineages. Cell fates are indicated as follows: sy, cells that fuse with the hyp7 syncytium; Pd, postdeirid neuron; se, seam cells. The time line indicates the first and second larval stages (L1 and L2).

(B) Representative *egl-20* mutant lineage. Arrows indicate divisions in which polarity reversals were observed. Polarity reversals occur in the first, second, and third divisions of the V5 cell lineage in *egl-20* mutants. Reversals at subsequent divisions occurred independently of the previous divisions. Polarity reversals were never observed in the first division of the V1-V4, and V6 lineages. The second division of these V cells is symmetric and thus cannot be examined for polarity reversals. Reversals were observed in the third division of the V3, V4, and V6 lineages. The reversals occurred mostly in the Vn.pa branches, except for one reversal in the V4.pp branch.

(C) Frequencies of polarity reversals at the first, second, and third divisions of the V-cell lineages in *egl-20(n585)* mutants. Polarity of the V-cell divisions was determined by looking at the positions of nuclei in staged animals using Nomarski microscopy. The number of animals (n) examined for the first division was 100; n=98 for the second division; n=104 for the third division, with the exception of the V5 lineage (n=99).



## **Appendix G: The temperature sensitive period (TSP) of V5 polarity determination in *egl-20(n585)* mutants**

### **Background**

The establishment of V5 polarity in *egl-20* mutants appears to be a temperature-sensitive process since all of the *egl-20* alleles that exhibit V5 polarity reversals are temperature-sensitive for the phenotype. Thus, an *egl-20*-independent system can polarize the V5 cell division correctly at low temperature but not at high temperatures. We asked when the polarity of the V5 cell division was established in *egl-20* mutants. To address this question, we performed a series of temperature shift experiments.

### **Materials and Methods**

Gravid *egl-20(n585)* hermaphrodites from populations cultured for at least two generations at either 15°C or 25°C were treated with alkaline hypochlorite to release their eggs. Larvae were staged by collecting newly hatched animals at 30 minute intervals and placing them on plates that had been preincubated at the initial temperature. To perform the "down-shift" experiment, staged animals on plates at 25°C were collected periodically in M9 media that had been preincubated at 15°C, pelleted briefly, and transferred to seeded plates that also had been preincubated at 15°C. To perform the "up-shift" experiment, staged animals growing at 15°C were collected in M9 media that had been preincubated at 25°C and transferred to plates preincubated at 25°C. The shifted animals were allowed to continue developing at the new temperature. V5 polarity was



determined after all V cells had divided once, and the P nuclei had descended into the ventral nerve cord.

## **Results**

We found that the temperature-sensitive period (TSP) of V5 polarity determination in *egl-20(n585)* mutants occurred prior to V5 cell division. Shifting *egl-20(n585)* mutants from the restrictive temperature (25°C) to the permissive temperature (15°C) prior to the time of V5 division suppressed the polarity reversal defect, whereas the reciprocal shift resulted in frequent V5 polarity reversals. Animals that were subjected to up-shifts or down-shifts after the time of V5 division exhibited the polarity phenotype characteristic of the original temperature. Thus, the TSP of V5 polarity determination in *egl-20* mutants suggests that polarity is established within the V5 cell and not in the V5 daughters. However, it remains possible that the TSP reflects the time when the temperature-sensitive component of the polarity-determining system is produced, rather than the time when it functions.

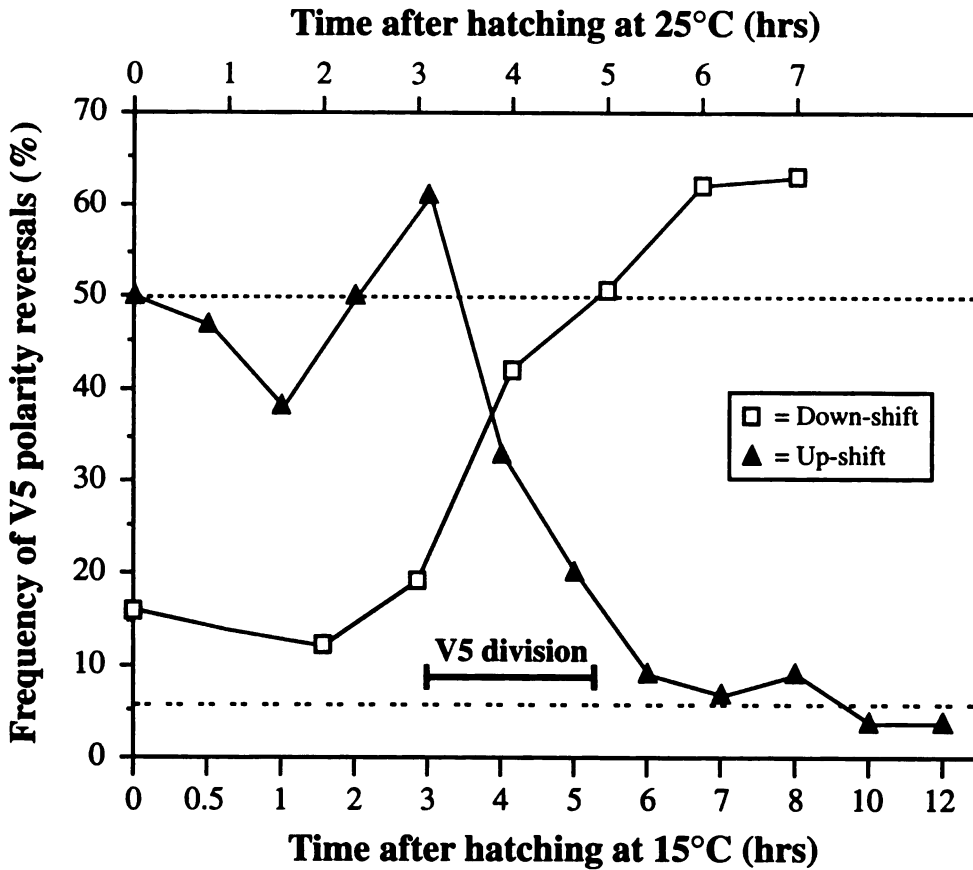


**Figure G.1.** The TSP for V5 polarity determination coincides with the time of the V5 cell division in *egl-20(n585)* mutants. The open squares represent animals grown at 25°C and shifted down to 15°C at various time points after hatching. The filled triangles represent animals grown at 15°C and shifted up to 25°C at various time points after hatching. The time of the V5 cell division is noted on the graph. The top and bottom dotted lines represent the frequency of V5 polarity reversals in animals grown constantly at 25°C and 15°C, respectively. Each time point consists of animals that have been synchronized within a half hour of each other.  $n > 30$  animals for each time point.

## Appendix H: Screening through candidate mutants for V cell polarity

### defects

### Materials and Methods

#### Strains

The following strains were used:

CF147 *lin-39(mu26)* III

CF162 *mig-2(mu28)* X

EV278 *mom-2(or42)* V/*DnT1* (IV;V)

EV311 *dpy-5(e61)* *mom-5(or57)* *IhT2* (I;III)

EV361 *mom-1(or10)* *unc-6(n102)* X/*szT1* (I;X)

EV431 *rol-1(e91)* *mom-3(or78)* *lin-7(e1413)* II/*mnC1*; *him-5(e1490)* V

EV446 *unc-13(e1091)* *mom-4(or30)* *IhT2* (I;III)

MT633 *lin-11(n389)* I; *him-5(e1467)* V

NJ36 *mig-2(rh17)* X

PS1037 *unc-24(e138)* *let-60(sy100dm)* *dpy-20(e1282)/let-60(n1046gf)* *unc-22(s7)* IV

*par-2(e2030ts)* III

#### Determining V5 polarity

All strains were scored at 25°C with the exception of *lin-11(n389)*, which was scored at 20°C. For the *mom* strains, I scored all the progeny from heterozygous parents. I assumed that 1/4 or 1/3 of the progeny would be homozygous for the *mom* allele, depending on the balancer. For each *mom* strain, n=100, except for *mom-3*, n=59.

#### Results

With the exception of the strain containing *mom-3(or78)* (EV431), I did not observe any V5 polarity defects in the candidate mutants that I examined. I observed two animals with reversed polarity of the V5 cell division among the EV431 progeny scored. Also among the EV431 progeny, I observed two animals in which the QL descendants

migrated anteriorly and two animals in which the QR descendants were located in positions posterior to the wild-type stopping points. Although the strain containing *mom-5(or57)* (EV311) did not exhibit any V cell polarity defects, I observed QL descendants which had migrated anteriorly in 4/47 left sides scored.

## References

*par-2* (Levitan et al., 1994)

*mig-2* (Hedgecock et al., 1987; Zipkin et al., 1997)

*lin-11* (Freyd et al., 1990)

*lin-39* (Clark et al., 1993; Wang et al., 1993)

*let-60* (Han and Sternberg, 1990)

*mom* genes (Rocheleau et al., 1997; Thorpe et al., 1997)

Clark, S. G., Chisholm, A. D. and Horvitz, H. R. (1993). Control of cell fates in the central body region of *C. elegans* by the homeobox gene *lin-39*. *Cell* 74, 43-55.

Freyd, G., Kim, S. K. and Horvitz, H. R. (1990). Novel cysteine-rich motif and homeodomain in the product of the *Caenorhabditis elegans* cell lineage gene *lin-11*. *Nature* 344, 876-879.

Han, M. and Sternberg, P. W. (1990). *let-60*, a gene that specifies cell fates during *C. elegans* vulval induction, encodes a ras protein. *Cell* 63, 921-931.

Hedgecock, E. M., Culotti, J. G., Hall, D. H. and Stern, B. D. (1987). Genetics of cell and axon migrations in *Caenorhabditis elegans*. *Development* 100, 365-382.

Levitan, D. J., Boyd, L., Mello, C. C., Kemphues, K. J. and Stinchcomb, D. T. (1994). *par-2*, a gene required for blastomere asymmetry in *Caenorhabditis elegans*, encodes zinc-finger and ATP-binding motifs. *Proceedings of the National Academy of Sciences of the United States of America* 91, 6108-6112.

Rocheleau, C. E., Downs, W. D., Lin, R., Wittmann, C., Bei, Y., Cha, Y. H., Ali, M., Priess, J. R. and Mello, C. C. (1997). Wnt signaling and an APC-related gene specify endoderm in early *C. elegans* embryos [see comments]. *Cell* 90, 707-716.

Thorpe, C. J., Schlesinger, A., Carter, J. C. and Bowerman, B. (1997). Wnt signaling polarizes an early *C. elegans* blastomere to distinguish endoderm from mesoderm [see comments]. *Cell* 90, 695-705.

Wang, B. B., Muller, I. M., Austin, J., Robinson, N. T., Chisholm, A. and Kenyon, C. (1993). A homeotic gene cluster patterns the anteroposterior body axis of *C. elegans*. *Cell* 74, 29-42.

Zipkin, I. D., Kindt, R. M. and Kenyon, C. J. (1997). Role of a new Rho family member in cell migration and axon guidance in *C. elegans*. *Cell* 90, 883-894.

**Table H.1 Mutant strains with wild-type V5 polarity.**

Gene	Molecular identity <sup>1</sup>	Rationale for examining <sup>2</sup>	(n)
<i>par-2(e2030ts)</i>	zinc finger, ATP-binding motifs	Required for asymmetric first cleavage in embryo	30
<i>mig-2(mu28)</i> null allele	Rho GTPase	May be required for cytoskeletal polarity	70
<i>mig-2(rh17)</i> activated allele	Rho GTPase	May be required for cytoskeletal polarity	45
<i>lin-11(n389)</i>	LIM homeobox gene	Required for asymmetric division of vulval precursor cells	58
<i>lin-39(mu26)</i>	<i>C. elegans</i> Hox gene	Patterns mid-body region	12
<i>let-60(n1046)</i>	let-60 = Ras	To determine if Ras pathway plays a role	50
<i>mom-1(or10)</i>	Porcupine homolog	Required for asymmetric EMS cell division	n.d. <sup>3</sup>
<i>mom-2(or42)</i>	Wnt homolog	Required for asymmetric EMS cell division	n.d.
<i>mom-4(or30)</i>	transforming growth factor $\alpha$ -activating kinase 1	Required for asymmetric EMS cell division	n.d.
<i>mom-5(or57)</i>	Frizzled homolog	Required for asymmetric EMS cell division	n.d.

<sup>1</sup> see References.

<sup>2</sup> see References.

<sup>3</sup> n.d. = not determined (see Materials and Methods).

## **Appendix I: Overexpression of *lin-17* causes *egl-20(-)* phenotypes.**

I constructed a *lin-17(n677); ncl-1(e1865)* strain carrying an extrachromosomal array for mosaic analysis of *lin-17*. The array *muEx67* contains pSH2(*lin-17+*) injected at 50 ng/μl, C33C3(*ncl-1+*) injected at 75 ng/μl and pTG96(*sur-5::gfp*) injected at 100 ng/μl. While scoring progeny from the mosaic strain at 25°C for controls, I noticed that animals carrying the array exhibited ectopic phenotypes that resembled *egl-20(-)* phenotypes. It is possible that *egl-20* negatively regulates *lin-17* for some phenotypes. Alternatively, excess LIN-17 might titrate away endogenous EGL-20. It will be necessary to cross the array into wild type and *egl-20(-)* animals to begin distinguishing between these two models.

**Table I.1.** Overexpression of *lin-17* causes *egl-20(-)* phenotypes

Genotype	QL descendants anterior <sup>a</sup> (%)	QR descendants posterior <sup>b</sup> (%)	V5 polarity reversed (%)	Abnormal phasmids <sup>c</sup> (%)
N2 <sup>d</sup>	0	0	0	0
<i>egl-20(n585)</i> <sup>e</sup>	99	82	50	0
<i>lin-17(n677)</i> <sup>f</sup> - array <sup>g</sup>	29 (76)	7 (60)	0 (68)	100 (166)
<i>lin-17(n677)</i> + array	86 (78) p < 0.0001	25 (80) p = 0.003	11 (83) p = 0.01	7 (137) p < 0.0001

All animals were examined at 25°C.

The number of animals (n) examined for each strain is shown in parentheses.

p-values relative to animals without the array were determined using Fisher's exact test.

<sup>a</sup> These numbers represent the fraction of QL.pax cells that were located anterior to V4.p.

<sup>b</sup> These numbers represent the fraction of QR.pax cells that were located posterior to V2.a.

<sup>c</sup> Dye fill assays were performed on young adults (2 days old at 25°C).

<sup>d</sup> n > 100.

<sup>e</sup> n > 100.

<sup>f</sup> This strain also contains the *ncl-1(e1865)* mutation.

<sup>g</sup> The extrachromosomal array contains pSH2 (*lin-17(+)*), C33C3 (*ncl-1(+)*) and pTG96 (*sur-5::gfp*).



## **Appendix J: Peptide antibodies against the EGL-20 protein**

I have designed an antibody against a peptide sequence from the EGL-20 protein. The 15 amino acid peptide sequence was selected from a unique region of EGL-20:

DYLPRPHYHSTDREH. I have received three bleeds each from two different rabbits at Research Genetics, Inc. The unpurified sera did not reveal a clear expression pattern, although there was some staining in the posterior body region. I used both the MH27 and LIN-39 fixation protocols on wild-type and *egl-20(n585)* worms. The unpurified sera are currently aliquoted and frozen at  $-80^{\circ}\text{C}$ . The peptide for affinity purification is stored at  $-20^{\circ}\text{C}$ .

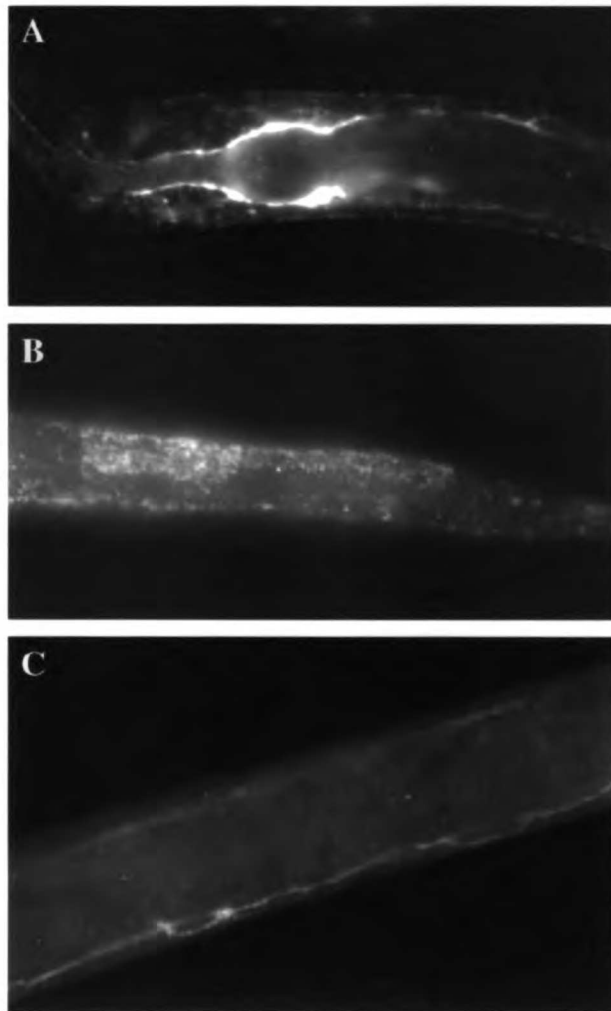


**Figure J.1.** Staining of wild-type animals with unpurified EGL-20 anti-sera #45585 (1:500 dilution). Animals were fixed as L1 larvae using the MH27 fixation protocol. All views are lateral with dorsal up and anterior to the left.

(A) Pharynx.

(B) Posterior body region.

(C) Ventral cord.

## **Appendix K: LIN-39 staining in *egl-20(n585)* mutants**

### **Background**

Previous work from our lab has shown that the posterior migrations of the QL descendants is dependent on the Hox gene *mab-5*, and the anterior migrations of the QR descendants is dependent on the Hox gene *lin-39*. In *egl-20(-)* animals, the QR descendants stop at positions that are posterior to the wild-type stopping points. It is not likely that *egl-20* regulates *lin-39* expression. If the sole function of *egl-20* was to activate *lin-39* expression in QR, then the double mutants should look like *lin-39(-)* single mutants. However, in *lin-39(-); egl-20(-)* double mutants, the QR descendants are shifted further posteriorly than in either single mutant (Harris et al., 1996). In addition, Naomi Robinson found that *lin-39::lacZ* expression in the QR.a and QR.p cells appeared to be normal in *egl-20(-)* animals. We stained WT and *egl-20(-)* animals with the LIN-39 anti-sera (developed by Julin Maloof) to determine whether the *lin-39* expression levels differed later in the Q lineages.

### **Materials and Methods**

We fixed and stained wild-type and *egl-20(n585)* larvae (4-6 hours old) that were grown at 25°C with the LIN-39 anti-sera as described by Maloof and Kenyon, 1998.

### **Results**

The staining was not very successful, but I was able to score a few animals from both strains. In the wild-type animals, the QR.paa and QR.pap cells showed strong staining,

whereas the QL.paa and QL.pap cells did not. In wild-type animals, *lin-39* is expressed in both the QL and QR cells initially, but it appears to be down-regulated later in the QL lineage. In *egl-20(n585)* animals, both QR.pax and QL.pax descendants showed strong LIN-39 staining. Thus, the defect in the anterior migration of the QR descendants in *egl-20(-)* animals does not appear to be due to a failure to activate *lin-39* expression.

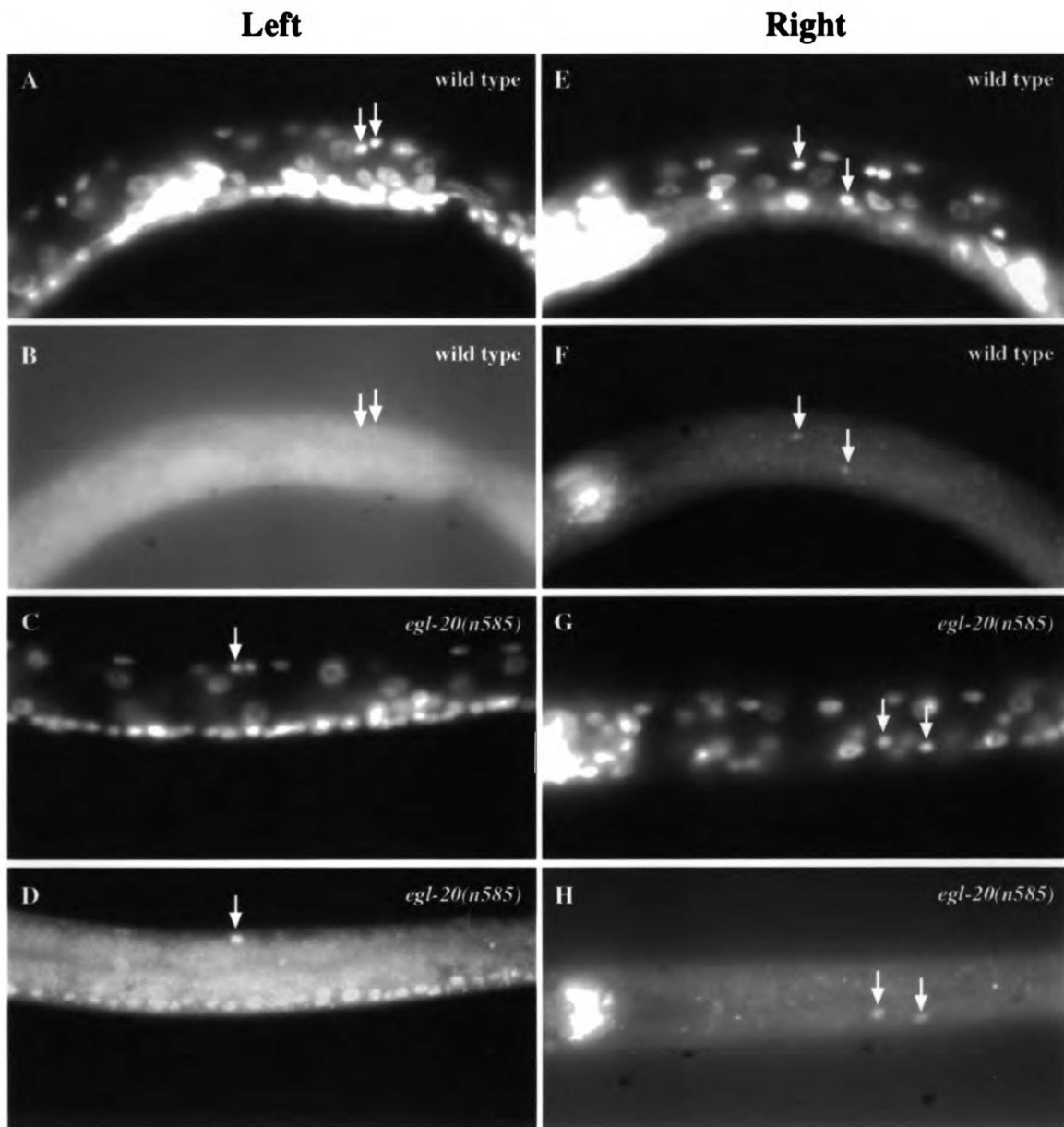
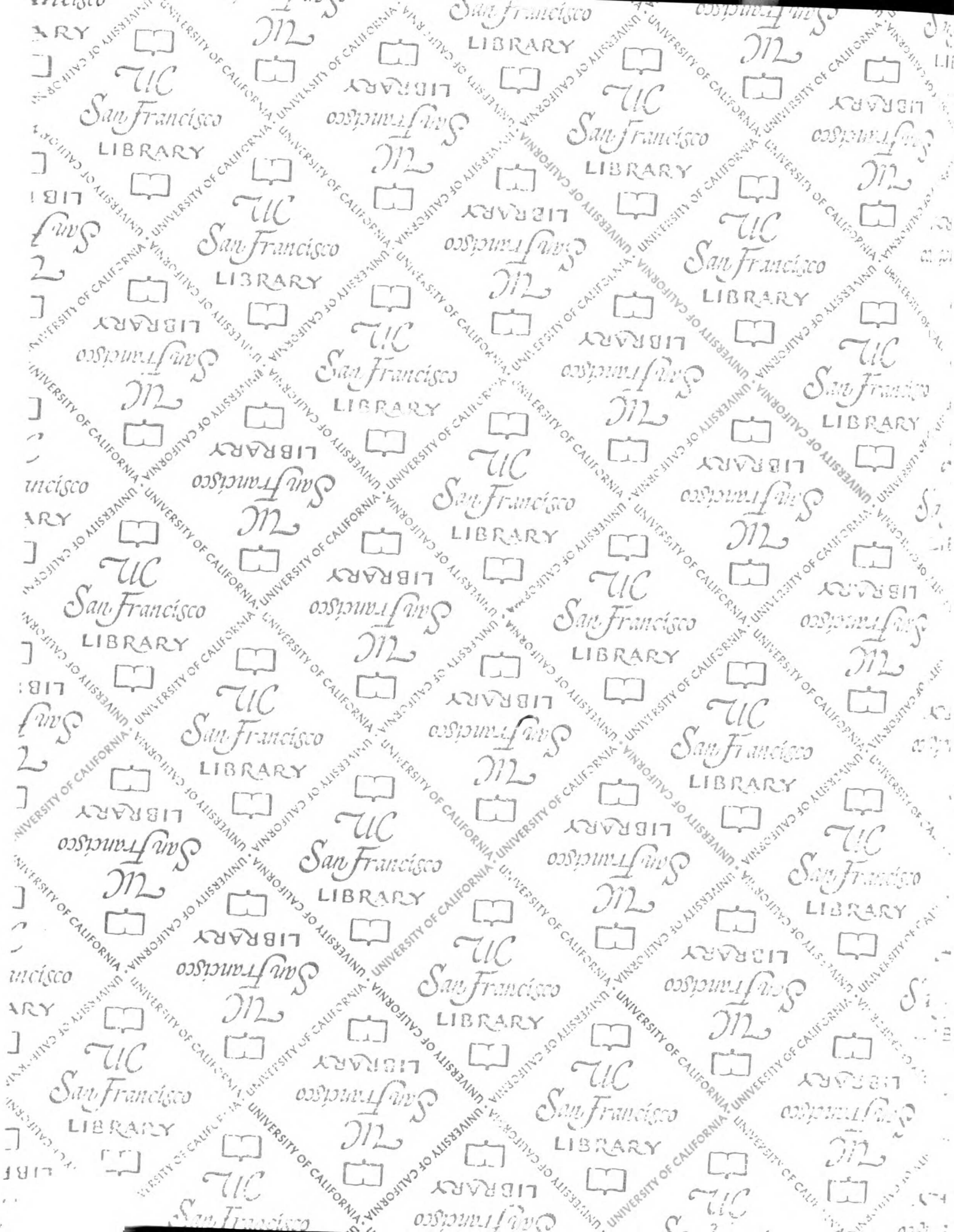


**Figure K.1.**  $\alpha$ -LIN-39 staining of wild-type (A, B, E, F) and *egl-20(n585)* (C, D, G, H) L1 larvae. All views are dorsal up and anterior to the left. DAPI images are provided to help in identification of the Q descendant nuclei. QL.pa and QR.pa descendants are indicated with white arrows.

UCSF LIBRARY



**For** Not to be taken  
from the room.  
**reference**

